SOME STUDIES ON REINFORCED EARTH FOUNDATION BEDS AND RETAINING WALLS

by

AMOL VASHISTHA

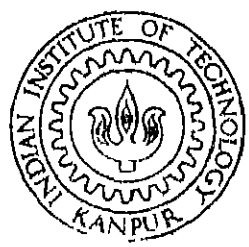

DEPARTMENT OF CIVIL ENGINEERING

INDIAN INSTITUTE OF TECHNOLOGY KANPUR

April, 1997

SOME STUDIES ON REINFORCED EARTH FOUNDATION BEDS AND RETAINING WALLS

A Thesis Submitted
in Partial Fulfillment of the Requirements
for the Degree of
Master of Technology

by

Amol Vashistha

to the

DEPARTMENT OF CIVIL ENGINEERING
INDIAN INSTITUTE OF TECHNOLOGY, KANPUR

April 1997

CE-1997-M-VAS-REI

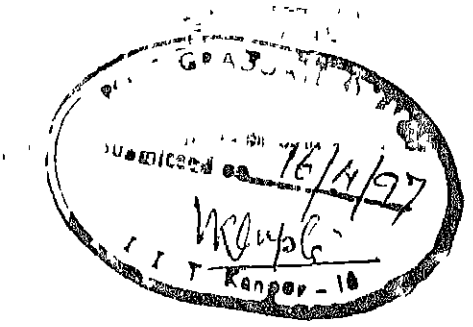

CERTIFICATE

This is to certify that the work contained in the thesis entitled SOME STUDIES ON REINFORCED EARTH FOUNDATION BEDS AND RETAINING WALLS by Amol Vashistha has been carried out under my supervision and that this work has not been submitted elsewhere for a degree

Dr. P. K. Basudhar,
Professor
Department of CIVIL Engineering,
Indian Institute of Technology, Kanpur.

Acknowledgements

I take this opportunity to, first of all, thank Dr P. K Basudhar, who has been a guide in the true sense of the word.

I would like to express my gratitude towards the Geotech. Faculty, Dr. Madhav, Dr. Kameswara Rao, Dr. Chandra, Dr. Dayal and Dr. Yudhbir for their enlightening lectures.

I would always be indebted to Dixitji for his patient hearings and suggestions at different stages of my thesis work

Its difficult to find words to express my feelings towards my batchmates, Raj, Ashu, Tiwari, Laxminarayana, Siva, Sharma, Rao and Arif, who have been the spark in my life here at IITK. I was indeed fortunate to have such a lively bunch with me in the Department. I would also like to thank Alok, Avi, MP, Vishal, Vivek, Pandu, RamP, Giridhar, Giri, Dash, Vikas, Bhole, Ravi, Tapan, members of the Hall cricket team, and all my friends whose names I could not mention here, for the great time in the Hall for the last 21 months.

Lastly, without my family's encouragement and blessings, I could never have reached this stage.

Abstract

Reinforcing earth with geosynthetics as a method of ground improvement has gained immense importance in recent times. The present study is concerned with two facets of reinforced earth namely, foundation beds and retaining walls The foundation beds reinforced with multiple layers of geosynthetics are analysed using FEM The soil geotextile interface is modelled as a contact problem instead of the conventional technique of adopting spring elements Parametric studies have been conducted for a homogeneous linearly elastic granular soil to determine the effects of the number of layers of reinforcements, the nature of load distribution and intensity, modular ratio and Poisson's ratio on settlements, tensile force distribution and stress distribution. The study reveals that the optimum placement depth is in the range of 0 4b - 0.5b and optimum spacing is 0 4b for all the cases. Lateral stress distribution indicates a strong effect of confinement while the shear stress distribution demonstrates the effectiveness of the reinforcement in reducing shear stresses in the soil mass The study has been validated by comparing results with FEM studies related to reinforced foundation beds.

The study also deals with optimal cost design of geosynthetic reinforced earth retaining walls subjected to static and dynamic loading. Choosing the length and strength of the reinforcement as a feasible design vector the Sequential Unconstrained Minimisation technique is used to arrive at an optimal cost of the reinforced earth wall. Optimal cost tables are presented for different combinations of loading and the developed procedure is validated by taking up an example problem. It is found from a typical example problem that savings of the order of 7 – 8% can be made over the standard design.

Contents

List of Figures

List of Tables

Chapter 1

Introduction

1.1 General

Reinforcements with geosynthetics as a method of treatment of soils of low bearing capacity is now an established ground improvement technique. Although, the systematic study of reinforced earth did not start until recently, to the villager in tropical Africa and Southern Asia, the practise of building houses and roads on fibre-reinforced earth is an age-old art. Reinforced soil structures are being used more frequently in system infrastructure such as bridge abutments, pavements, railway foundations, air strips, working platforms for oil drilling, etc. The concept of reinforced earth was developed in 1960's by a French Engineer, Henri Vidal The concept involves the increase in load carrying capacity of a composite formed by the soil mass and reinforcement due to the development of tensile stresses in the reinforcement and the shear bond with the surrounding soil. Excellent field performance of the reinforcements confirm the advantages pertaining to this type of construction.

Different types of Geosynthetics are available in the market, viz geotextiles, geogrids and geomats Action of each of these differs in many ways when used as an inclusion in the soil. In contrast to the geomats and geogrids, geotextiles do

not offer any bending resistance Geogrids offer more frictional resistance against pullout Geosynthetics are increasingly being used in the construction of reinforced earth structures, such as, retaining walls, embankments, soil foundations, etc

The construction of reinforced soil foundation has considerable potential as a cost-effective alternative to conventional methods of support In this technique, one or more layers of geosynthetic reinforcement and controlled fill material are placed beneath the footing The purpose is to provide a suitable operating surface on which loads may be carried without the subgrade failing or deforming excessively

Retaining walls as earth structures are frequently constructed for a variety of applications, most common being bridge abutments and road construction They are required where a slope is uneconomical or technically infeasible When selecting a retaining wall type, mechanically stabilized earth (MSE) walls should always be considered MSE (i e. reinforced soil) walls are basically composed of some type of reinforcing elements, e. g geosynthetics in the soil fill to resist lateral earth pressures When compared to conventional retaining wall systems, reinforced earth retaining walls have significant advantages They are very cost effective, especially for walls in fill embankment cross sections Furthermore, these systems are more flexible than conventional earth retaining walls such as reinforced concrete-cantilever or gravity walls Therefore, they are suitable for sites with poor foundations and seismically active areas.

A proper understanding of the performance of any reinforced structure is achieved through large scale model tests. However, economic considerations pertaining to the conduct of such tests have encouraged development of numerical and analytical modelling techniques Such techniques can be used to study, in detail, the various parameters associated with the mechanism and simulate varied field conditions.

Sophisticated theoretical predictive models may be adopted for complementing conventional analysis on large/important projects where the anticipated conditions

are such that the validity of simplified approaches may be questioned

In the following section, a brief literature review pertaining to the behavior of a footing under strip loading resting on reinforced bed and the design aspects of reinforced earth-retaining walls is presented Based on the literature review, scope of the work has also been outlined.

1.2 Brief Literature Review

The behavior of footings resting on reinforced beds and reinforced earth walls have drawn the attention of geotechnical research community and much work has been reported in literature However, only those literature pertaining to strip loading on reinforced beds are presented here mainly due to the reasons of space and brevity Another reason for the decision to work only with this type of loading as major constructions like highways and embankments impose such type of loading analytical and experimental studies on reinforced earth walls has also been presented.

1.2.1 Reinforced Foundation Beds

In order to predict the behavior of the reinforced earth beds, the various methods that have been originally developed for unreinforced soils have further been extended to study the effect of inclusion The theoretical predictive techniques that have been proposed, fall in one of the following four categories based on limit equilibrium methods, lumped parameter models, theory of elasticity solutions and finite element methods. A brief review of literature pertaining to each of the above methods is presented as follows.

Limit Equilibrium Methods

Giroud and Noiray (1981) made an analysis of the unpaved road behavior with and without geotextile as reinforcement. They considered the effect of geotextile in increasing the bearing capacity of the soil This method is based on the consideration

of the "tension membrane" effect for the case of plane strain reinforced unpaved road deforming under the action of a single application of dual wheel load Assuming an allowable rut depth, load spread angle, suitable geometric configuration and firm anchorage of the reinforcement, the strain in the reinforcement was calculated. On knowing the strain, the tension in the reinforcement is computed Design charts were proposed for the reduction in road base thickness, due to reinforcement effect of geosynthetic, for various traffic intensities

Ingold and Miller (1982) proposed a theory for bearing capacity of footings on reinforced clay considering an equivalent undrained strength of reinforced clay A number of layers of reinforcements spaced at a certain distance were considered Considering the force equilibrium of an element of soil spliced between two layers of reinforcement, they presented an expression for equivalent shear strength to the soil They derived an equation for the bearing capacity of reinforced cohesive soil. Comparison of the predictive results with the model test results has shown a close agreement.

Lumped Parameter Models

Madhav and Poorooshasb (1989) proposed a new model which consists of Pasternak shear layers, Winkler springs and a newly proposed rough membrane to represent the mechanical response of a granular fill geosynthetic–soft soil system. The displacements of soil and tension in fabric were obtained by satisfying the force equilibrium, coupled differential equations. They reported that the soil settlement decreases and tends to become uniform with increasing rigidity of shear layer It was proposed that the geosynthetic should be placed within the granular fill rather than laying it directly on soft ground.

Poorooshasb (1991) developed a unified approach to the solution of three classes of problems, viz. (i) mats supported on point loads, uniformally distributed or symmetrically distributed loads. (ii) mats bridging over voids appearing in the

subgrade after construction. (iii) mats placed over non-uniform forms of ground subsidence In the analysis, the reinforcements are assumed to be rough enough so that no slippage takes place The granular fill is considered as a strain hardening plastic material having a yield function, f The special assumption regarding mode of deformation is that all the vertical planes in unloaded system remain both vertical and plane after loading has been imposed The results demonstrated the usefulness of the transform function developed on the basis of the above assumptions, in obtaining solutions to the problems of geosynthetic reinforced granular mats

Gofar and Bourdeau (1994) described an analytical model based on the stochastic theory of stress diffusion. The model accounts for the effect of fill compaction and confinement as well as the boundary interferences with the stress diffusion mechanism

Ghosh and Madhav (1994) studied the settlement, confinement and membrane effects of reinforced granular fill- soft soil system These studies were undertaken by modifying the models proposed by Madhav and Poorooshasb (1988,1989) As in the previous study the 'rough membrane' element is incorporated for single layer of reinforcement assuming horizontal transfer at the soil-reinforcement interface. The model is generalized by incorporating non-linear response of the soft soil and fill under plane strain loading condition. Parametric studies indicated that at large deformations, the vertical component of the tensile force in the reinforcement resists the applied load from acting directly over the soft soil. The membrane effect is significant for low values of shear stiffness of the granular fill. A reinforcement length of 3b was found to be sufficient to improve foundation response

Ghosh and Madhav(1994) developed another model to incorporate the confinement effect of a single layer of reinforcement. It is quantified in terms of average increase in confining pressure due to the reinforcement, from which modified shear stiffnesses of the granular fill surrounding the reinforcement are obtained. The

parametric studies indicates that while the membrane action improves the footing response, the confinement effect further enhances it The confinement effect is more pronounced when shear stiffness of the granular fill is large

Shukla and Chandra (1994) proposed a foundation model to incorporate the compressibility of the granular fill by attaching a layer of Winkler springs to the Pasternak shear layer The parametric studies indicates that the consideration of the compressibility of the granular fill results in a significant increase in the settlement of reinforced soil

Theory of Elasticity Solutions

Binquet and Lee (1975a) are the pioneers in carrying out an analytical study on the bearing capacity of reinforced soil beds Using the Boussinesq's stress distribution, they calculated the shear stress distribution on the plane of reinforcement and the maximum tensile stress in the reinforcement They also defined the locus of the maximum shear stresses with depth The distance x_0 along the length of the reinforcement where the shear stress is maximum, is a function of the depth of reinforcement and the soil properties They suggested values of maximum shear stress as $0.3q_0$ at a depth of $0.25b$ and around $0.1q_0$ at a depth of $2b$, where q_0 is the intensity of the applied loading and b, the width of the footing. The normal force on the reinforcement due to the loading was obtained by integrating the vertical stress over the area of reinforcement. The authors considered three failure mechanisms viz. pullout, tension failure of the reinforcement and shear failure of the soil above the reinforcement. They assume that the tension in the reinforcement is inversely proportional to the number of reinforcing layers. Based on this assumption, they have given expression for the tension as a function of shear stresses and normal stresses at that depth, and the bearing capacity ratio (BCR), defined as the ratio of average contact pressure for the reinforced soil to that of unreinforced soil.

Pitchumani (1992) presented an analysis for the reduction in settlement due to an

inclusion of strip reinforcement within the soil mass An elastic continuum approach was used and the solution given by Mindlin (1936) was numerically integrated to study the effect of shear stresses along the strip on the settlement reduction at the surface Curves presented show the effect of length of the strip, distance and depth of the strip on the settlement reduction. The optimum depth of placement of the topmost layer is found to be 0 25b, b being the width of the footing

Finite Element Method (FEM)

Brown and Poulos (1981) demonstrated how a finite element model of reinforced earth could be used to investigate the increase in bearing capacity and stiffness of a foundation due to the placement of the reinforcement. The various components of the reinforced soil structure, are considered seperately. incorporating an elasto-plastic soil model obeying Mohr-Columb failure criterion The reinforcement strip is treated as elastic with zero flexural stiffness transmitting axial forces only. The model accounts for slip at the reinforcement-soil interface. Two cases, a footing on a homogeneous soil and a footing on a foundation incorporating a cavity or a pocket of soft soil were studied The results of the finite element study show similar patterns of behavior to the laboratory model test results. The analysis shows that the quantity of reinforcement required to produce some significant increase in bearing capacity is high, and since the limit state of the reinforcement soil bond is reached at an early stage, the reinforcement soil slip (rather than the stiffness of the reinforcing material) is the governing criterion. The analysis brings out that the provision of the reinforcement helps in spreading the load, thereby causing mobilization of soil resistance over a wider area and a shallow depth.

Andrawes et al , (1982) presented a finite element analysis to predict the load settlement behavior of soil geotextile system using variational approach to obtain the stiffness matrix for the soil elements. The geotextile was represented by linear elements with no bending stiffness. The soil geotextile interaction was assumed to

be only frictional and simulated by spring elements of zero length connecting the nodes of soil elements to those of geotextile elements Results obtained from this analysis were compared with those obtained from model tests which consisted of a geotextile reinforced sand layer loaded to failure by a strip loading The measured and predicted data for load settlement curve showed that, when geotextile was placed at a depth of 0 5 times the width of the footing, the difference in these values were within 10 percent of the peak footing load For the case where the geotextile was placed at a depth equal to the width of the footing, the difference is again within 10 percent, but only upto 0 85 times the peak load Beyond this the predicted value diverges and grossly overestimates the bearing capacity of the footing The reason could be the local shear failure of soil, which could not be accommodated in finite element procedure.

Love et al., (1987) formulated a finite element program in order to verify their model tests capable of handling large displacements and strains The subgrade was modelled as elastic perfectly plastic material The fill material was modelled as an elastic frictional material obeying Matsuoka yield criterion. The reinforcement was treated as perfectly rough, to simulate no slip condition Yielding of the reinforcement was also not considered based on observation made in model tests. It was also assumed that the reinforcement cannot take compressive stresses. The results of this analysis compare well with those obtained with model tests for reinforced and unreinforced cases The results indicated that reinforcement prevents the shear stress on its upper surface from being transmitted to the clay layer below. The membrane action was mobilized at large displacements, leading to large increase in normal pressure both above and below the inclusion. The membrane tension profile displayed a slight dip directly underneath the footing, confirming that tension in reinforcement is not constant under the footing.

Rowe and Soderman(1987) discussed the choice of the finite element and constitutive models and validation of the results against bench mark solutions demonstrated, both from field evidence and theoretical analysis, that the reinforcement plays a relatively small role at low load levels since the soil is essentially elastic Significant strain in the geotextile begin to develop with increasing plasticity and in fact most of the strain develops after a contiguous plastic region has developed in the soil

Burd and Hulsby (1989) presented a finite element model capable of computing the behavior of a reinforced unpaved road deforming in plane strain The calculations were based on the use of Von Mises plasticity model for the clay subgrade and a model based on the Matsuoka yield function for the granular fill The reinforcement was modelled using elastic membrane elements The formulation was based on a large strain, large displacement approach. The mesh used was based on six-noded isoparametric triangular elements to model the soil and three noded membrane elements to model the reinforcement. The finite element method was used to back analyze laboratory scale model tests in which a footing has been jacked automatically into a model reinforced unpaved road There was a good agreement in the load displacement curve for reinforced and unreinforced systems between the model test results and finite element results The authors commented that the finite element model may be used to obtain values for parameters that are necessary for a full understanding of the behavior of reinforced unpaved road, but are difficult to measure in physical tests. The authors presented plots of two such parameters viz strain in the reinforcement and normal stresses acting on the reinforcement. They concluded that the finite element model is useful in estimating values of those parameters that are difficult to measure through model tests

Burd and Brocklehurst(1990) desribed a small displacement Finite Element study to investigate the mechanism of reinforcement in a plane strain reinforced unpaved road under the action of single monotonic load The fill and the clay are both

modelled by six-noded triangular elements with three noded membrane elements used to model the reinforcement which is placed directly at the base of the fill over the whole width of the mesh An elastic-perfectly plastic model was used to model the clay subgrade and an elastic-perfectly frictional model is used for the fill where the plastic behaviour is modelled by a non-associated flow rule The reinforcement is modelled as a perfectly elastic material with an infinite yield stress in tension and zero yield stress in compression. The only parameter varied was the reinforcement stiffness. No slip was allowed at the soil-reinforcement interface and geometric non-linearity was excluded The computed results agreed well with previously published limit state models A particular feature was that the increase in reinforcement stiffness causes substantial increase in the magnitude of the interface stress and reinforcement force.

Patel and Chandreshekhran (1992) formulated a FEM program to analyze two structures, viz a strip footing and a road/pavement rail track on reinforced soil subgrades. The soils were represented by four noded quadrilateral elements and geotextile by straight linear elements. The interface was assumed to be purely frictional and simulated by spring elements of zero lengths connecting the nodes of soil elements to those of inclusion elements. The results indicated best improvement at a depth of 0.55b, the depth of the top layer of the reinforcement. They also concluded that failure mass predicted by FEM analysis is deeper than that predicted by Bearing Capacity theory Varying E_s and E_g values have shown that there is greater potential for improvement in weaker soils

Wilson-Fahmy and Koerner (1993) presented a finite element model to represent soil–geotextile interaction using an incremental load transfer $1-D$ finite element type of analysis to study the behavior of geogrids embedded in sand under a pullout condition. The conversion of $2-D$ structure of geogrids into an equivalent $1-D$ structure while still retaining its $2-D$ properties was elaborated

Otani et al , (1994) performed bearing capacity analysis of geogrid reinforced foundation ground using rigid plastic finite element method A series of parametric studies by changing the reinforcement conditions, i.e , length, depth and strength of geogrid were conducted Results showed that the bearing capacity increases as depth and length of reinforcement increases but there exists an optimum depth at which the maximum reinforcement effect is mobilized.

Desai (1995) presented a nonlinear finite element analysis of the problem of strip footing resting on reinforced sand bed The non-linear behaviour of sand was modelled by a hyperbolic reversible stress-strain relationship. The geotextile was modelled as a new isoparametric element It was discretized into a set of membrane and contact elements while the sand continuum was discretized into eight-noded isoparametric elements. They concluded that the geotextile reinforcement contributes to reduction in settlements of vertically loaded strips and the major principal stress direction at a point in sand is a function of magnitude

Gharpure(1995) conducted FEM studies to predict the load-deformation behaviour of a geotextile reinforced sand bed subjected to strip loading. The soil-geotextile interface was modelled by defining the contact conditions at the interface rather than the conventional joint elements The parametric studies were carried out to find the optimum placement depth of the reinforcement, variation of shear and tensile forces along the reinforcement, effects of the nature of load distribution, effect of modular ratio,etc. The author concluded that the optimum placement depth of a single layer of reinforcement is 0 6b and that at optimum placement depth, the modulus of elasticity of the geotextile if increased beyond 200 times the modulus of elasticity of soil, does not further reduce the settlements

Raghvendra et al., (1996) extended Binquet and Lee's approach for the design of reinforced soil bed as a two layered system. They used a general purpose Finite Element program, FEAP using four noded quadrilateral elements to find the optimal

thickness of the upper granular layer Stress distribution obtained from FEM analysis was used to calculate non-dimensional parameters for estimating the mobilization of tension in the reinforcement They suggested that these non-dimensional parameters together with selected design variables could be used to calculate the thickness and length of the reinforcement required to satisfy the performance criterion on settlement and bearing capacity

Sitharam et al.,(1996) conducted Finite Element Studies to obtain the nature of tensile distribution along the reinforcement for a reinforced soil bed A nonlinear confining stress-strain dependent behaviour model was used for the soil elements Finite Element Analysis was carried out with different types of reinforcement and loading was applied sequentially in increments. They concluded that the tensile force distribution along the length of the reinforcement is non-linear Higher the reinforcement stiffness, higher was the tensile force Another observation was that the location of the maximum tensile force depends on the type of the reinforcement.

Experimental Investigations

Binquet and Lee (1975b) investigated the mechanisms and potential benefits of using reinforced earth slabs to improve the bearing capacity of granular soil. They conducted model tests with stiff footings on reinforced foundations for three conditions - homogeneous deep sand, sand above an extensive layer of very soft material and sand above a finite size pocket of very soft material. The reinforcing material consisted of $13mm$ wide strips of household aluminium foil. Tests were conducted for linear density ratio, defined as the total width of strips per unit width of footings, of 0.425. Three series of tests were conducted. The results of these tests showed that the load settlement and the ultimate bearing capacity of the footing could be improved by a factor of about two to four times above the bearing capacity of an unreinforced soil under identical conditions. Results were obtained regarding the effects of the depth of the top layer of reinforcement and number of layers of

reinforcement It was observed that the bearing capacity ratio (BCR) continued to improve with increasing number of layers upto 6 to 8, beyond which there was little additional improvement It was also observed that the optimum location of the top strip is at a depth of $0.3b, b$ being the half width of footing and with further increase in this depth, the BCR value decreases. They observed that pullout failure generally occurred with lightly reinforced slab ($N < 2$), whereas tie-breaking which occurred in the uppermost layers was generally associated with heavily reinforced slabs ($N > 4$)

Akinmusuru and Akinbolade (1981) conducted a series of laboratory model tests with square footings on a deep homogeneous sand bed reinforced with flat strips of rope fibre material and undertook parametric studies. The results indicated that bearing capacity was maximum when the topmost layer of the reinforcement is at a depth of $0.5b$ from the base of the footing, where b is the width of the footing The optimum vertical spacing of the reinforcement was found to be less than $0.5b$ For spacing greater than that, the BCR decreased sharply and the rate of decrease became low for spacing greater than b. They concluded that increasing the number of layers beyond three does not contribute much to bearing capacity improvement

Fragaszy and Lawton (1984) conducted a series of laboratory model studies to determine the influence of soil density and reinforcing strip length on the load settlement behavior of reinforced soil The tests were conducted on reinforced and unreinforced sand. The results showed that when BCR is calculated at a settlement equal to 10 percent of the footing width, the BCR is independent of soil density. When calculated at a settlement of 4 percent of the width of the footing, the percentage increase in the bearing capacity appeared to be less for loose sands than for dense sands. As strip length was increased from $3b$ to $7b$, BCR increases rapidly but beyond that additional strip length does not appear to increase the BCR significantly. Comparison of their results with those reported by Binquet and Lee

for earth slabs showed good agreement in respect of the observation that the bottom layer of the reinforcement breaks first The authors commented that the equations developed by Binquet and Lee are very sensitive to the value of friction angle at failure

Guido et al , (1986) presented a comparison of results of laboratory model tests to study the behaviour of geogrid and geotextile reinforced earth slabs The parameters studied were the coefficient of friction between soil and geotextile, pullout resistance between geogrid and soil, depth below the footing for the first layer of reinforcement, vertical spacing of the layers, number of layers, width size of square sheet of reinforcement and tensile strength of the reinforcement. The geotextile used was Du Pont Typar 3401 and geogrid was Tensar SSI grid. They concluded that for both the cases, BCR decreased with increasing depth of top layer upto a critical depth of b, beyond which it remained practically constant As the vertical spacing was increased, BCR decreased. The number of reinforcement layers showed an optimum value of three, further increase in the number did not contribute significantly to BCR enhancement.

Love et al , (1987) conducted small scale model tests to study the effectiveness of geogrid reinforcement, placed at the base of a layer of granular film on the surface of soft clay. To make the modelling as realistic as possible, the various components were scaled by factor of 4. The reinforcement used is a version of Tensar SS geogrid. In the tests, monotonic loading was applied by a rigid footing under plane strain condition, to the surface of reinforced and unreinforced system for a range of fill thicknesses and subgrade strengths Deformation of the subgrade and the geogrid were measured from photographs. Load in the footing was measured by a load cell and displacements by a Linear Variable Displacement Transducer (LVDT) The result of the model study indicated that the geogrid reinforcement tends to reduce the shear stress transmitted to the surface of the clay subgrade The authors

opined that the failure mechanisms in the clay are mobilized at small deformations of the fill and therefore large deformations are not necessary for the benefits of the reinforcements to be filled. At large deformations, where these are permissible, additional benefit was obtained from the membrane action of reinforcement

Ramaswamy et al , (1992) conducted model tests on circular footings resting on reinforced clay they studied the influence of depth of a single layer below the footing, number of layers, thickness of grid material, anchorage length, sand-cover on both sides of the reinforcement and soaking of compacted soil on the BCR Similar to earlier studies, their conclusions were that bearing capacity increased with increase in the number of inclusion layers and thickness of geogrid They concluded that there is substantial increase in BCR if the geogrid reinforcement is covered by sand on both sides The bearing capacity of soaked reinforced soil was found to be greater than soaked unreinforced soil

Giroud et al., (1993) with their laboratory shear box tests showed that the relationship between the interface shear strength and the stress normal to the interface is not linear (as it is assumed generally) and a hyperbolic expression represents a behavior close to the actual one

Khing et al., (1993) conducted model tests on a strip foundation supported by a sand layer reinforced with layers of geogrids (punctured sheet drawn $PP/HDPE$ co-polymer). The results indicated that the maximum benefits of geogrid reinforcements in increasing the bearing capacity was obtained when the depth of top layer of reinforcement was less than b, the foundation width. A reinforcement placed below tha foundation at a depth of more than 2.25 times the foundation width did not contribute to any increase in the BCR Maximum benefit was achieved when the minimum width of the geogrid layers was about six times the foundation width.

Omar et al , (1993) carried out model tests for the ultimate bearing capacity of strip and square foundation supported by geogrid reinforced sand They concluded

that for development of maximum bearing capacity, the effective depth of the reinforcement should be about $2b$ for strip foundation and 1 $4b$ for square foundation The maximum depth of placement of the first layer of reinforcement should be less than about b to take advantage of the intrusion The maximum width of the reinforcing layers required for mobilization of maximum BCR was found to be about $8b$ for strip foundation and 4 $5b$ for square foundation

Yetimogulu et al , (1994) performed laboratory model tests as well as Finite Element analysis to investigate the bearing capacity of rectangular footing on sand bed reinforced with a single layer of reinforcement Both the methods revealed that there is an optimum reinforcement embedment depth, 0 $3b$, at which the bearing capacity was highest The studies also showed that there is an optimum vertical spacing of between 0 $2b$ and 0 $4b$ for sand beds with multiple layers of reinforcement. The bearing capacity of reinforced sand was also found to increase with reinforcement layer number and size when the reinforcement is placed within a certain effective zone, which is approximately within $1.5b$ from both the base and edge of the footing.

Adams et al., (1997) performed large-scale field tests to investigate the potential benefits of geosynthetic-reinforced soil Two different types of geosynthetics were used . stiff biaxial geogrids and geocells. They found that BCR was maximum when the depth of the top layer was less than $0.5b$ At low strains, depth of the top layer within $0.25b$ showed good results Effective zone for the reinforcement was between $0.25b$ and $0.5b$ for one and two layer case and between 0 $5b$ and $1.5b$ for three layer case.

1.2.2 Reinforced Earth Walls

Investigations of reinforced earth retaining walls involve the state of stress inside the soil mass, the forces mobilized along the reinforcement, the forces acting on the wall facing and model tests on these walls Various design procedures have also been

developed for the reinforced earth walls The Literature review is presented in the following section

Lee et al.,(1973) studied the use of reinforced earth for earth retaining structures The basic assumptions and results of the analysis were checked and found to be realistic by comparing the results with the observations made on model walls For ideal uncomplicated conditions, a cost analysis indicated that reinforced earth walls may cost as little as one-half the cost of conventional walls Maximum tensile forces in the ties were calculated and compared with the tensile strength to ensure adequate safety against breaking. Observations of failure heights for tie-breaking cases showed that there was little significant difference in failure heights for dense sand and loose sand They proposed that a better method of analysis of stress distribution within the ties and the backfill may lead to a more nearly optimum distribution of tie dimensions and therefore to more economical designs

Kennedy et al., (1980) presented an analysis to estimate the forces mobilized in the reinforced wall subjected to a surcharge strip load. An estimate of the maximum traction force in a reinforcing element was deduced by a modification of the Terzaghi's formula for the conventional rigid retaining wall They also proposed a simple distribution for the traction force in a reinforcing element, and to estimate the force transmitted to the facing of the wall. They also concluded that the surcharge strip loads applied outside the top extremity of the failure wedge do not generate significant forces either in the reinforcement or on the facing

Jewell and Milligan (1985) considered deformations of soil structures reinforced by extensible materials to ensure that the deflections at the end of construction and due to creep of the Reinforcement during the life of the structures are of a serviceable magnitude.They presented an analysis procedure linking an equilibrium stress field in which a constant mobilised angle of friction is assumed, with a strain increment or displacement field in which a constant angle of dilation is assumed Charts were

derived for horizontal deflection at face of the wall and the vertical settlement behind the crest of the wall for an ideal length layout at ideal and uniform spacing Similar charts were also derived for truncated length layout

Labba and Kennedy (1986) conducted both experimental and theoretical studies to assess the maximum tensile forces mobilized in a reinforced wall subject to a vertical surcharge strip load or the combined action of vertical and horizontal surcharge strip loads They developed a simple design method for determining the maximum magnitude of the tensile force and its distribution with depth of the reinforced earth backfill The ability of the wall system to transfer stress from overstressed regions to those regions where the reinforcing elements not yet reached their full frictional or strength capacity, in order to maintain internal equilibrium, was incorporated in the analysis. It was concluded that the stress transfer was greatly influenced by the surcharge load magnitude and its location, i e distance from the wall face

Juran et al., (1989) conducted laboratory model study on the performance and failure mechanisms of reinforced soil retaining walls, using different reinforcing materials, namely woven polyester geotextile strips, plastic grids, and non-woven geotextile strips. The model walls were instrumented to obtain measurement of stresses in the reinforcements, displacements at different points along the reinforcements, displacement of the facing, and to identify, using coloured sand, the failure surface in the soil. The results indicated the importance of confinement of the reinforcement on the structural performance.

Leshchinsky and Boedeker(1989) presented an approach for stability analysis of geosynthetic reinforced earth over firm foundations. The internal stability analysis was based on variational limiting equilibrium and satisfied all equilibrium requirements Two extreme inclinations of reinforcement tensile resistance were investigated: orthogonal to the radius defining the geosynthetic sheet, and horizontal,

signifying the as-installed position It was found that the required embedment length is longer for the orthogonal inclinations The external stability analysis was carried out by using the bilinear wedge method The results of both type of analysis were presented in the form of design charts

Juran et al ,(1990) argued that neither of the working stress method and the limit equilibrium method consider the fundamental requirement of strain compatibility between the soil and the reinforcement nor do they provide any evaluation of the effect of the soil dilatancy and extensibility of the reinforcement on the mobilized tension forces and structural stability. They presented a strain compatibility design approach that is fundamentally based on the analogy between the plane strain shear mechanism that develops along a potential failure surface in the actual structure and the response of the reinforced soil material to simple shearing.

Claybourn and Wu (1993) reviewed six published design methods, namely, Forest Service method, Broms method, Collin method, Bonaparte method, Leshchinsky and Perry method, and Schemertman method They made a comparative study of the design concepts involved in each of these methods and the results obtained by each of these methods. The computed results were then compared with the observations made on the test walls. They found that the differences in the design results stem primarily from the significant disparity in defining allowable reinforced strength and safety factors, and to a lesser degree, from discrepancies among the methods of analysis viz the lateral earth pressure distribution.

Singh and Basudhar (1993) presented the application of a generalized approach to the estimation of the lower bound bearing capacity of reinforced soil retaining walls by using Finite Element technique in conjunction with non-linear programming to isolate optimal solution. The analysis was based on a rigid-plastic model for reinforced soil, treating it as a macroscopically homogeneous anisotropic material No slipping phenomenon was considered at the soil-reinforcement interface The stress

field was the design vector subject to constraints arising from interface equilibrium and external boundary conditions as well as no-yield criterion The results when compared with data available in Literature showed good agreement

McGown et al , (1994) outlined the Limit State approach to the design of polymer reinforced walls, slopes and embankments. The approach was shown to be applicable and it was suggested that a single integrated approach based on identifiable kinematic models can be generated for the reinforced structures

Wong et al , (1994) conducted a series of model tests to study the failure model of a geotextile reinforced soil wall The backfill was uniform fine sand and the reinforcement was a woven polyester with a strength of $47Kn/m$ A uniform surcharge pressure of up to 250 KPa was applied on top of the model A two part wedge type of failure with the slope plane passing between two reinforced layers was checked in the design. They concluded that sliding failure may be critical if surcharge load is applied behind the reinforced block. Their results did not support pullout and overturning failure modes.

Karpurapu et al., (1995) described Finite Element models that were used to simulate the behaviour of two instrumented large-scale geosynthetic reinforced model walls The walls were constructed using dense sand-fill and layers of geosynthetics attached to two different facing treatments. The model walls were taken to collapse using a series of uniform surcharge load applied at the sand-fill surface. The authors adopted a modified form of constitutive hyperbolic model that included a dilation parameter to simulate the behaviour of granular soil The results showed that FEM models and constitutive models can predict important features of wall performance fairly accurately

Bastick and Segrestin (1996) applied double wedge equilibrium method to reinforced earth and analysed taking safety coefficients or weighing factors into account. They compared this method with the commonly used coherent gravity method and

global stability method Consistent results were shown provided that the safety was correctly ensured

Hyodo et al , (1996) studied the displacement of a reinforced earth wall using a small model involving two kinds of geosynthetic strips namely rubber and high density polyethylene (HDPE) Varying lengths of strip reinforcement were tested in dry Ako Sand. They observed that higher the tensile stiffness of the reinforcement, smaller is the wall displacement for full transfer of active force to the reinforcement Furthermore, the strains measured along the strip provided information on the behaviour of the strip when subjected to, firstly active force and later an additional pull out force

Porbaha and Goodings (1996) tested 24 reduced scale models of vertical and steeply sloping (1H:6V) reinforced soil walls using Kaolin as backfill, reinforced with a non woven geotextile simulant and loaded to failure under increasing self weight in the geotechnical centrifuge. The models were constructed on either firm or rigid foundation and different lengths of reinforcements were used. The tests showed that in vertical walls, failure developed entirely within the reinforced zone when $L/H \geq 0.75$. For steeply sloped walls, this threshold occurred when $L/H \geq 0.67$ Better performance was observed for models on firm foundations Tension cracks in the backfill led to stress concentration in geosynthetics and it was suggested to avoid their development in practice.

Ling et al., (1996) conducted a seismic analysis of reinforced soil structures using a pseudo-static approach. Based on the analysis, design charts were developed for a reinforced wall and the effects of seismic inertia force were investigated. For soils with small friction angle, ϕ, or for large seismic intensities, direct sliding stability concerns lead to impractically long reinforcement lengths. Therefore, the authors proposed that a permanent displacement limit should be used in the design so that direct sliding from an earthquake can be tolerable. The authors obtained yield

acceleration of the reinforced soil block in a two-part wedge mechanism for a factor of safety against direct sliding equal to unity

Nishimara et al., (1996) investigated the resistance against earthquake of ten geogrid-reinforced soil walls following the Hyogo earthquake They found that although the earthquake caused some settlements and cracks in the foundation, the walls themselves were free of deformations Analysis based on two design methods proposed by GRB and PWRI in Japan, revealed that stability was critical at horizontal seismic coefficients of 0 1 to 0.2 The failure modes were circular slip or two-part wedge sliding They proposed that stability will be enhanced by adequately increasing the length of the geogrid in the upper portions of the reinforced zone

1.3 Motivation and Scope of the work

Considering the importance of the use of geosynthetics as a reinforcing material for foundation beds, much work has been done by researchers all over the world. The various approaches discussed above for the analysis of reinforced foundation beds have their own pros and cons The Limit Equilibrium approach, albeit simple, suffers from the limitation of not considering the deformations of the soil. Similarly, in theory of elasticity approach, the analysis approach is simplified by considering an equivalent elastic modulus for the reinforced zone. It is also not able to predict the nature and magnitude of stresses at the critical interface of soil and geosynthetic. The Lumped Parameter models are more general and can be applied to a variety of situations. In terms of computational cost and understanding the overall behaviour of the system, these models have an advantage But their utility is again limited if stresses and displacements at various points in the continuum are to be found out Model tests, though quite reliable, have economic constraints since it becomes extremely difficult and expensive to perform these tests with all different combination of parameters.

FEM modelling enjoys a considerable advantage over all other approaches and experimental observations, since parameters can be easily varied for a comprehensive study and details of stress distributions and displacements can be determined throughout the system. This is particularly useful for studying the soil-geosynthetic interface.

Review of literature reveals that when multiple layers of reinforcements are used, the reinforced zone is generally homogenized and analysis is carried out by considering the zone to be very stiff, having very high modulus of elasticity. It has already been pointed out that such procedures do not give the correct representation of the stresses developed in the medium. As such there is a need to analyze the reinforced bed considering each reinforcement as a seperate entity. Gharpure(1995) developed a computer program utilizing FEM to analyze reinforced sand beds with a single layer of reinforcement. The objective of the present work is to improve upon the developed computer program in order to incorporate multiple layers of reinforcements.

The importance of reinforced earth retaining walls is easily recognizable. Although a number of design approaches have been developed and analytical studies carried out, optimal cost studies to check the economic feasibility of such walls have not yet been attempted. As such an attempt has been made here to develop a general procedure to arrive at an optimal cost estimate of a retaining wall reinforced with geosynthetics formulating the problem in the frame of non-linear programming. Studies have been made with regard to optimum cost of both geogrid and geotextile-wrap walls under static and dynamic loading.

Chapter 2 deals with the Finite Element Analysis of the reinforced foundation beds. The optimum cost design of the geosynthetic reinforced earth walls is discussed in Chapter 3. In Chapter 4, the scope of the future work has been presented.

Chapter 2

Finite Element Analysis of Reinforced beds

2.1 Problem Formulation

2.1.1 General

Finite Element Method (FEM) is well recognized as a very powerful and versatile numerical tool used for solving continuum mechanics problems Numerous examples of its application to model reinforced soil can be found in the literature. As already discussed in chapter 1, the same has been adopted in the thesis also. In the following sections, the soil-geotextile interaction mechanism is described and then the use of the FEM in finding the response of reinforced soil bed subjected to superimposed loads has been presented. The procedure was originally developed by Gharpure (1995) for a single layer of reinforcement. The same has been extended here to study the effects of multiple layers of reinforcements. For the sake of completeness, the analysis procedure is presented in detail

2.1.2 Soil-Geotextile Interaction Mechanism

Reinforced Foundation beds are classified as internally stabilized load bearing systems which are dependent upon the interaction mechanism of the soil and reinforcement. Within this system, shear transfer occurs through the interface by the mobilization of the induced tensile force in the embedded reinforcement. The process by which forces and strains are transmitted from the soil to the reinforcement depends on the soil-reinforcement friction in case of granular soils, soil-reinforcement interlock in case of geogrids and adhesion in case of undrained loading of soft clays. The tensile force distribution within the reinforcement solely depends on interface stress transfer law (Mohr-Coulumb's Law). The tensile forces induce corresponding compression in the soil as long as there is no slippage between the soil and the reinforcement. This additional compression increases the confining pressure on the soil. As a result, the soil can take more axial load. This is the 'confinement effect' Since mobilized shear stresses confine the surrounding soil, the effect will be maximum directly below the footing. Refer Fig 2.1.

Moreover, at large strains, the lateral displacements of the granular fill due to the applied load are large enough to mobilize the full shear resistance at soil-reinforcement interface. As a consequence, the geotextile, which does not have any bending strength, takes the shape of a hanging string. Due to the tension induced, it lifts the overlying soil. The applied load is distributed over a wider area on the soil underneath. Vertical pressure and settlement in the zone below the footing are thus reduced. Additionally, differential settlements are reduced due to induction of extra pressure and settlement on the soil away from the footing. Refer Fig. 2.2.

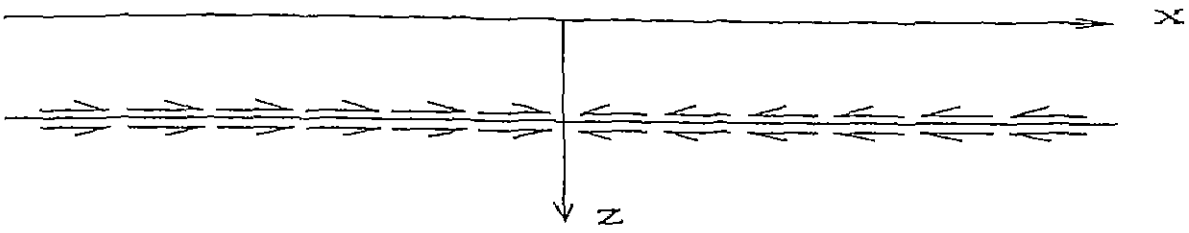

SHEAR STRESSES IN SOIL

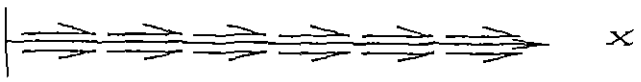

STRESSES ON REINFORCEMENT

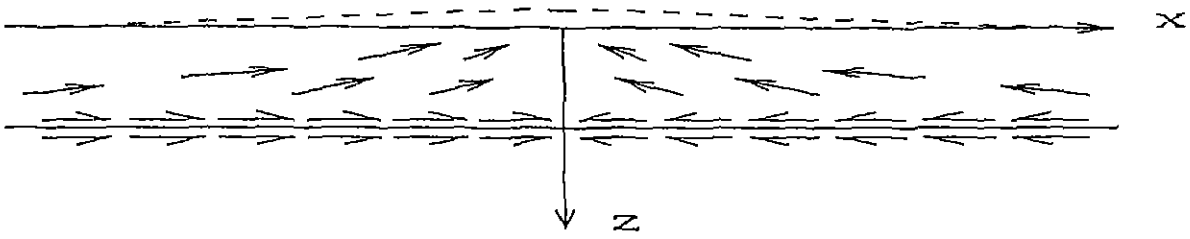

SETTELMENT REDUCTION OF SURFACE

Figure 2 1· Mechanism of Confining Effect

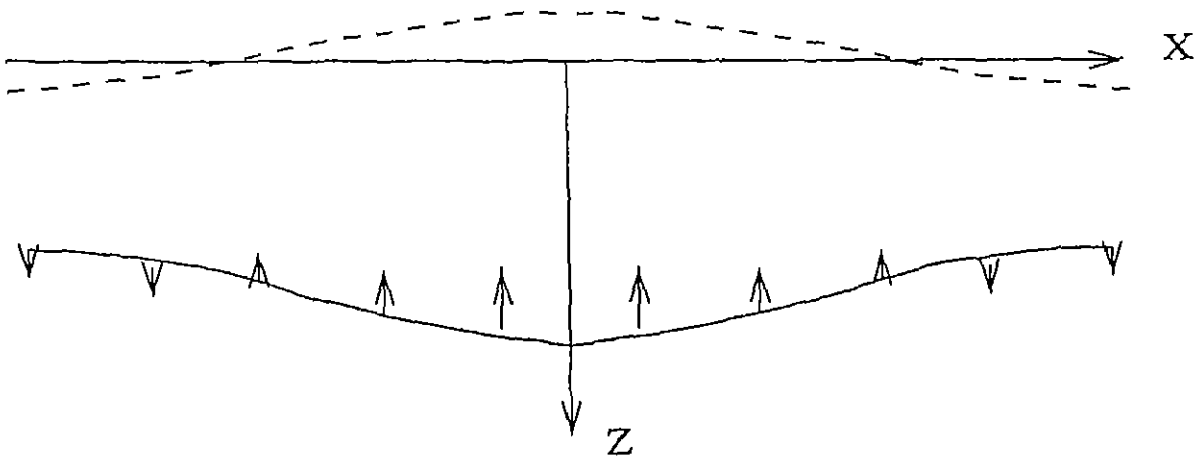

DIFFERENTIAL SETTELMENT REDUCTION OF SURFACE

(STRING EFFECT)

Figure 2 2· Mechanism of String Effect.

2.1.3 Statement of The Problem

Fig 2 1 3 shows a strip load of width b having (a) uniform intensity of loading (for flexible foundations) and (b) parabolic distribution of loading (for rigid foundations) acting on a semi infinite elastic half space A number of reinforcing geosynthetic layers are placed from a depth d with spacing s. The settlement response of the footing and the stress behaviour is to be studied for different reinforcement and soil conditions The soil is assumed to be homogeneous with constant Young's Modulus.

The method developed has been validated by taking up case studies and comparing the obtained results with experimental and theoretical solutions available in the literature. Parametric studies have been conducted to study the effect of important factors on the stress-deformation behavior of reinforced beds.

2.2 Analysis

2.2.1 Assumptions :

The following assumptions are made in the analysis :

1 The soil is considered as a linearly elastic material

2 The geotextile is also considered as a linearly elastic material

3. Length of the footing is very long in comparison to the width of footing so that plane strain condition prevails.

4. The Soil-Geotextile interaction is based on

   - Friction between soil and geotextile,
   - Adhesion between soil and geotextile,
   - String effect.

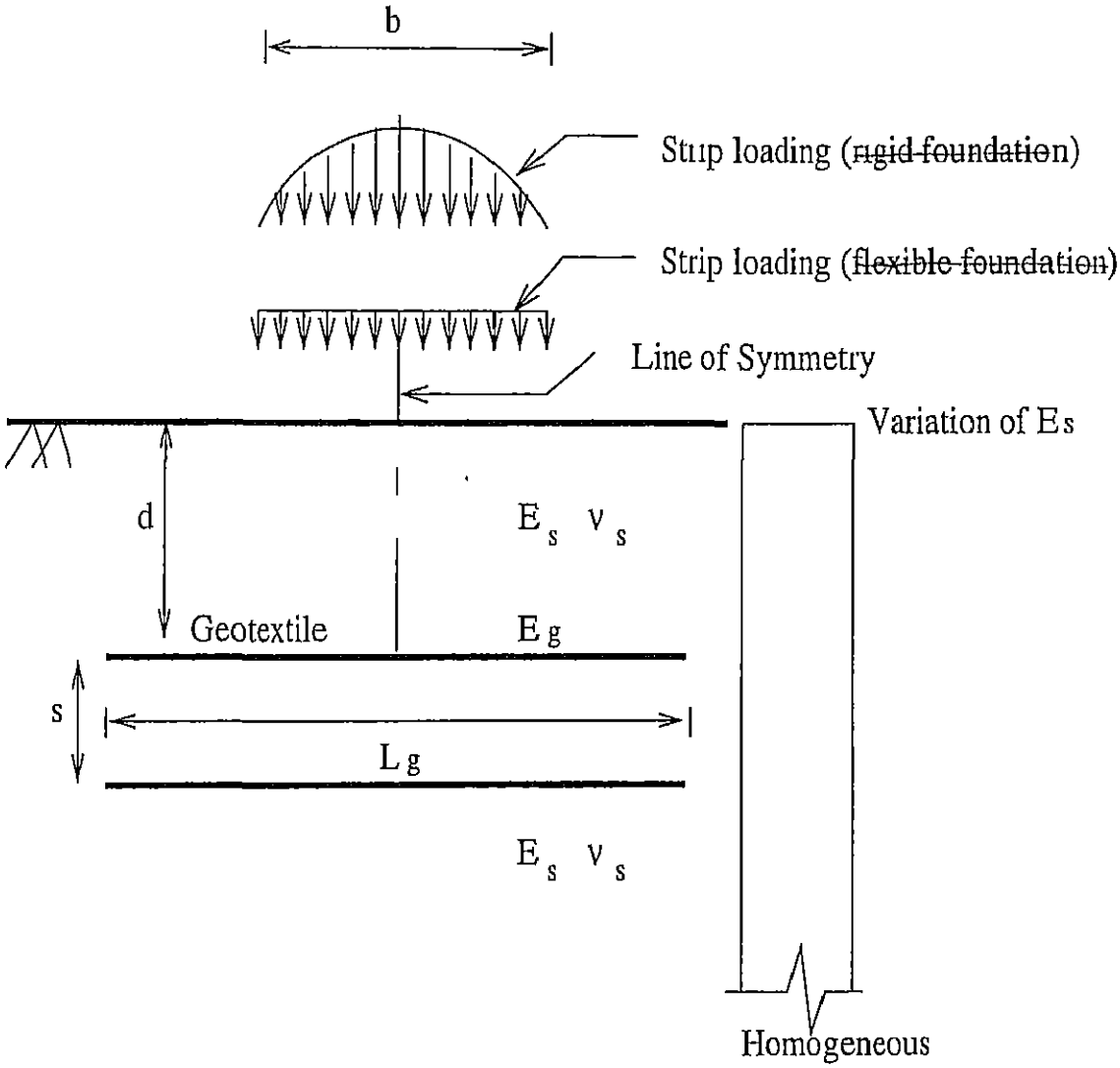

PROBLEM DEFINITION SKETCH

5 In comparison with the soil dimensions, the thickness of geotextile is negligible However, thickness is considered while calculating stresses in geotextile

2.2.2 Finite Element Formulation of The Soil Bed :

The finite element procedure used is basically that for solving continuum load-displacement problem. It consists of four main steps discretization of the continuum, selection of approximating function; derivation of elemental stiffness matrices and analysis of the element assemblage.

The Problem domain is discretized by dividing it into a number of elements. The soil has been discretized using four noded rectangular elements and the geotextile inclusion has been discretized using linear elements. The complete problem geometry and mesh details are shown in Fig 2 3

For a typical soil element, the following approximation to the dependent variables u and v (displacements in x and y direction respectively) is chosen

$$\left\{ \begin{array}{c} u \\ v \end{array} \right\} = \left[\begin{array}{ccccc} N_1 & 0 & N_2 & 0 & \cdots \\ 0 & N_1 & 0 & N_2 & \cdots \end{array} \right] \left\{ \begin{array}{c} u_1 \\ v_1 \\ u_2 \\ v_2 \\ \vdots \end{array} \right\} \tag{2 1}$$

which can be written as

$$\{u\} = [N]\{u\}^e. \tag{2.2}$$

Here the functions N_i (shape functions) are bilinear functions of natural coordinates (ζ, η) and $\{u\}^e$ is the elemental displacement vector. The chosen shape functions satisfy the completeness and compatibility conditions required for convergence. For

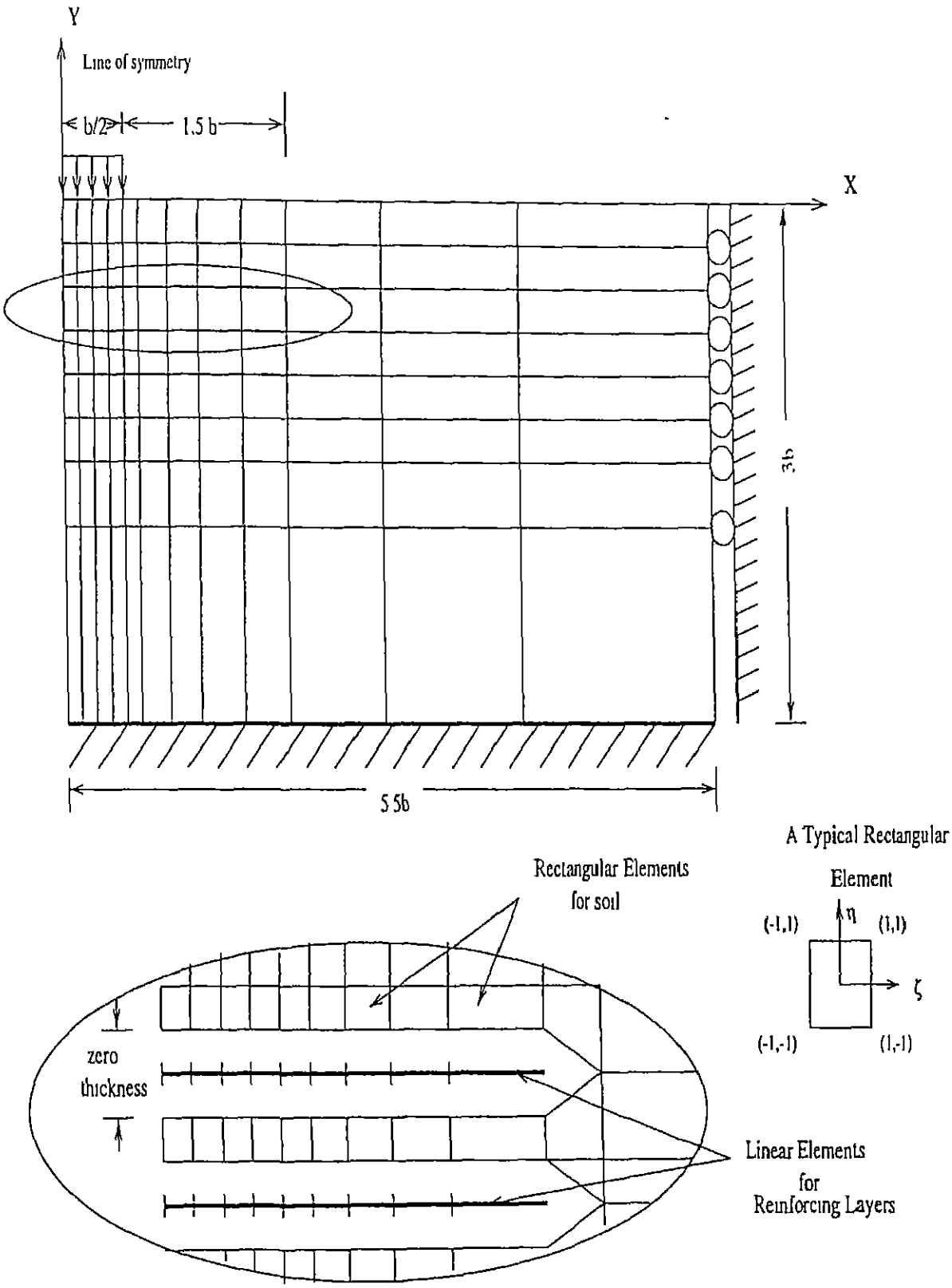

Figure 2 3. Problem Geometry and Mesh Details

a plane strain problem, the strain vector has only three components

$$\{\epsilon\} = \begin{Bmatrix} \epsilon_{xx} \\ \epsilon_{yy} \\ \gamma_{xy} \end{Bmatrix} \tag{2 3}$$

The strain vector is related to the displacement vector $\{u\}$ by

$$\{\epsilon\} = [L]\{u\} \tag{2 4}$$

where

$$[L] = \begin{bmatrix} \frac{\partial}{\partial x} & 0 \\ 0 & \frac{\partial}{\partial y} \\ \frac{\partial}{\partial y} & \frac{\partial}{\partial x} \end{bmatrix} \tag{2 5}$$

Substitution of approximation (Eqn. 2 2) into (Eqn 2 4) leads to

$$\{\epsilon\} = [L][N]\{u\}^e = [B]\{u\}^e \tag{2.6}$$

where the matrix $[B]$ is given by

$$[B] = \begin{bmatrix} N_{1,x} & 0 & N_{2,x} & 0 & \cdots \\ 0 & N_{1,y} & 0 & N_{2,y} & \cdots \\ N_{1,y} & N_{1,x} & N_{2,y} & N_{2,x} & \cdots \end{bmatrix}. \tag{2 7}$$

For a linearly elastic material, the stress-strain relation is usually expressed as

$$[\sigma] = [D]\{\epsilon\} \tag{2 8}$$

where the elasticity matrix $[D]$ for a plane strain problem is given by

$$[D] = \frac{E_s}{(1+\nu_s)(1-2\nu_s)} \begin{bmatrix} 1-\nu_s & \nu_s & 0 \\ \nu_s & 1-\nu_s & 0 \\ 0 & 0 & (1-2\nu_s)/2 \end{bmatrix}. \tag{2 9}$$

The potential energy Π of an elastic body can be expressed as

$$\Pi = \frac{1}{2}\int_{\Omega}\{\epsilon\}^T\{\sigma\}dA - \int_{\Omega}\{u\}^T\{f\}dA - \int_{\Gamma}\{u\}^T\{\tau\}dl \tag{2.10}$$

where $\{u\}$, $\{\epsilon\}$, $\{\sigma\}$, $\{f\}$ and $\{\tau\}$ are vectors of displacements, strains, stresses, body forces and surface tractions respectively Ω denotes the area of the body and Γ is the boundary of the body where the tractions are specified. Substitution of the relations (2.2), (2 6), (2 8) into the expression (2.10) for the potential energy leads to

$$\Pi = \sum_{e=1}^{n}\left[\frac{1}{2}\{u\}^{eT}[k]^e\{u\}^e - \{u\}^{eT}\{q\}^e\right] \tag{2.11}$$

Here n is the number of elements,

$$[k]^e = \int_{\Omega_e}[B]^T[D][B]dA \tag{2 12}$$

is the element stiffness matrix and

$$\{q\}^e = \int_{\Omega_e}[N]^T\{f\}dA + \int_{\Gamma_e}[N]^T\{\tau\}dl \tag{2.13}$$

is the element load vector. Further, Ω_e is the area of the element e and Γ_e is that part of its boundary which is common to Γ.

The expression (2.11) can be written in terms of the global matrices as follows :

$$\Pi = \frac{1}{2}\{U\}^T[K]\{U\} - \{U\}^T\{Q\} \tag{2.14}$$

and the minimization results in

$$[K]\{u\} = \{Q\}. \tag{2 15}$$

Here

$$[K] = \sum_{e=1}^{n}[k]^e \tag{2.16}$$

is the global stiffness matrix,

$$\{Q\} = \sum_{e=1}^{n} \{q\}^e \tag{2.17}$$

is the global load vector and $\{U\}$ is the global displacement vector. The summation sign in equations (2.16), (2.17) means the matrices $[k]^e$ and $\{q\}^e$ are to be expanded first to the global size and then added.

Note that the evaluation of B-matrix (Eqn. 2.7) involves x and y derivatives of the shape functions N_i. However, N_i are given as the functions of the natural coordinates (ζ, η). The derivatives can be calculated as follows. By chain rule

$$\begin{Bmatrix} \frac{\partial N_i}{\partial \zeta} \\ \\ \frac{\partial N_i}{\partial \eta} \end{Bmatrix} = \begin{bmatrix} \frac{\partial x}{\partial \zeta} & \frac{\partial y}{\partial \zeta} \\ \\ \frac{\partial x}{\partial \eta} & \frac{\partial y}{\partial \eta} \end{bmatrix} \begin{Bmatrix} \frac{\partial N_i}{\partial x} \\ \\ \frac{\partial N_i}{\partial y} \end{Bmatrix} = [J] \begin{Bmatrix} \frac{\partial N_i}{\partial x} \\ \\ \frac{\partial N_i}{\partial y} \end{Bmatrix}. \tag{2.18}$$

Thus

$$\begin{Bmatrix} \frac{\partial N_i}{\partial x} \\ \\ \frac{\partial N_i}{\partial y} \end{Bmatrix} = [J]^{-1} \begin{Bmatrix} \frac{\partial N_i}{\partial \zeta} \\ \\ \frac{\partial N_i}{\partial \eta} \end{Bmatrix}. \tag{2.19}$$

The matrix [J] is called the Jacobian matrix. It can be evaluated from the relationship between the two coordinate systems. The relationship is given by

$$x = \sum_{i=1}^{4} N_i(\zeta, \eta) x_i^e \tag{2.20}$$

$$y = \sum_{i=1}^{4} N_i(\zeta, \eta) y_i^e \tag{2.21}$$

where (x_i^e, y_i^e) are the nodal coordinates and N_i are the same shape functions as used in the approximation of u and v. Thus the chosen element is an isoparametric element.

2.2.3 Finite Element Formulation Of the Geotextile :

The Geotextile layer is represented by straight line elements without any bending stiffness as shown in Fig 2 3. For the two different types of mechanisms, the geotextile element is modeled differently

For the confining effect of geotextile due to tension, the element is modeled as an axial element with linear approximation for the displacement in x direction The same variational approach as used for 2-D soil elements is used The corresponding stiffness matrix becomes

$$[k_x]^e = E_g A_g / l^e \begin{bmatrix} 1 & -1 \\ -1 & 1 \end{bmatrix} \tag{2.22}$$

where A_g is the cross sectional area and l^e is the length of the element.

For the string effect, a transversely distributed load p as shown in the Fig. 2.4 is

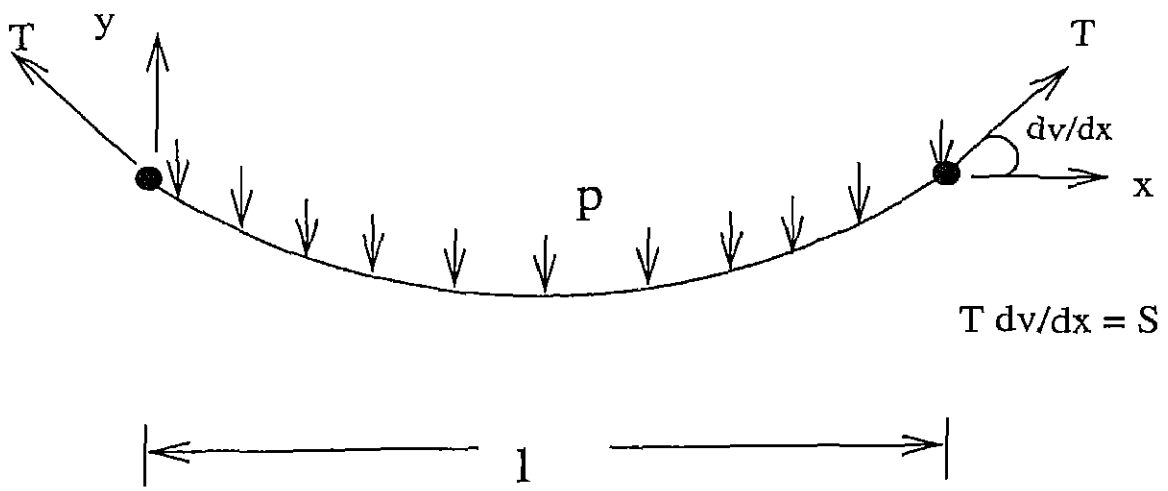

Figure 2.4: Definition Sketch for String Effect

considered. The variational functional for this case is

$$I = \int_0^l [\frac{1}{2} T (\frac{dv}{dx})^2 - pv] dx - (Sv) \mid_0^l \tag{2 23}$$

where v is the displacement in y-direction, T is the tension in the string and S is the vertical component of T at each end. Again using the same procedure as used for 2-D soil element, the minimization of variational function gives the following stiffness matrix

$$[k_y]^e = \frac{T}{l^e}\begin{bmatrix} 1 & -1 \\ -1 & 1 \end{bmatrix} \tag{2.24}$$

Note that the stiffness matrix for the confinement effect is related to the x-direction displacements while that due to the string effect is related to the y-direction displacements. The combined stiffness matrix can be arranged as

$$[k]^e = \frac{1}{l^e}\begin{bmatrix} E_g A_g & 0 & -E_g A_g & 0 \\ 0 & T & 0 & -T \\ -E_g A_g & 0 & E_g A_g & 0 \\ 0 & -T & 0 & T \end{bmatrix}. \tag{2.25}$$

Finite Element Modeling of the Interface :

In general practice, the soil geotextile interface behavior is modeled by introducing interface elements. This can be achieved in a number of ways, like, the use of joint element of zero or nonzero thickness, node compatibility spring element or by composite layer model.

The joint element formulation is derived on the basis of relative nodal displacements of the soil elements surrounding the interface as shown in Fig. 2.5, where the subscripts n and s indicate the normal and tangential (shear) components while the subscript r stands for the relative quantity.

Another common approach is to join the adjoining three nodes by springs as shown in Fig. 2.6. In this type of formulation, the spring elements ensure compatibility of

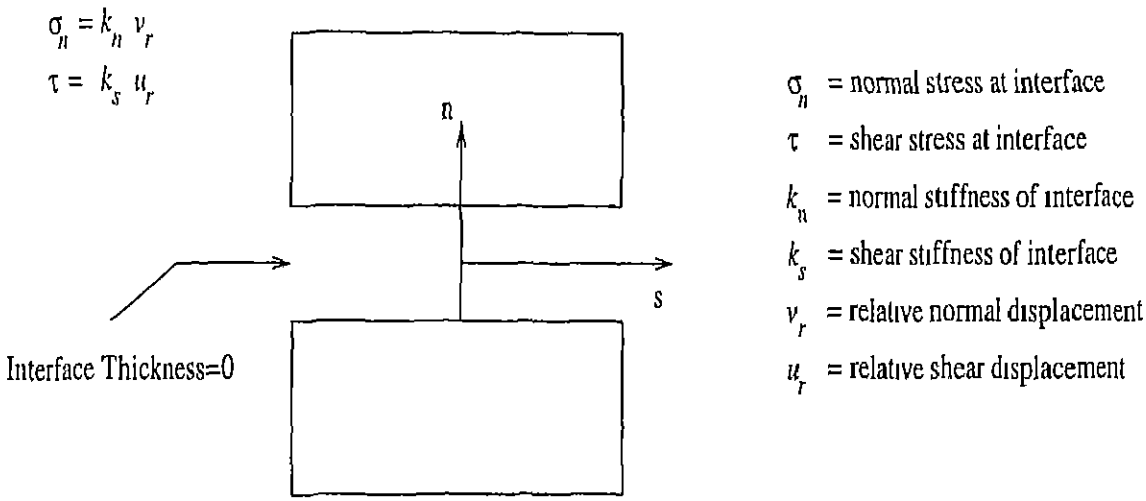

Figure 2.5: Joint Element of Zero Thickness

the displacements between the adjoining nodes until the Mohr-Coulomb's criteria is reached. It replaces the compatibility conditions by failure conditions and dilatancy equation once the interface strength is exceeded based on some assumed constitutive relationship (*e.g* Andrawes et al (1983) used a hyperbolic model) to represent the interface behavior

The composite layer model involves a beam-membrane-type four noded element with large deformation capability. This provides flexural stiffness and local membrane effect but does not allow slip between the reinforcement and soil. Therefore this is particularly suitable for geogrid type of reinforcement.

In the present work, no interface element is used but the interface is modeled as a contact problem. Referring to Fig. 2.7, the soil-geotextile interaction is represented by the following contact conditions

1. *Force equilibrium conditions* : For vertical forces at contact nodes

$$(F_y)_i + (F_y)_j + (F_y)_k = 0 \tag{2.26}$$

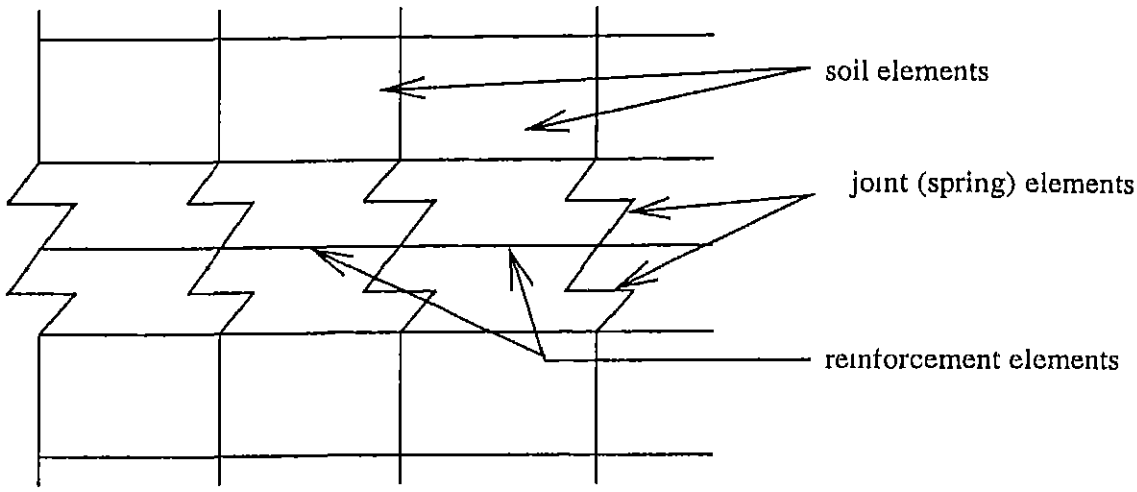

Figure 2.6: Node Compatibility Spring Elements

and for horizontal forces at contact nodes

$$(F_x)_i + (F_x)_j + (F_x)_k = 0. \tag{2.27}$$

2. *Displacement conditions* No separation is allowed between the soil and geotextile hence the vertical displacement condition at contact nodes is defined as

$$(v)_i = (v)_j = (v)_k \tag{2.28}$$

Horizontal displacement condition depends on the occurrence of slip between the soil and geotextile at a particular node For no slip, horizontal displacement compatibility is defined separately for the top and bottom soil nodes as slip can occur on either side of reinforcement. Thus

$$(u)_i = (u)_k, \tag{2.29}$$

$$(u)_j = (u)_k \tag{2.30}$$

For slip between the soil and geotextile, nodal force condition describing the Mohr-Coulomb criterion replaces the displacement compatibility condition as

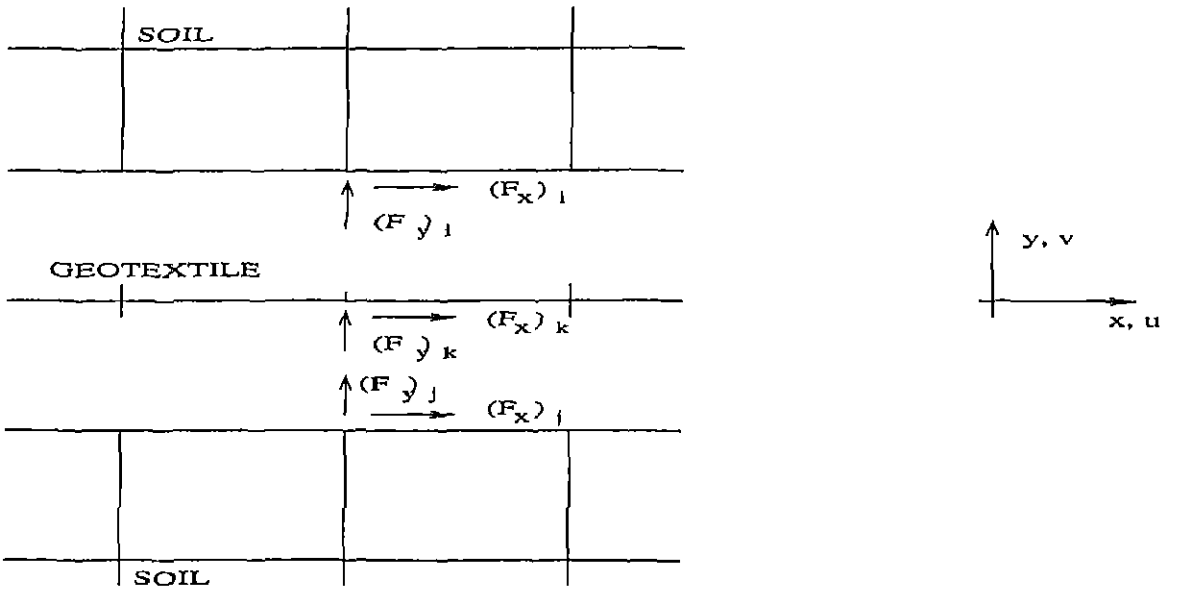

Figure 2 7 Modeling of the interface

follows.

$$(F_x)_i = (F_y)_i tan\phi^* + c^* l^e, \tag{2.31}$$

$$(F_x)_j = (F_y)_j tan\phi^* + c^* l^e \tag{2 32}$$

where ϕ^* is the frictional angle between the soil and geotextile and c^* is adhesion per unit area For parametric study adhesion is taken as zero.

2.2.4 Analysis Of Element Assemblage :

After evaluating the stiffness matrices for the individual elements, the stiffness matrix $[K]$ for the whole system is assembled. The basis of assembly is that the value of the displacement at a node is the same for each element sharing the node. As the reinforcing layer nodes are not connected with the soil nodes, the assemblage takes the shape as shown in Fig 2.8

The next step is to modify the stiffness matrix, (a) for Soil-Geotextile interaction mechanism as explained in the previous section and (b) for boundary conditions

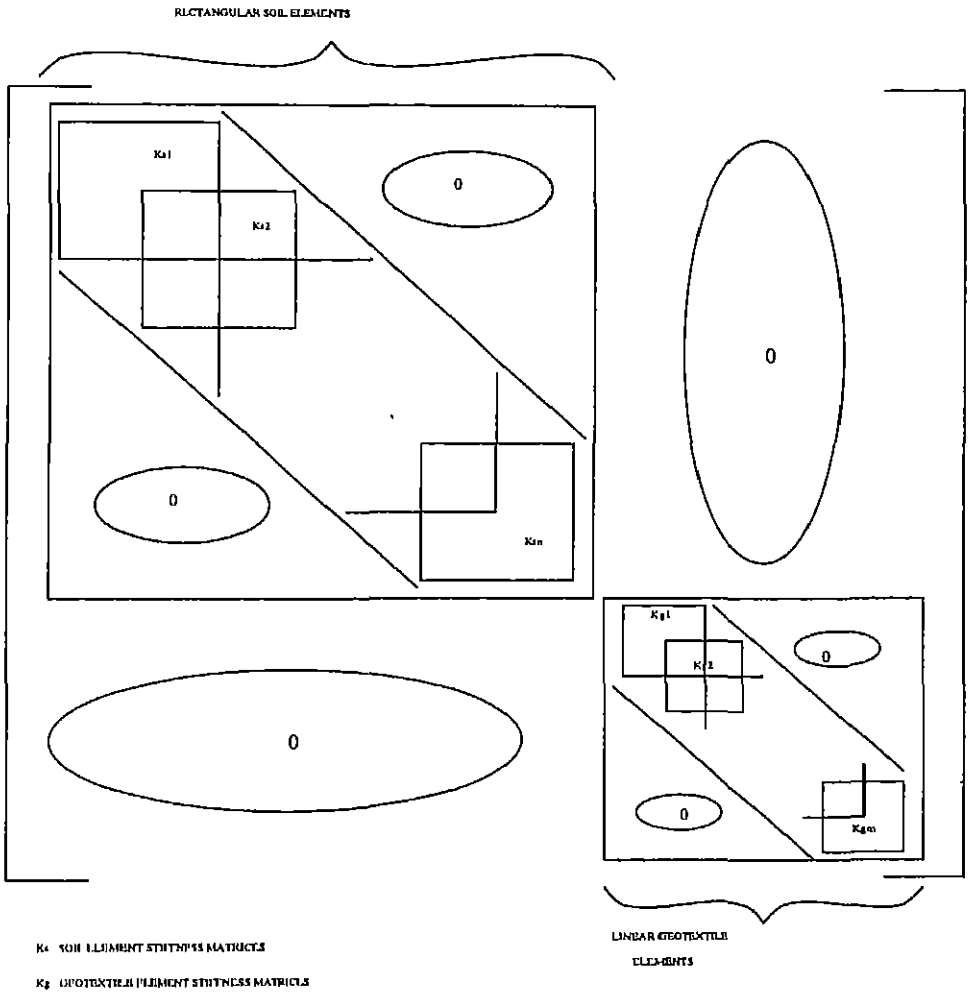

Figure 2 8. Assemblage of Stiffness Matrices

which includes zero or nonzero displacements at specific boundary nodes (The roller supports show that only vertical displacements are allowed and fixed support shows no displacement in either direction is allowed). Then the load vector $\{Q\}$ is calculated from the given loading condition (uniform, parabolic etc.). This is followed by the solution of the simultaneous equations for the unknown displacements. Finally from the known displacements, the nodal forces and strains and stresses for each element are calculated to yield the complete solution.

To check the slip conditions at interface, the forces at these nodes should be known Hence the solution requires iterations In the first iteration, no slip is considered between the interface nodes and the check for slip condition is made in the second iteration The iterations continue till slip conditions for all the nodes for two successive iterations remain the same

2.2 Results, Discussion and Conclusions

2.2.1 Input Parameters

The footing of width b is placed on a granular bed . The size of the domain for FEM analysis is chosen to be 5.5 times the width of the footing from the central axis along X direction and 3 times the width of the footing along Z direction Owing to the symmetry of the problem, only half of the layer need be analyzed The geosynthetic layers are placed such that these extend by 1 5 times the width of the footing beyond the edge of the strip loading. Analysis have been carried out with meshes of size 24×16 elements and 12×8 elements.

Soil Parameters .

Angle of Internal Friction, $\phi = 35°$;

Poisson's Ratio, $\nu = 0\ 49$;

Modulus of Elasticity of Soil, $E_s = 30$ MPa;

Geosynthetic characteristics :

Modulus of Elasticity of Geotextile, $E_g = 4$ GPa,

thickness = 7mm;

2.2.2 Parametric studies

Four cases have been investigated.

1. Unreinforced case This has been simulated using identical modulus of elasticity values for soil and geotextile

2 Single Layer of reinforcement.

3. Two layers of reinforcement.

4. Three layers of reinforcement

Table 2 1 Effect of number of layers on settlements Uniform Distribution of loading

Case	Maximum Settlement (cm)	*percent reduction*
unreinforced	4 42	0 0
single layer	4.07	7 87
two layer	3 86	12 61
three layer	3 70	16 23

The results obtained for these cases with homogeneous soil subjected to uniform distribution of loading are as follows:

- *Settlement profile:*

The settlement profile for the four cases are shown in Fig. 2 9 As expected, at $z = 0$, settlements along X direction are least when three layers of reinforcements are placed Settlement is observed to reduce more and more with addition of each layer of reinforcement.To get a quantitative idea, the corresponding percentage reduction in maximum settlement over the unreinforced case is illustrated in Table 2 1 The Fig. 2 9 also shows that increase in the number of layers of reinforcements causes significant reduction in settlements upto a distance of $0.5b$ from the centre of footing along X direction Beyond this distance, there is no appreciable impact of increasing the number of reinforcing layers on the settlement characteristics

To get an idea of the effect of nature of loading on the settlement profile, the settlement profile was plotted for the case of parabolic distribution of loading also. The profile obtained as in Fig. 2.10 shows similar trends to the uniform loading case. The percentage reduction in maximum settlement over the unreinforced case is illustrated in Table 2.2. Expectedly, the maximum settlements for the Parabolic loading case are more than the corresponding ones for the Uniform loading case. For a comparative view, the settlement profile for the unreinforced case and three layers

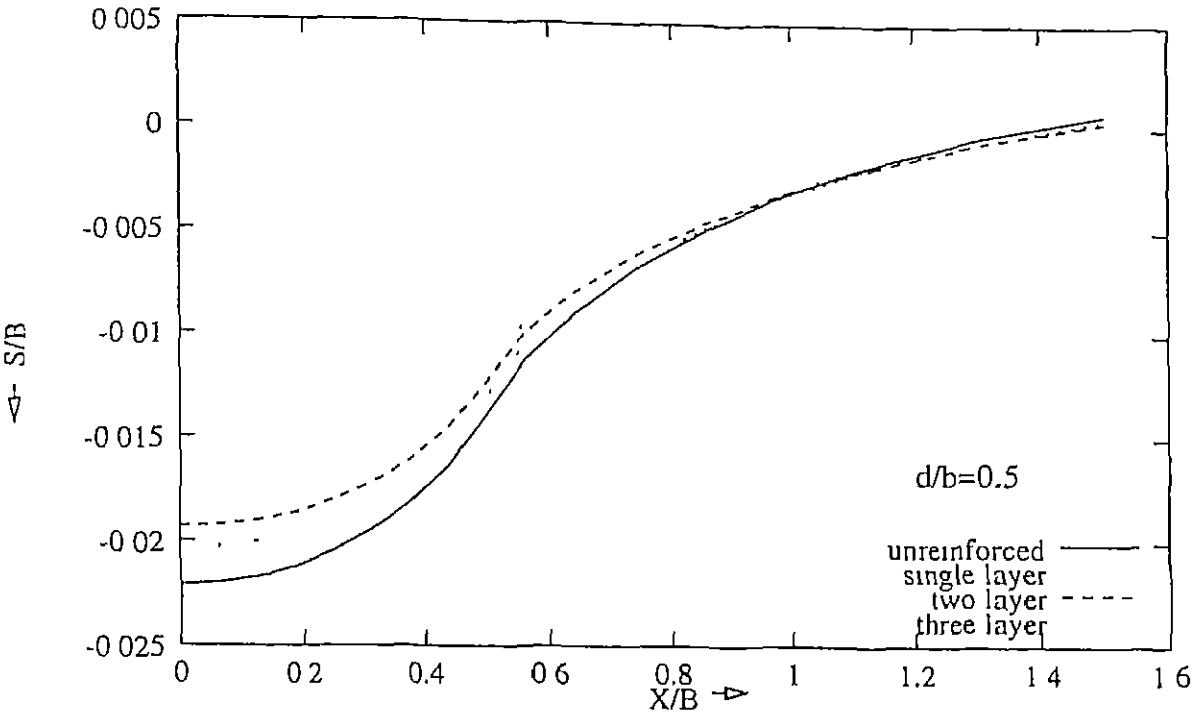

Figure 2.9 Surface Settlement Profile for UDL

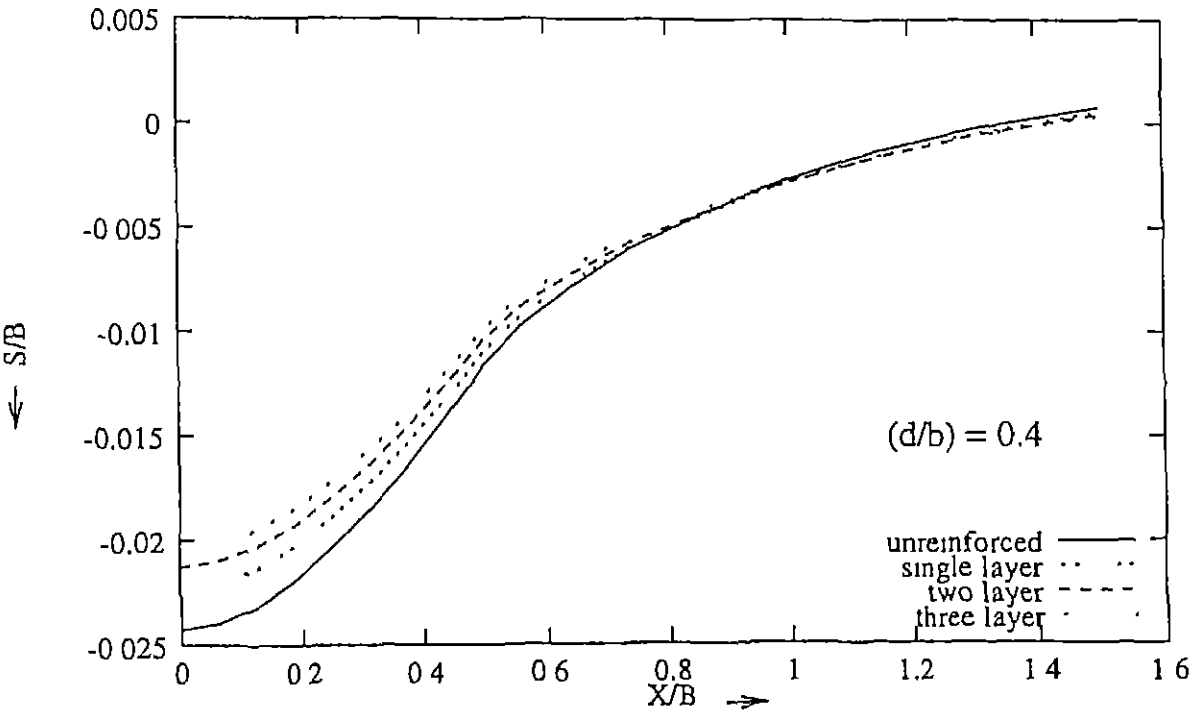

Figure 2.10: Surface Settlement Profile for PDL

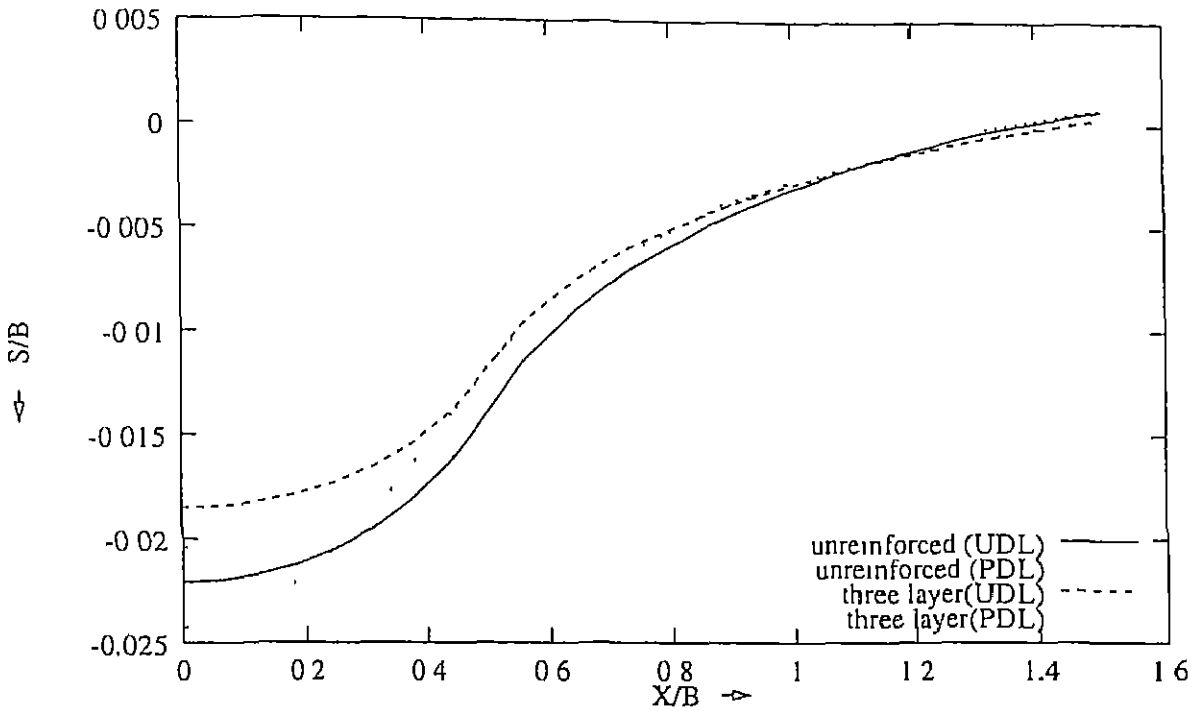

Figure 2.11: Comparison of surface Settlement Profile for UDL and PDL case(unreinforced and three layer case)

Table 2 2· Effect of number of layers on settlements· Parabolic Distribution of loading

Case	Maximum Settlement (cm)	*percent reduction*
unreinforced	4 86	0.0
single layer	4 48	7.72
two layer	4 26	12.31
three layer	4 09	15 83

of reinforcements are plotted for both the loading distributions in Fig. 2 11. The fig shows that a rigid footing, corresponding to the parabolic loading case, settles more at the centre of the loading as compared to the flexible footing Beyond the edge of the footing, $X/B = 0\ 5$, the parabolic loading case shows lesser settlements than the Uniform loading case.

- *Effect of embedment on settlements:*

To study the effect of embedment depth (the depth at which the first reinforcement layer is placed), the embedment ratio, d/b has been varied from 0 3 to 0 8 with increments of 0 1 for all three cases of reinforcements The obtained results have been presented in Fig 2.12 It can be seen from the figure that as the embedment ratio is varied from 0.3 to 0.5, settlement reduces, but any further increase in the embedment ratio causes increased settlements. Table 2 3 shows maximum settlements

for various d/b ratios and the percentage reduction in settlements for the corresponding value obtained for unreinforced case It can be noted that the percentage reductions in settlement over the unreinforced case for different d/b ratios fall within a very narrow zone for a particular case The optimum placement depth for all reinforcement cases is 0.5b. It agrees excellently with experimental investigations carried out by Akinmusuru et al(1981) and Ramaswamy et al(1992) The maximum percentage reductions in settlement values at optimum placement depth are 7.87, 12.61 and 16.3 for single layer, two layer and three layer case respectively

Similar studies have been conducted for a Parabolic distribution of loading. The results obtained for the three cases are presented in Fig. 2 13 For all the cases, the maximum settlements show a decreasing trend as d/b is varied from 0 3 to 0 4. Further increase of embedment ratio causes an increase of settlements too Table 2.4 shows maximum settlements for various d/b ratios and the percentage reduction in settlements for the corresponding value obtained for the unreinforced

Table 2 3. Effect of embedment ratio on settlements: UDL case

case	d/b	maximum settlement (cm)	*percent reduction*
unreinforced	0 0	4 4205	0 0
single layer	0.3	4 1159	6 89
	0 4	4 0806	7.69
	0.5	4 0727	7.87
	0.6	4 0809	7.68
	0.7	4 0975	7.31
	0 8	4.1181	6.84
two layer	0.3	3 9072	11.61
	0 4	3.8676	12.51
	0 5	3 8631	12 61
	0 6	3 8788	12 25
	0 7	3.9050	11.66
	0 8	3.9362	10.96
three layer	0.3	3 737	15.54
	0 4	3 6999	16 30
	0 5	3 7030	16.23
	0 6	3.7270	15.69
	0 7	3.7617	14.90
	0 8	3 8009	14 02

case. Thus, the optimum placement depth for Parabolic Distribution of Loading for all cases of reinforcements is 0 4b, although the variations in percentage reduction in settlements are almost insignificant for a particular case of reinforcement. The maximum percentage reductions in settlement over the unreinforced case at the optimum embedment ratio are 7.72, 12.3 and 15 84 for single layer, two layers and three layers of geosynthetic respectively.

- *Effect of spacing on settlement:*

To study the effect of spacing between the layers at the optimum placement depth, the spacing ratio, s/b, has been varied from 0.2 to 1.2 for two layer case and 0.2 to 0 8 for three layer case It is evident from Fig 2.14, that the settlements reduce as s/b is varied from 0 2 to 0 4 and then show an increasing trend as s/b is increased further. The variation is more pronounced for three layer case. This agrees well with model tests conducted by Yetimogulu et al(1994) and Singh (1988)

Quantitatively, Table 2 5 shows maximum settlements for different s/b ratios and percentage reductions over the unreinforced case It clearly shows that the optimum spacing for both two and three layer case is 0.4b and the corresponding percentage reduction in settlements being 11 57 and 16 27 respectively.

- *Effect of Poisson's Ratio on settlements:*

The effect of Poisson s ratio on settlements at the centre of the loading has been studied and the results are shown in Fig 2.15. The Fig 2 15 shows that an increase in Poisson's ratio over the whole range of ν_s varying from 0 3 to 0 49 (drained and undrained condition) leads to an increase in percentage reduction in settlement over the unreinforced case.

The effect is more pronounced for the undrained case ($\nu_s = 0\ 49$) as is evident from Table 2 6 The corresponding maximum percentage reduction in settlement

Table 2 4 Effect of embedment ratio on settlements PDL case

case	d/b	maximum settlement (cm)	*percent reduction*
unreinforced	0 0	4 837	0 0
single layer	0 3	4 51	7 14
	0.4	4 482	7 72
	0 5	4 489	7 57
	0 6	4 507	7 21
	0 7	4 531	6.71
	0 8	4 551	6 3
two layer	0 3	4 272	12 04
	0 4	4 259	12 30
	0 5	4 275	11 98
	0 6	4 305	11 36
	0 7	4 34	10 66
	0 8	4 377	9 88
three layer	0 3	4 098	15 64
	0 4	4 088	15.84
	0 5	4.114	15.3
	0 6	4 154	14.47
	0 7	4.199	13 55
	0 8	4 24	12 72

Table 2 5 Effect of spacing ratio on settlements, ($d/b = 0\ 5$)

case	s/b	maximum settlement (cm)	*percent reduction*
unreinforced	0 0	4.4205	0 0
two layer	0.2	3.9130	11.48
	0.4	3.9089	11.57
	0.6	3.9210	11 30
	0.8	3 9409	10.85
	1.0	3 9643	10 32
	1.2	3.9894	9 75
three layer	0.2	3.7149	15 96
	0 4	3.7013	16 27
	0 6	3 7445	15 29
	0 8	3 8096	13 82

Table 2 6 Effect of Poisson's ratio on Settlements, $(d/b) = 0\ 5$

ν_s	unreinforced	one layer		two layer		three layer	
	settl (cm)	settl (cm)	% diff	settl (cm)	% diff	settl. (cm)	% diff
0 499	1 919	1 766	-7 97	1 657	-13.66	1 573	-18 04
0 45	2 615	2 481	-5.12	2 383	-8 89	2 303	-11.92
0 40	3 128	3 032	-3 67	2 958	-5 44	2 896	-7.42
0 35	3 574	3 508	-1 83	3 454	-3 34	3 406	-4 64
0 30	3 986	3 943	-1 09	3 903	-2 08	3 867	-2 99

values are 7 97, 13 66 and 18 04 for single layer, two layer and three layer case respectively The reason for such behaviour is that in the undrained case, the soil is at its stiffest state and so the settlements are less than those for drained case

Effect of Modular Ratio on settlements

The Modular Ratio is the ratio of the stiffness of the geotextile and the stiffness of the soil and thus, reflects the strength of the reinforcement. Fig 2 16 shows the effect of Modular Ratio, E_g/E_s, at $d/b = 0.5$, on the maximum settlements at the centre of the loading for the three reinforced cases The figure shows that as the Modular Ratio increases, i. e. stiffer reinforcement is chosen, the settlements decrease at an increasing rate, but the decrease is at a constant rate beyond Modular Ratio equal to 400.

Variation of tensile force in reinforcement:

Due to the soil-reinforcement interaction, tensile forces are mobilized in the reinforcement. The tensile force in the top layer of reinforcement have been plotted in Fig. 2.17 for all the three reinforced cases. Predictably, the tensile forces are maximum for the single layer case and minimum for the three layer case There is a sharp decrease in tensile force from the centre to the edge of the loaded area

Thereafter, the tension in the geosynthetic varies more gradually till it becomes zero at the edge of the reinforcement

For the two layer case, upto a distance of 0 $3b$ from the centre in the X direction, the top layer of the geosynthetic shows more tension than the lower layer (Fig 2 18) Beyond that distance, the lower layer shows greater tension The results are comparable qualitatively to the FEM studies conducted by Burd and Brocklehurst (1990) and Love et al (1987) Model tests conducted by Love (1987) and Gourc et al (1985) also show a dip in tension profile directly beneath the footing The extent of significant tension is an indication of the required width of the reinforcement in the soil bed

Tensile force distribution has also been plotted for the case of Parabolic Distribution of loading in Fig 2 19 As in the previous case, the mobilized tensile forces are maximum for the single layer case A comparative plot of tensile forces in the first layer of reinforcement for the cases of Uniform and Parabolic case of loading shown in Fig 2 20 predictably shows a direct relation between the tensile force and the load intensity. The increase in tensile force is in the range of 10-15% for the parabolic loading case over the uniform loading case, directly below the footing. Beyond the edge of the footing, the Uniform loading case shows greater tension in the reinforcement for both single layer and three layers case

An attempt was made to study the effect of load intensities and Modular Ratio on the tensile force distribution along the reinforcement Fig 2 21 shows the tensile force distribution for load intensities of 10, 100, 200 and 500 KN/m for a Modular ratio of 200. It illustrates that the reinforcement becomes more effective at higher load levels as greater mobilization of tensile forces takes place at these levels.

To study the effect of stiffness of the reinforcement on the tensile force distribution, tensile forces are plotted in Fig. 2.22 for a constant loading of $100KN/m$ and varying modular ratio It can be observed that a stiffer reinforcement shows a

distinct peak tensile stress near the centre of the loading while the reinforcements with very low stiffness show a uniform tensile force distribution The results of the study of effect of load intensities and the modular ratio on tensile force distribution agree well qualitatively with similar FEM studies conducted by Sitharam et al (1996)

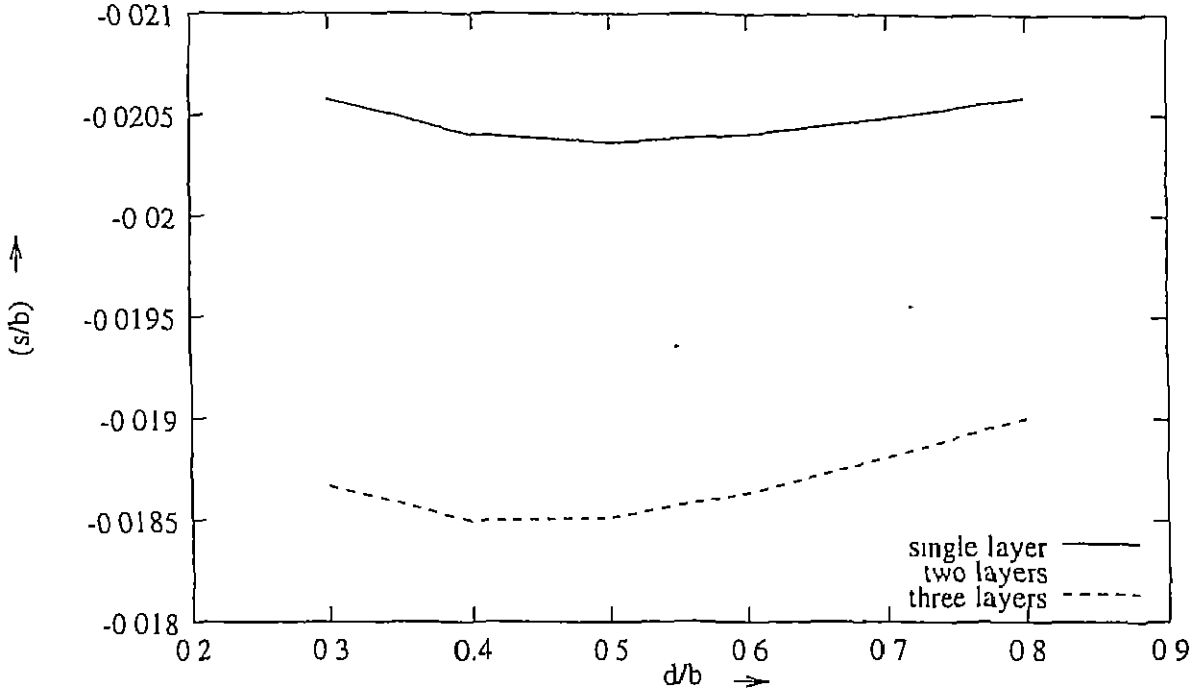

Figure 2.12 Effect of Embedment ratio on settlements UDL case

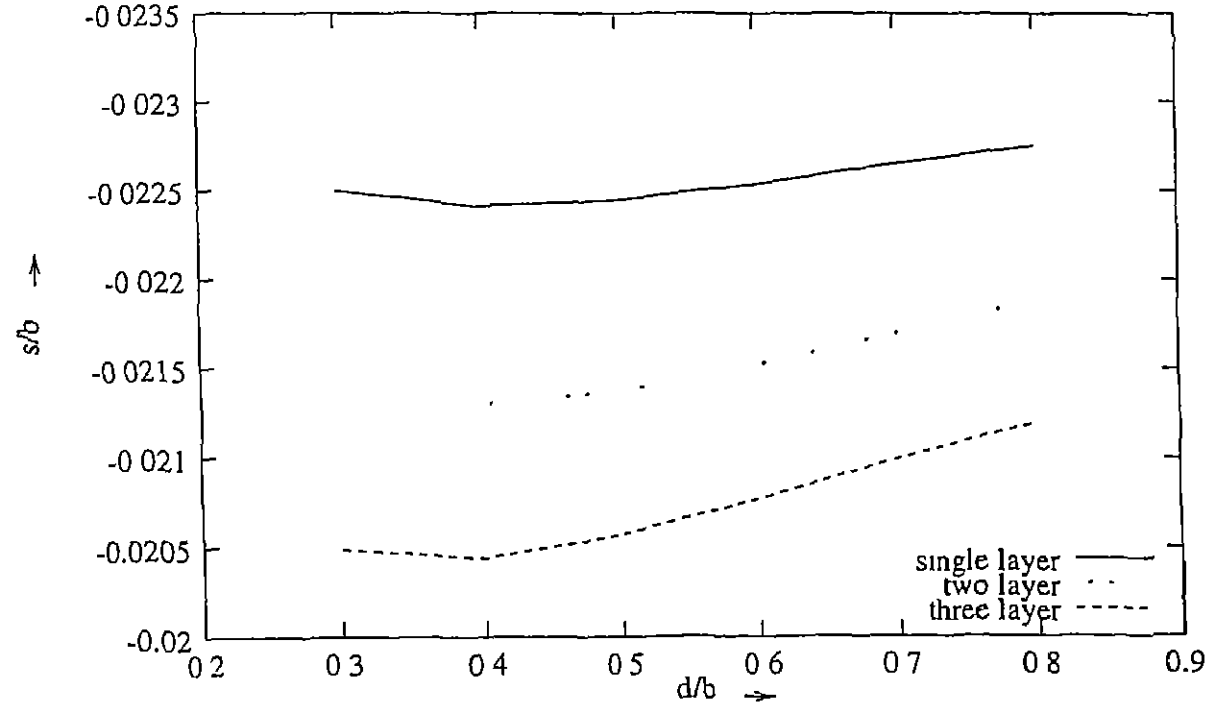

Figure 2 13· Effect of Embedment ratio on settlements .PDL case

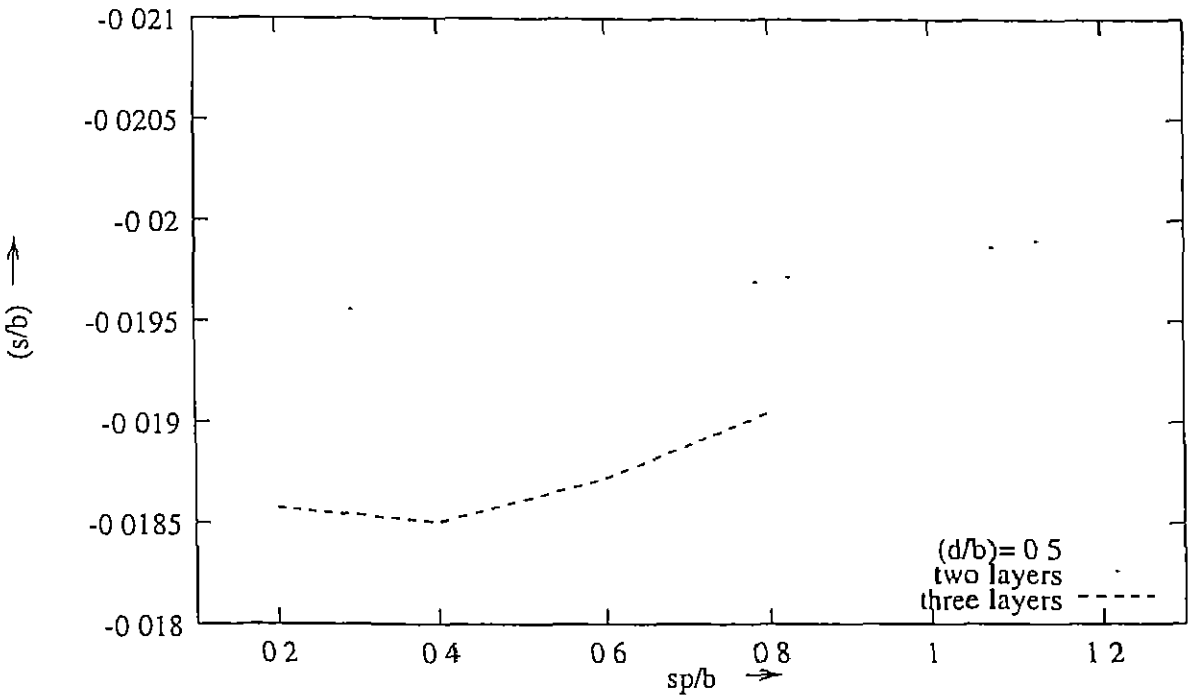

Figure 2.14. Effect of spacing on settlements UDL case

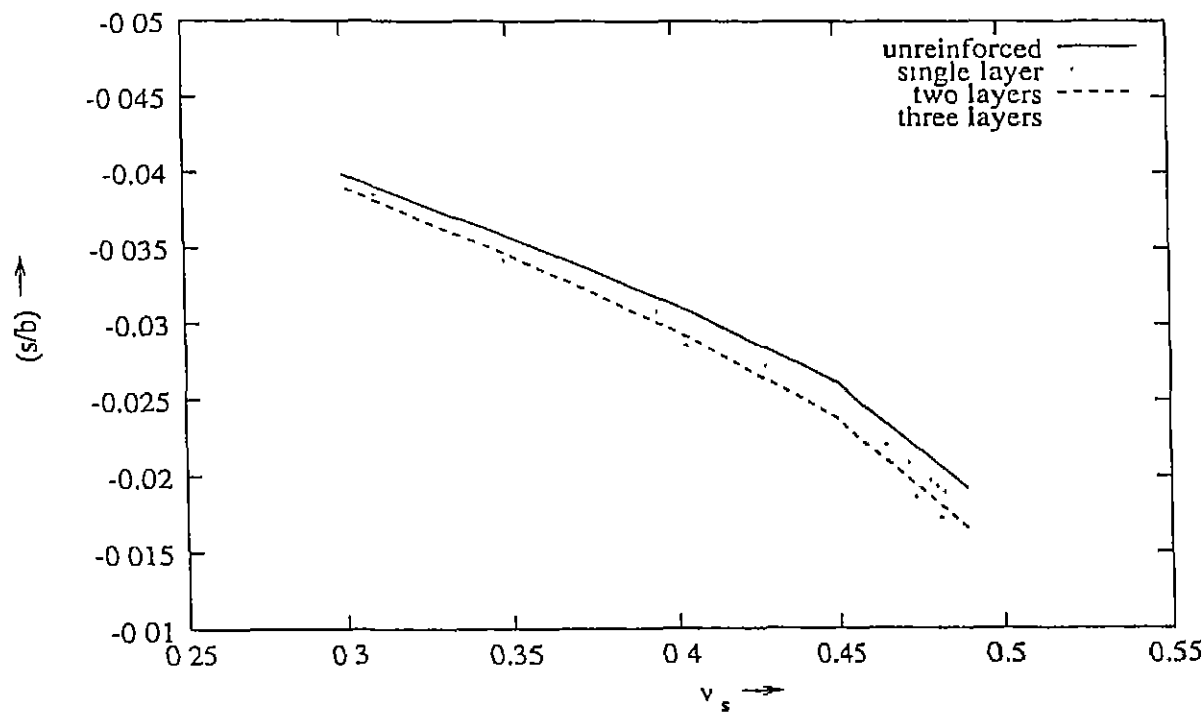

Figure 2.15· Effect of Poisson's ratio on settlements .UDL case

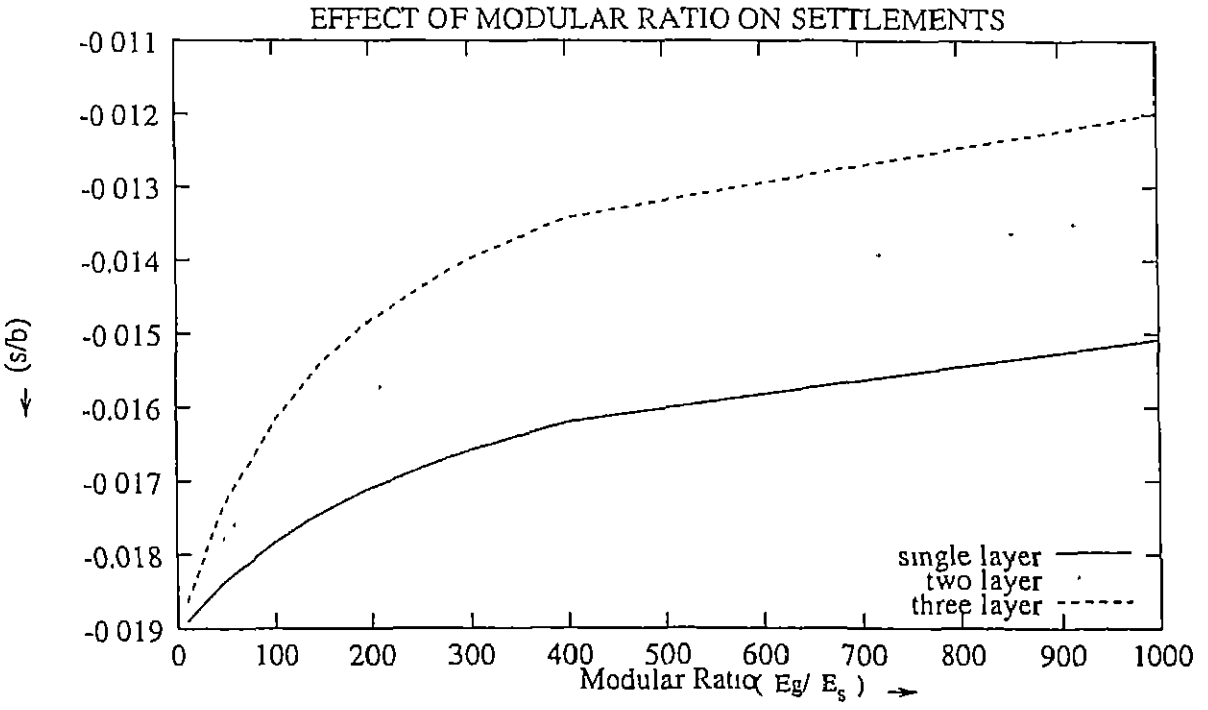

Figure 2.16 Effect of Modular ratio on settlements :UDL case

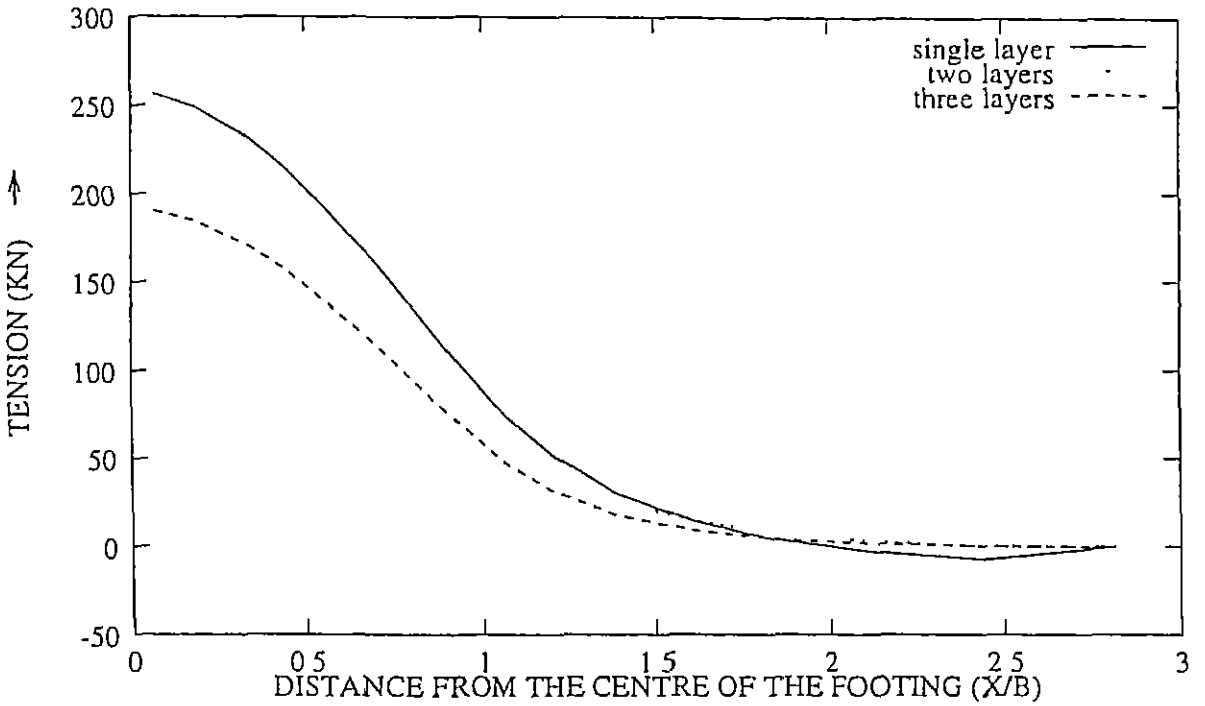

Figure 2 19 Tensile force distribution for top layer of geosynthetic PDL case

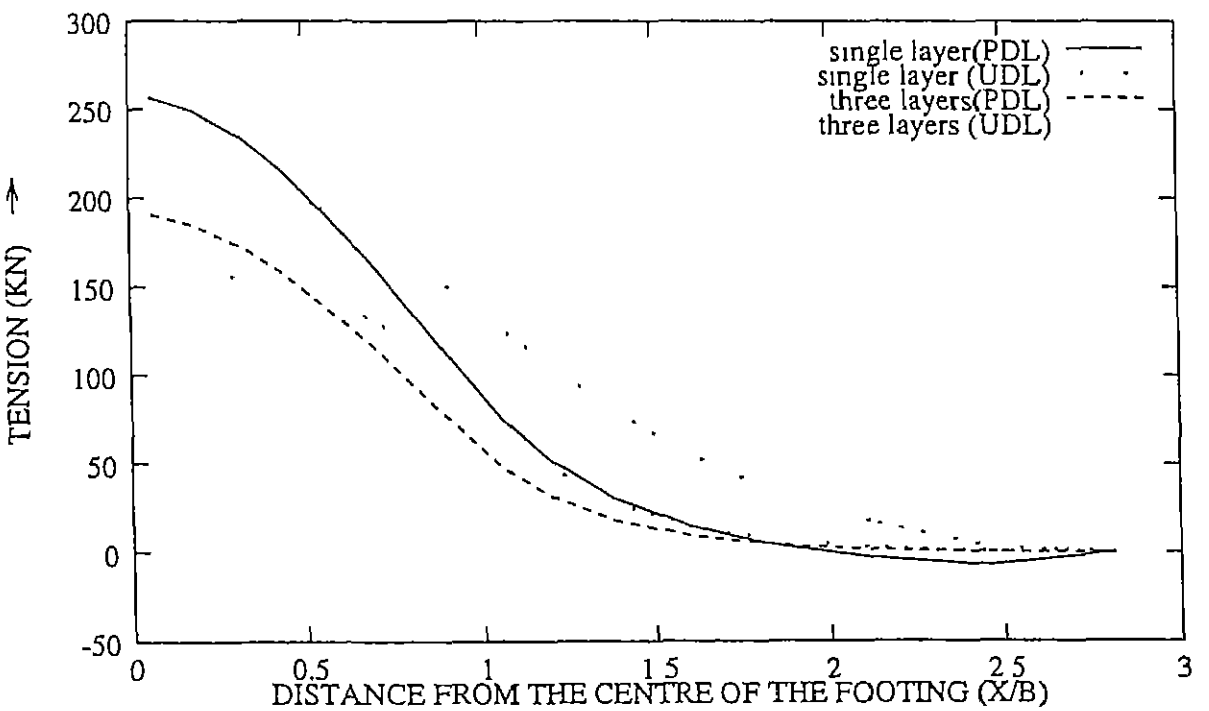

Figure 2 20 Comparison of Tensile force distribution for top layer of geosynthetic UDL and PDL

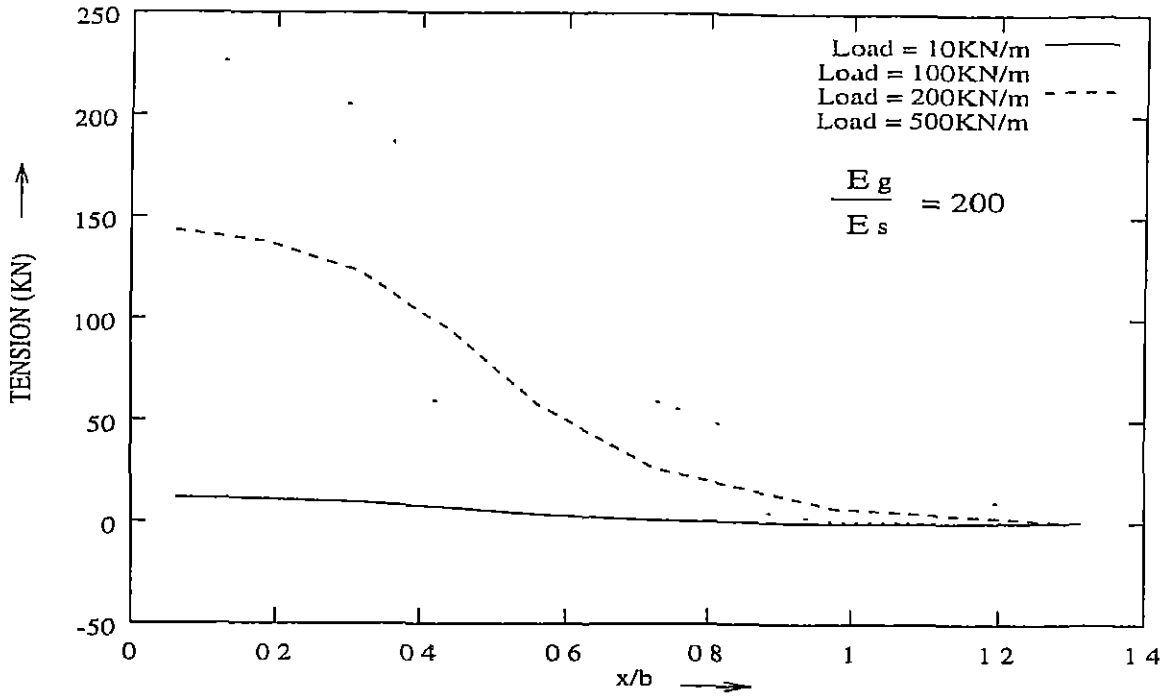

Figure 2 21 Effect of load intensity on Tensile force distribution, $E_g/E_s = 200$

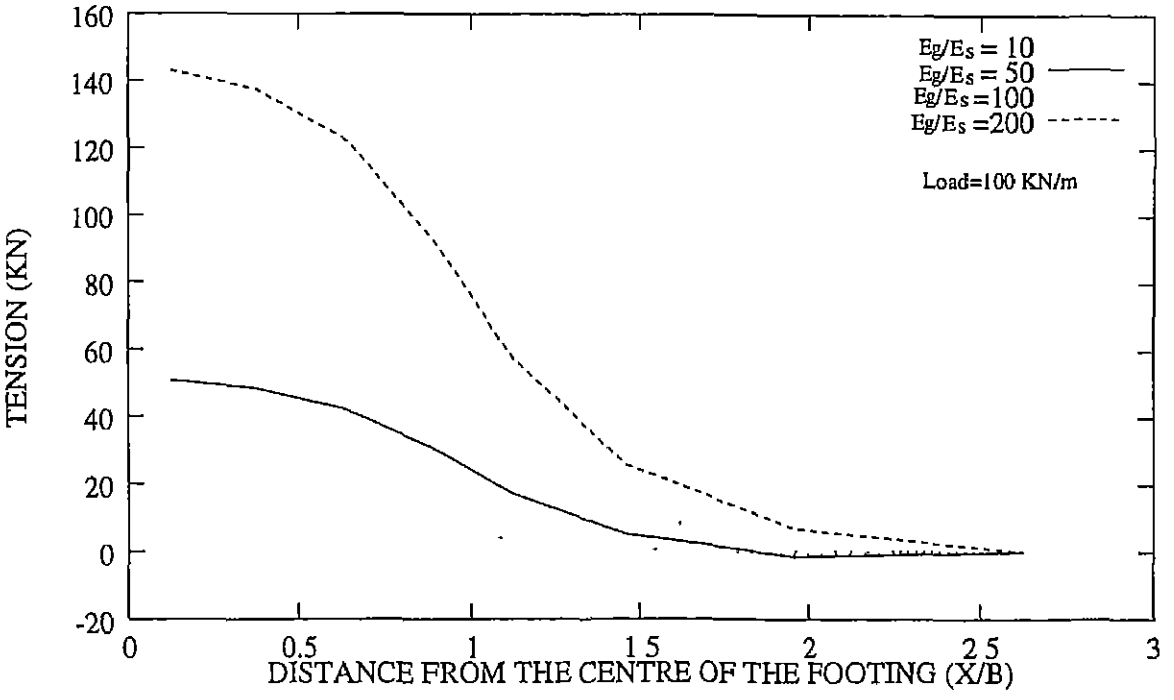

Figure 2.22 Effect of Modular Ratio on Tensile force distribution, UDL=$100KN/m$

Distribution of stresses:

Normal stress:

Plots of distribution of vertical normal stress at different vertical cross-sections are taken at 0 063m, 0.19m, 0 31m, 0 44m, 0 94m, 1.6m, 2.81m and 5 11m from the centre of the footing Figures 2 23 to 2 26 show the distribution of vertical normal stress for all the four cases Expectedly, for sections nearer the centre of the loading, stresses are higher than for those further away from the centre The stresses follow the general trend of Theory of Elasticity solution Stresses tend to decrease sharply for the sections nearer the centre whereas the variation is more gradual for sections further away Similar trends are observed for all the four cases

In Figures 2 27 and 2 28 the stresses for all the cases at each vertical section are compared For shallow depths, the stresses are nearly the same for each case but for depths greater than the reinforcement depth, the three layer case shows more stresses than the two layer, single layer and unreinforced case The percentage increase over the unreinforced case varies in the range of 7-10 for three layer case, 6-8 for two layer case and 2-4 for single layer case For sections at 1.06m and 1.6m which are at distances greater than b from the centre of loading, the three layer case shows the least stresses for shallow depths The percentage reduction being of the order of 3-4 %

The tension developed in the reinforcement due to the interfacial friction induces a horizontal force in the opposite direction in the soil mass which acts as a lateral restraint, producing the effect of confinement. The lateral restraint produces an additional vertical force on the effective area of the inclusion which causes additional normal stress in the reinforced zone. This may be the cause of increased vertical stresses in the top layers as observed from Fig. 2 27 and Fig. 2 28. Perhaps, due

to reduction in the confinement effect away from the centre, sections at 1 06m and beyond show lesser stresses for the reinforced cases

In the available literature, such studies regarding stresses using the confinement effect have not been presented and thus, the values obtained by the present study could not be compared with the other solutions The above observation is contrary to the general expectation that increasing the number of layers of reinforcements causes reduction in the stresses

Raghvendra et al (1996) studied the effect of increased number of reinforcing layers on stresses by considering the reinforcement zone being stiffer for more number of reinforcement layers. They have chosen the stiffness of the reinforced zone as ten times that of the zone below it The results obtained by the present study, after modifying the developed computer program on similar lines, agree qualitatively with those obtained by Raghvendra et al from FEM studies (Fig 2.29 and Fig. 2.30) Due to inadequacy of data available for the problem solved by the authors, only qualitative comparison could be made Since all other results of parametric study are consistent with experimental and theoritical studies in this field, the reason for the apparent anomalous behaviour may lie in the 'confinement effect' Even though care has been taken to get convergent solutions with appropirate mesh sizes, the calculation of stresses may not be that accurate as for that one needs a very fine mesh Effect of finer mesh on the stresses needs to be investigated further.

For the two layer case, a plot of normal stress in the reinforced zone agrees, qualitatively, with the Finite Element studies conducted by Burd and Houlsby (1989). The plot, Fig 2.31 indicates reduction in normal stress across the reinforcement. The stress difference arises due to the curvature of the reinforcement and tends to reduce the magnitude of the normal stress acting on the soil below the geotextile.

Lateral stress:

The benefits obtained from reinforced soil results from the generation of frictional

forces at soil-reinforcement interface These forces are analogous to the increase in confining pressure, thus restricting lateral strains in the soil As a result, Fig 2 34 and Fig. 2 35 indicate higher lateral stresses for the reinforced cases as compared to the unreinforced case For sections beyond the reinforced zone in X direction, the diminishing of confinement leads to higher lateral stresses for the unreinforced case Figures 2 32 and 2 33 show the distribution of lateral stresses, individually, for the unreinforced case and the three layer case. At distances beyond the edge of the footing ($X = 1\ 6m, 2\ 81m, etc$), where the tensile forces reduce, the reduction in confinement effect causes a corresponding reduction in lateral stresses for the reinforced cases As a result, at these sections, the lateral stresses are less for the reinforced cases as compared to the unreinforced case

Shear Stress:

The lateral streses in the fill generate shear stresses. If the reinforcement is absent, these shear stresses are sustained directly by the soil and so have a detrimental effect on the bearing capacity In the reinforced case, the shear stresses are assumed to be sustained wholly by the geosynthetic Thus, the presence of the reinforcement causes a reduction in the outward acting shear stresses leading to better performance of the fill under the superimposed load. Plots of shear stress for the four cases are shown in Figures 2 36 to 2 39 The comparison, as in previous cases, is shown in Fig. 2 40 and Fig 2.41. The plots highlight the effectiveness of increasing the number of reinforcing layers in reducing the shear stresses. The fact that the shesr stresses are sustained wholly by the reinforcement is brought out by observing the abrupt reduction in shear stresses in the reinforced zone for all the three cases

Shear stresses acting on the reinforced zone are plotted for the two layer case. The resulte agree qualitatively with the findings of Burd and Brocklehurst (1990). They have showed (Fig 2 42) that the shear stresses reached a peak at about 0 7b from the centre of the loading The present study shows (Fig 2 43) that the shear

stresses reached a peak at a distance of about 0 5b, the edge of the loaded area, from the centre of the footing

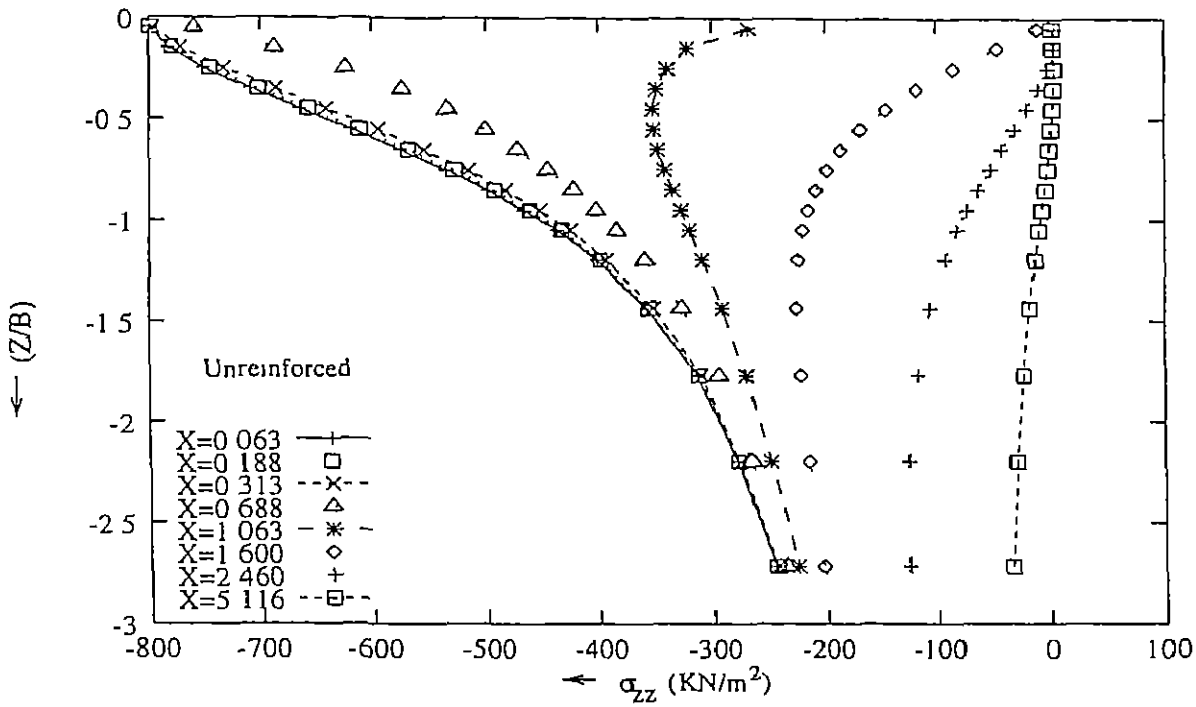

Figure 2 23 Vertical Distribution of Normal Stresses Unreinforced case

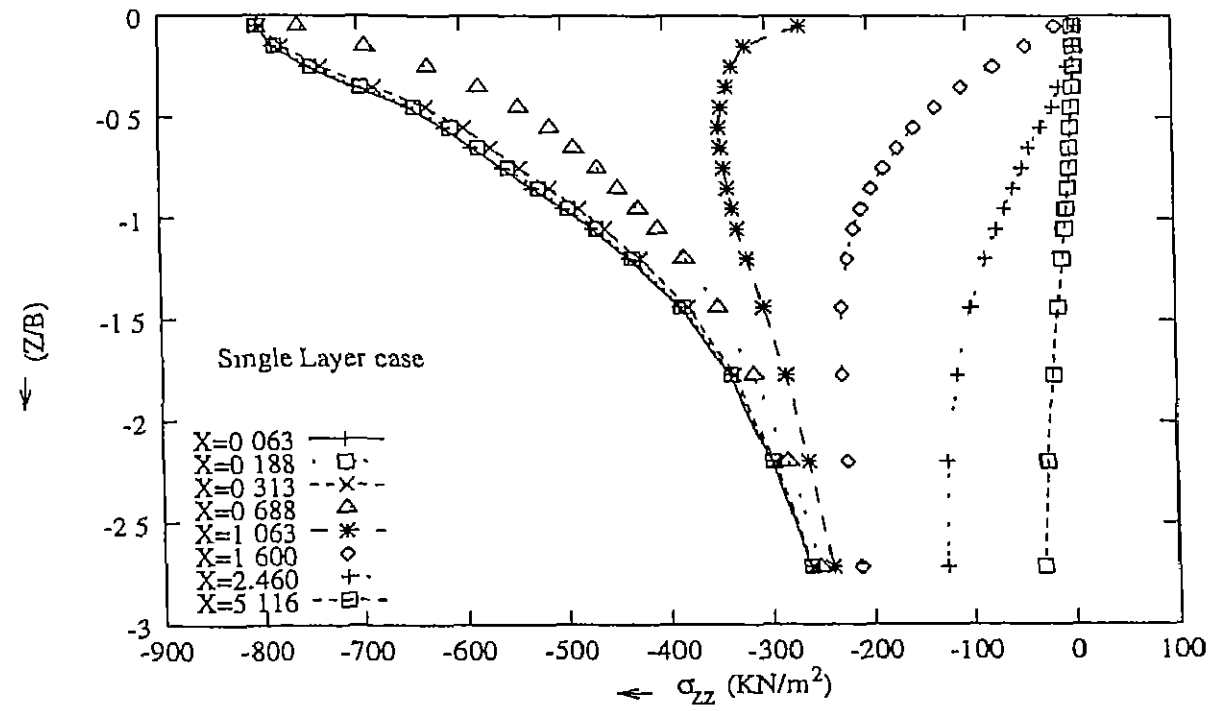

Figure 2.24 Vertical Distribution of Normal Stresses· single layer case

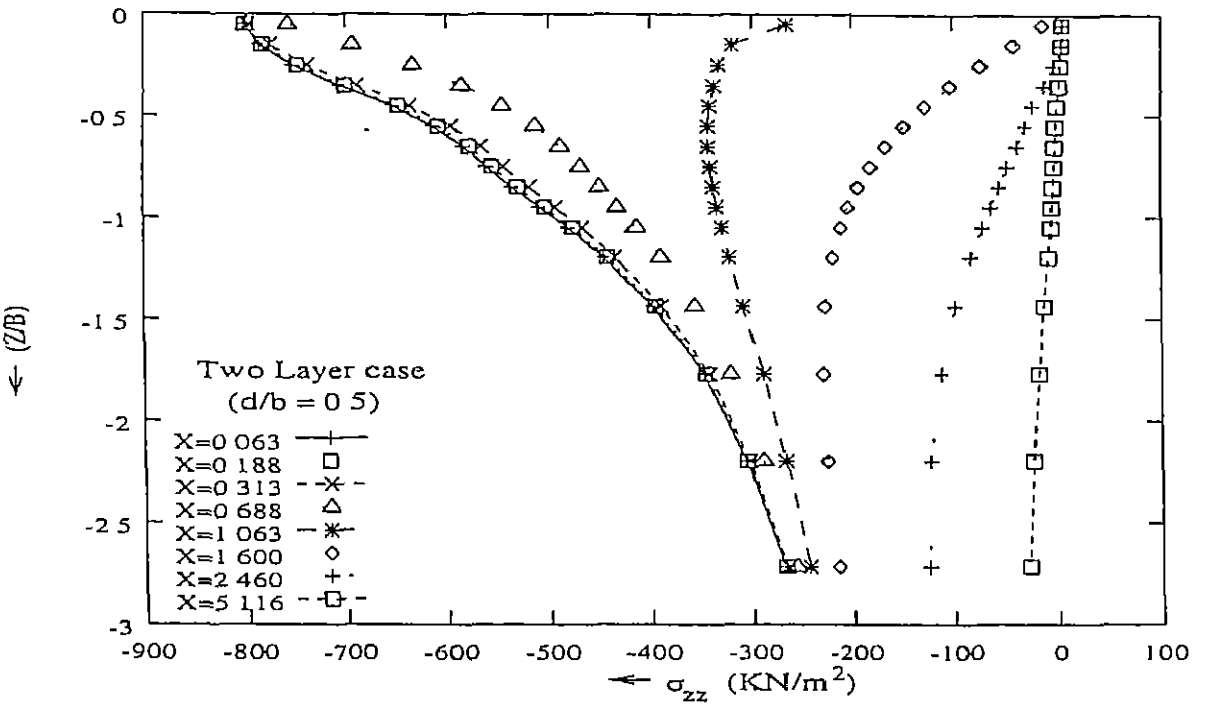

Figure 2 25. Vertical Distribution of Normal Stresses. two layer case

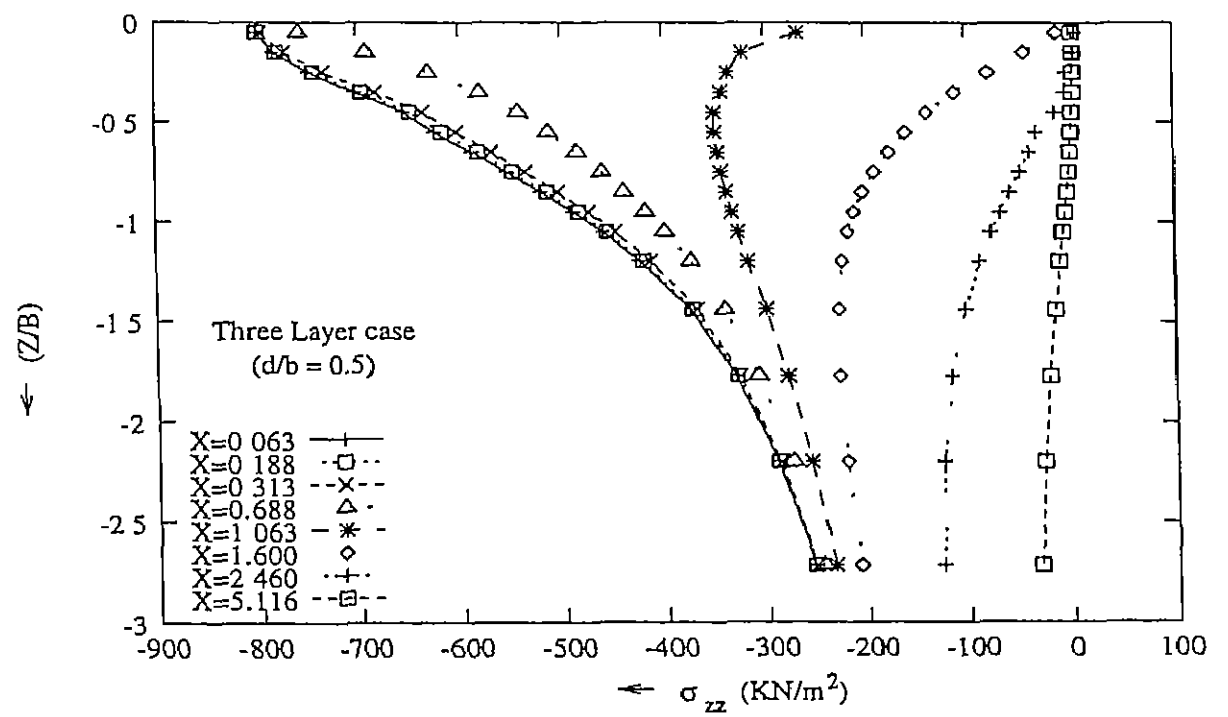

Figure 2.26. Vertical Distribution of Normal Stresses· three layer case

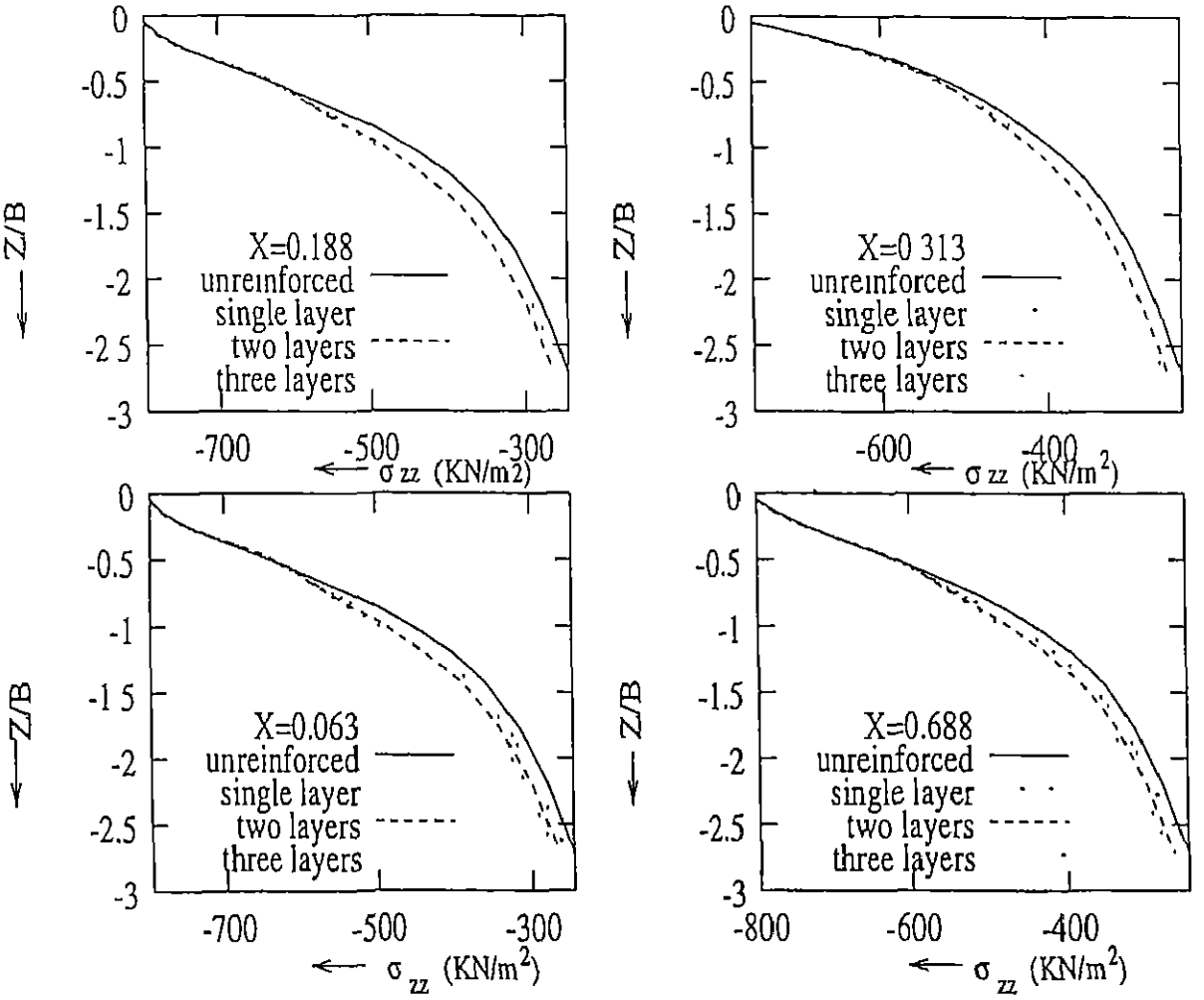

Figure 2 27. Vertical Distribution of Normal Stresses Comparison

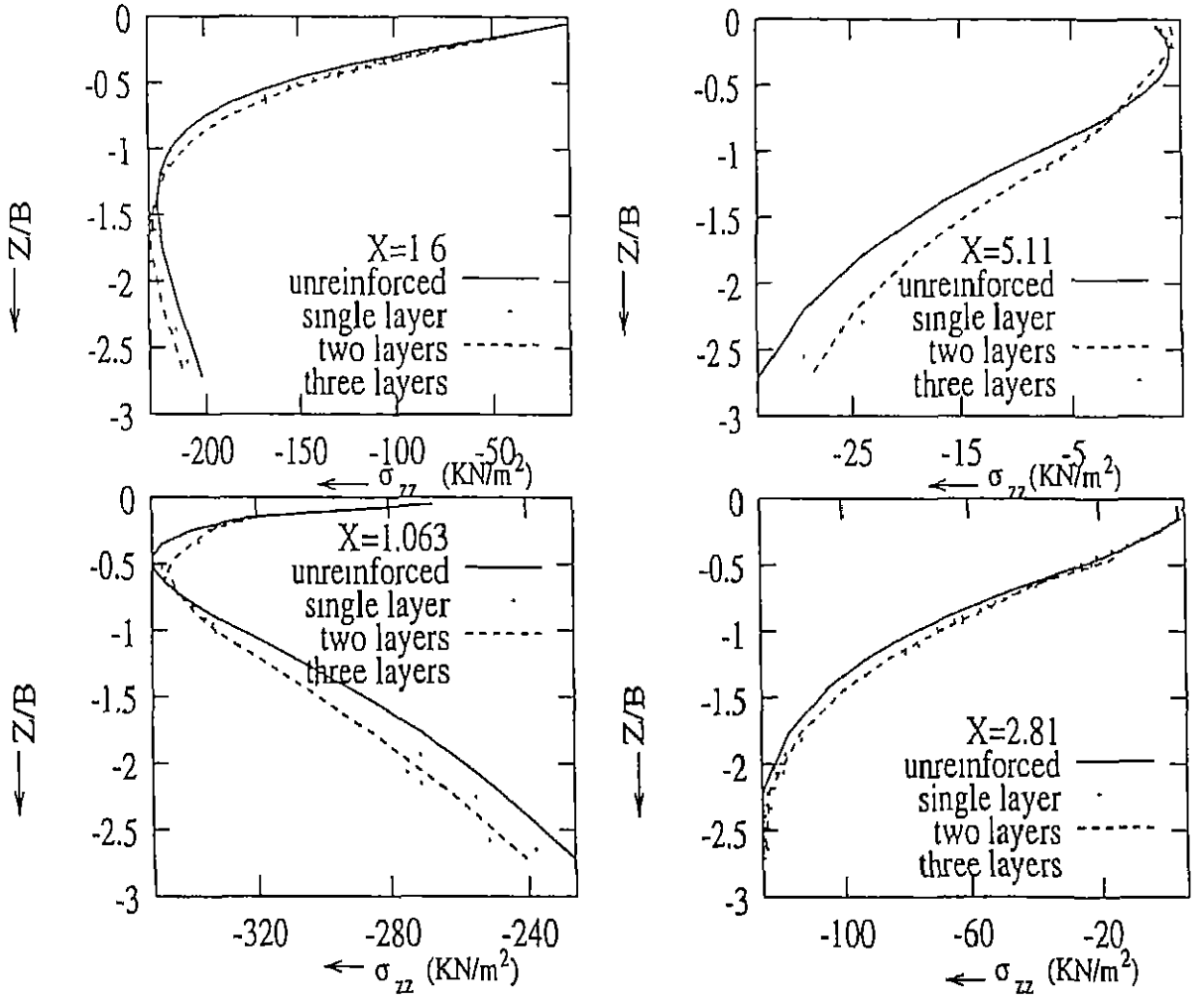

Figure 2 28· Vertical Distribution of Normal Stresses· Cmparison

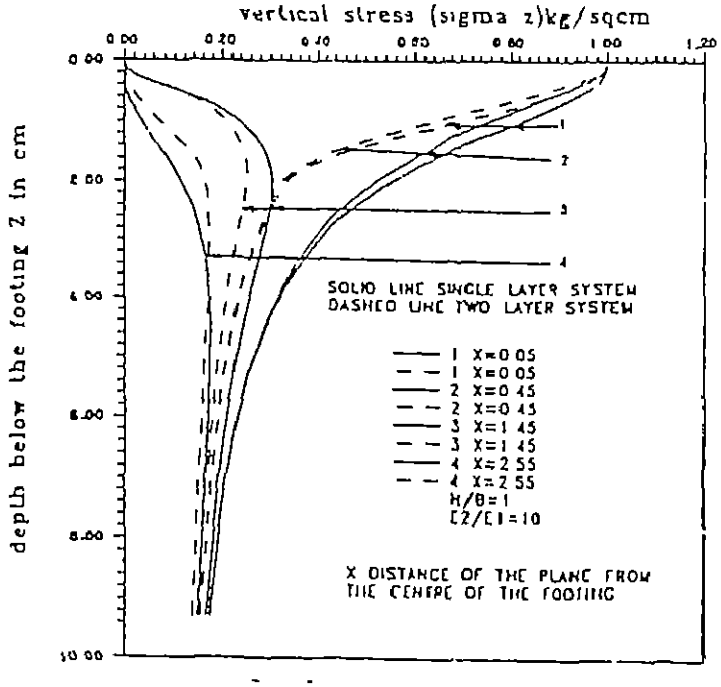

Figure 2.29: Vertical Distribution of Normal Stresses (Raghvendra et al(1996)

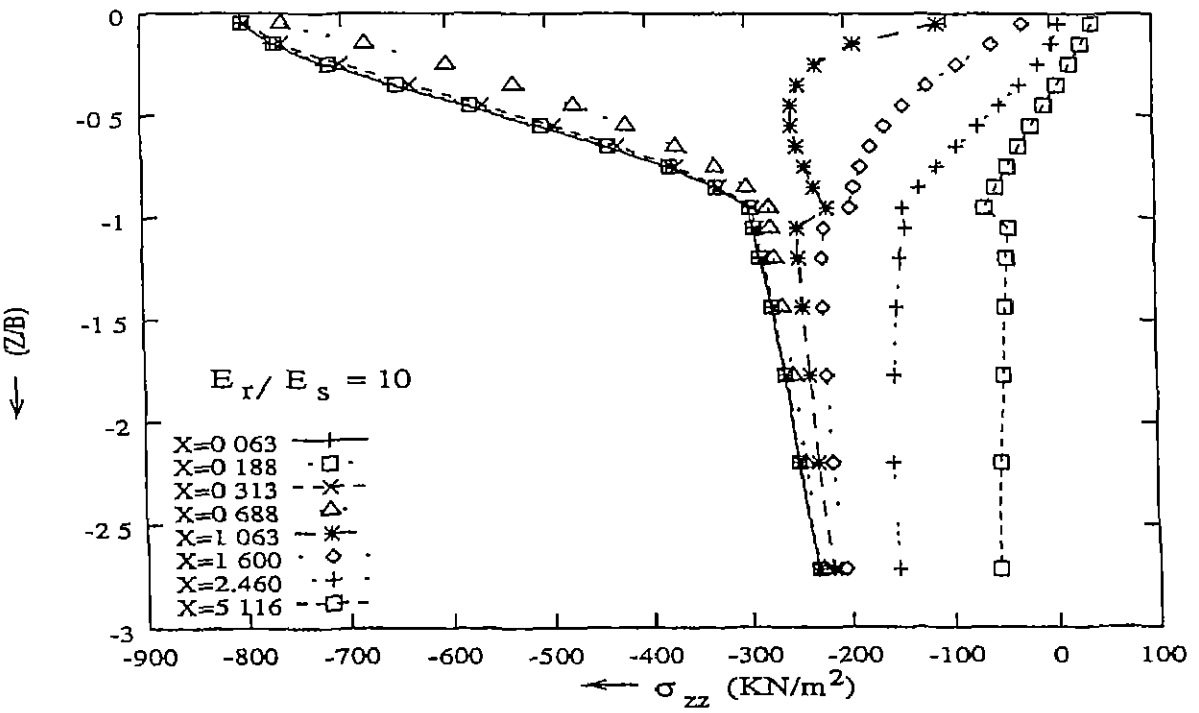

Figure 2.30: Vertical Distribution of Normal Stresses (Validation problem, $E_r/E_s = 10$)

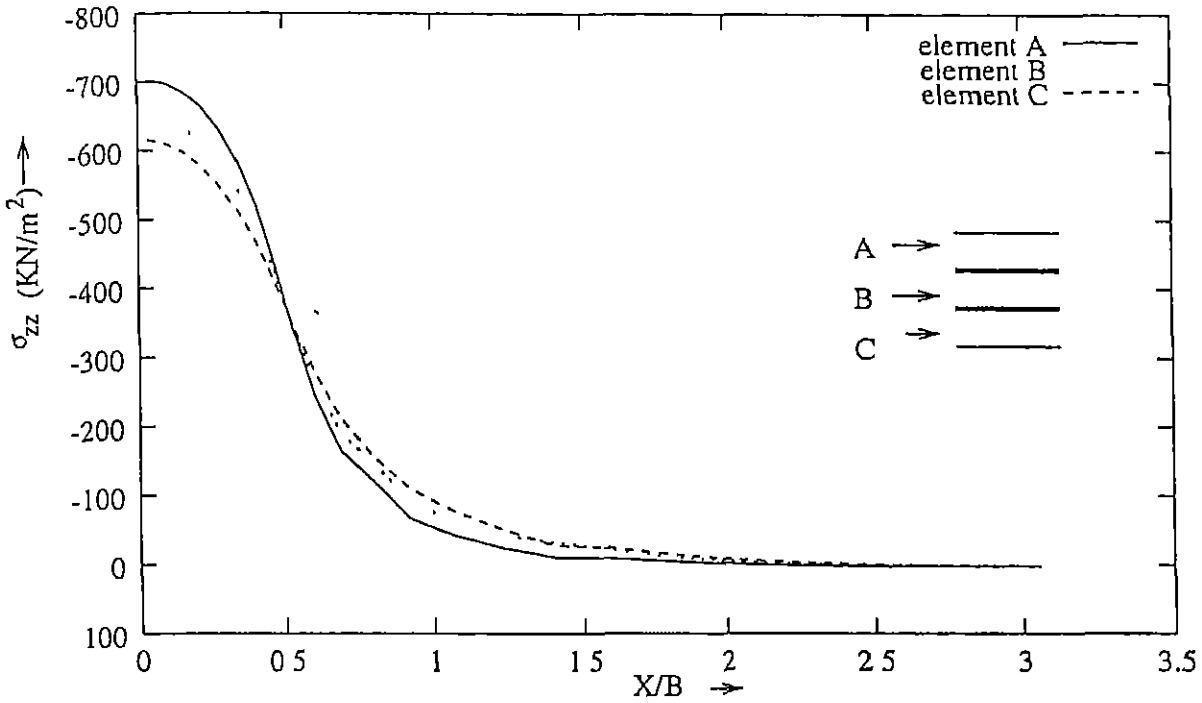

Figure 2 31 Distribution of Normal Stresses in reinforced zone . Two layer case

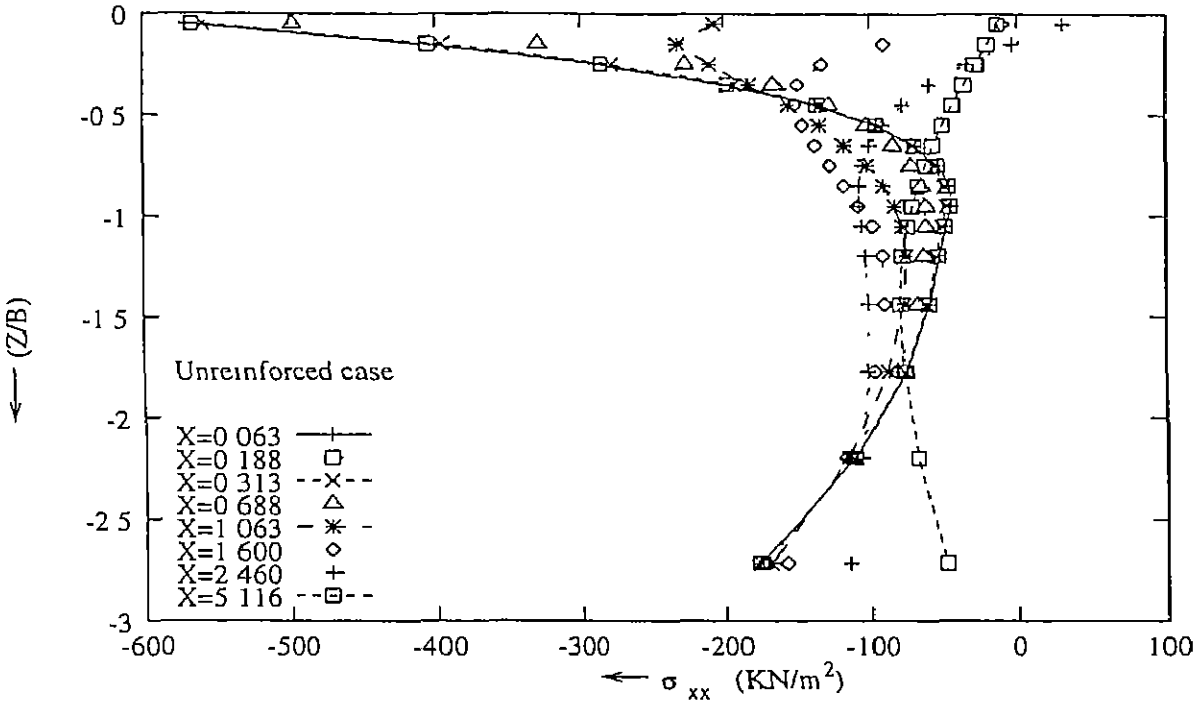

Figure 2 32 Vertical Distribution of Lateral Stresses Unreinforced case

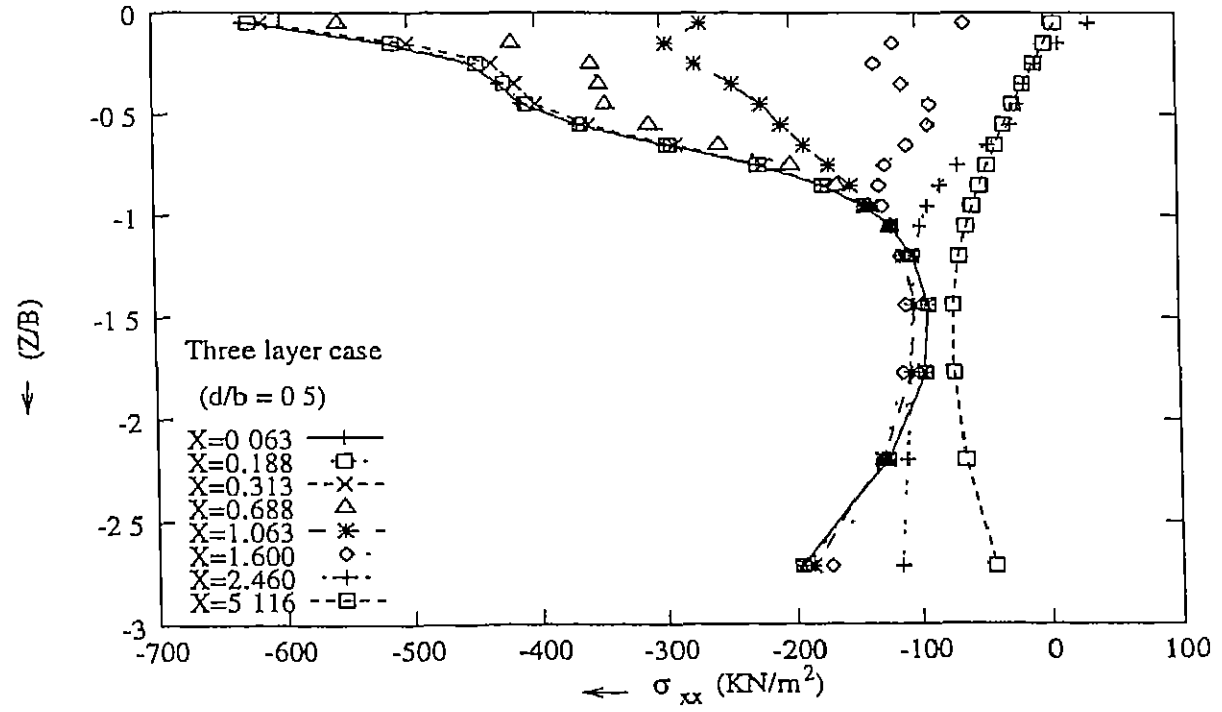

Figure 2 33 Vertical Distribution of Lateral Stresses. Three layer case

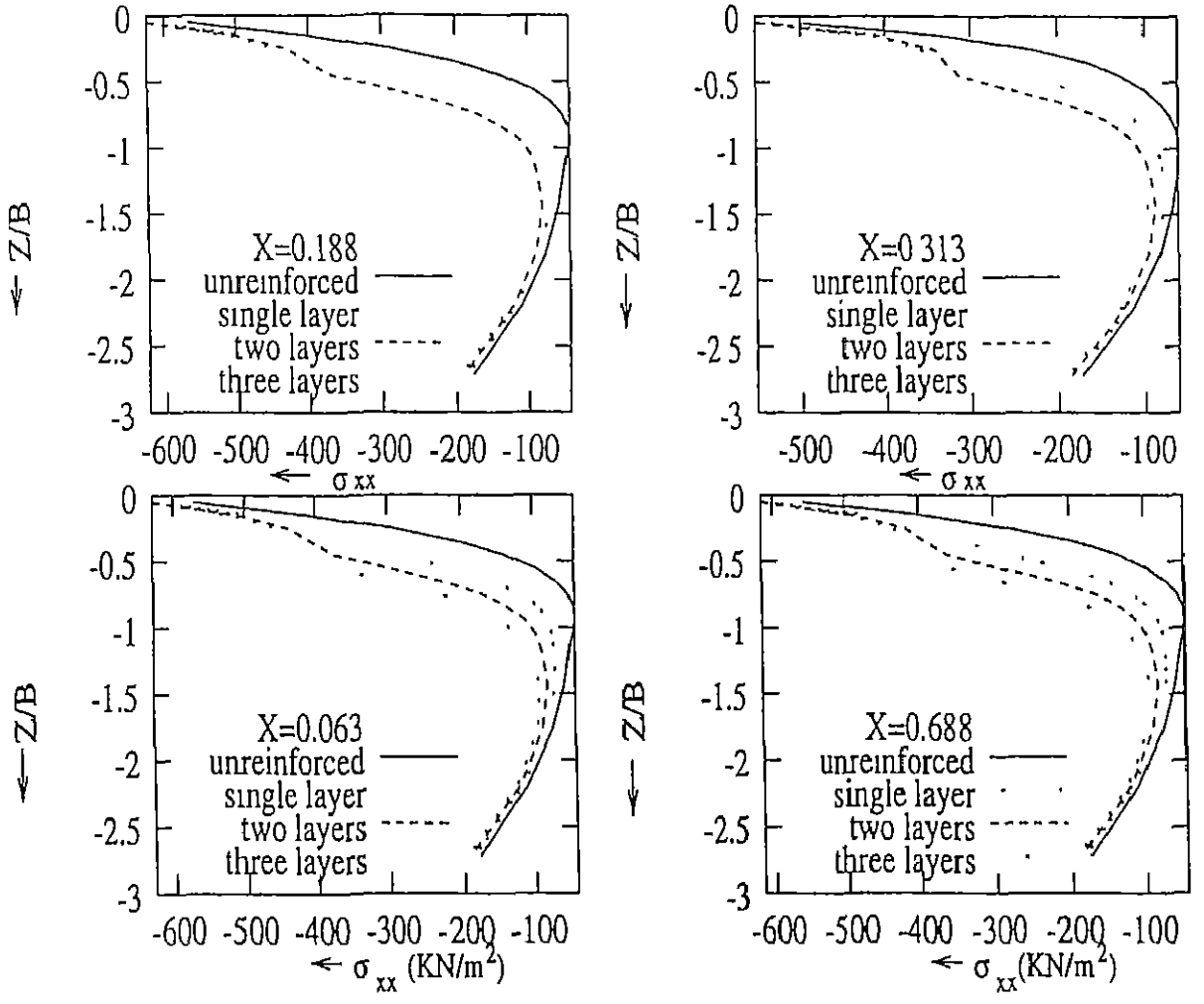

Figure 2 34. Vertical Distribution of Lateral Stresses Comparison

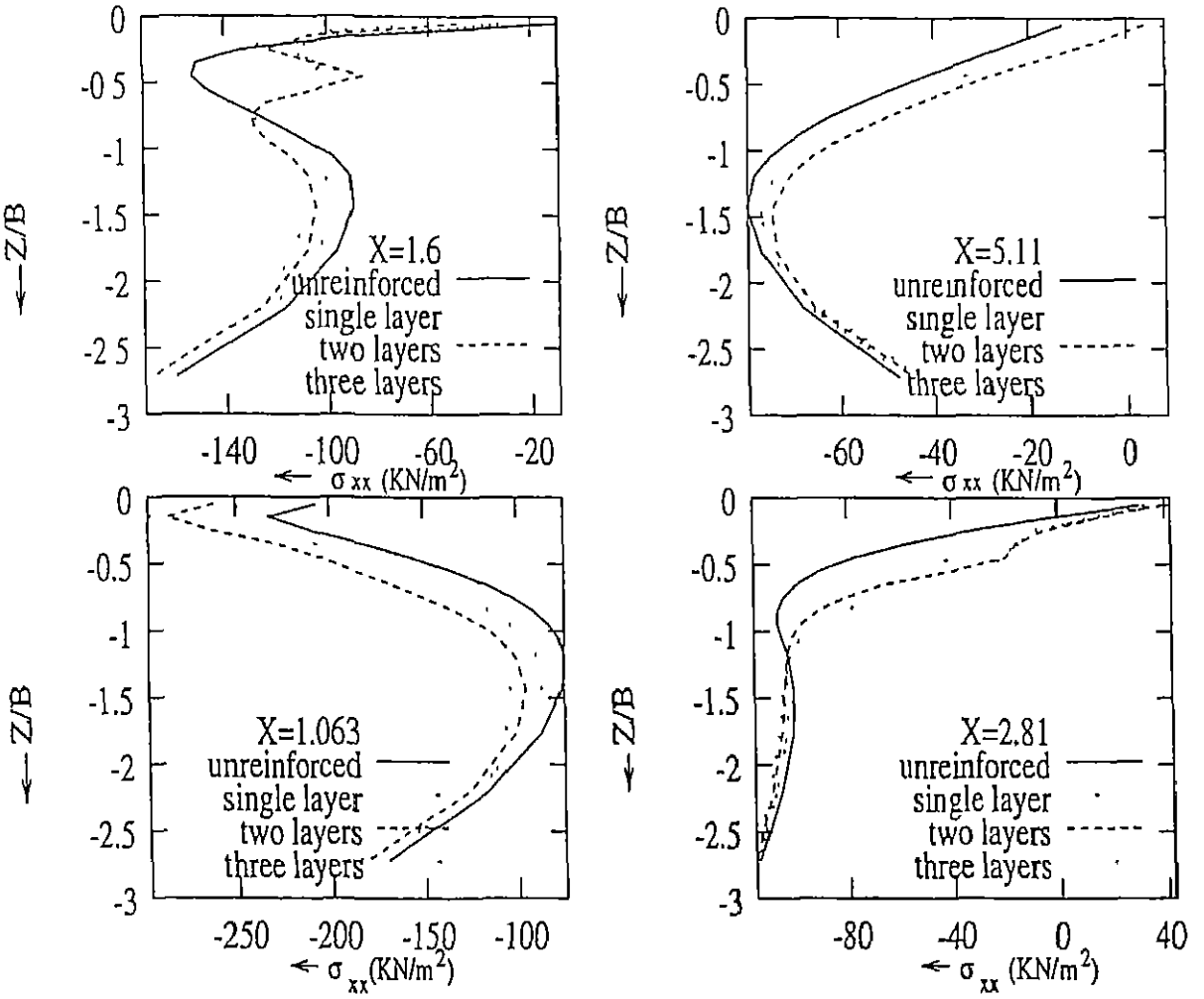

Figure 2 35 Vertical Distribution of Lateral Stresses· Comparison

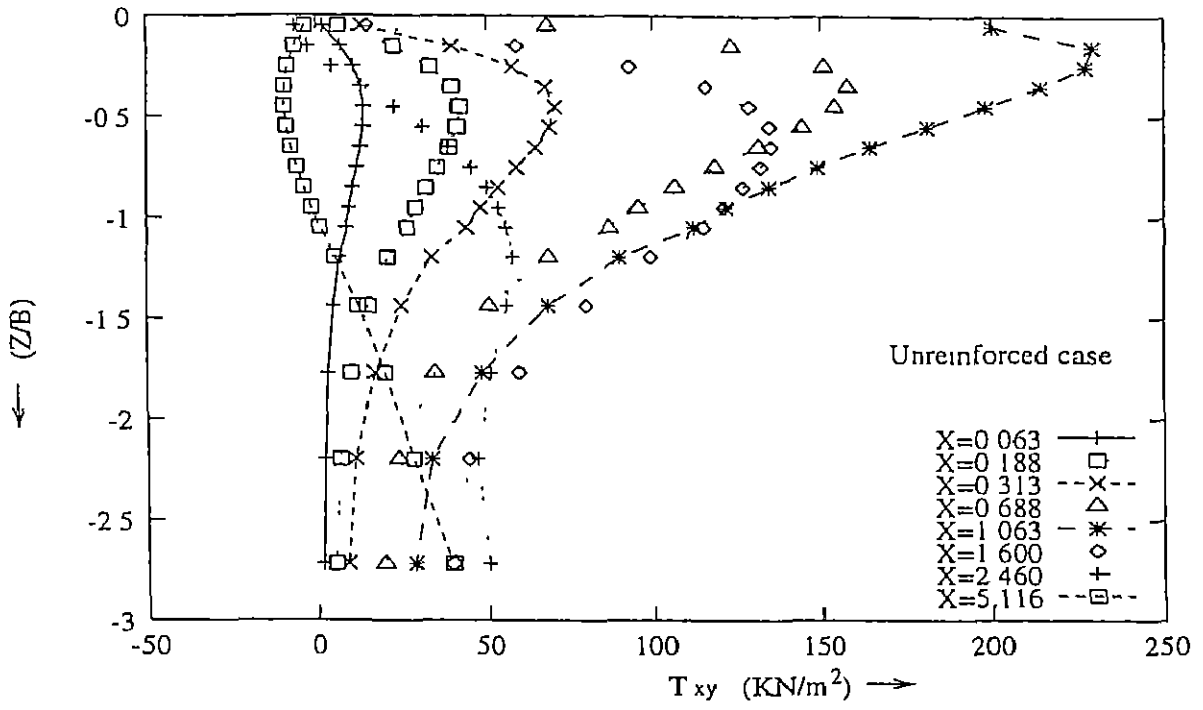

Figure 2 36 Vertical Distribution of Shear Stresses Unreinforced case

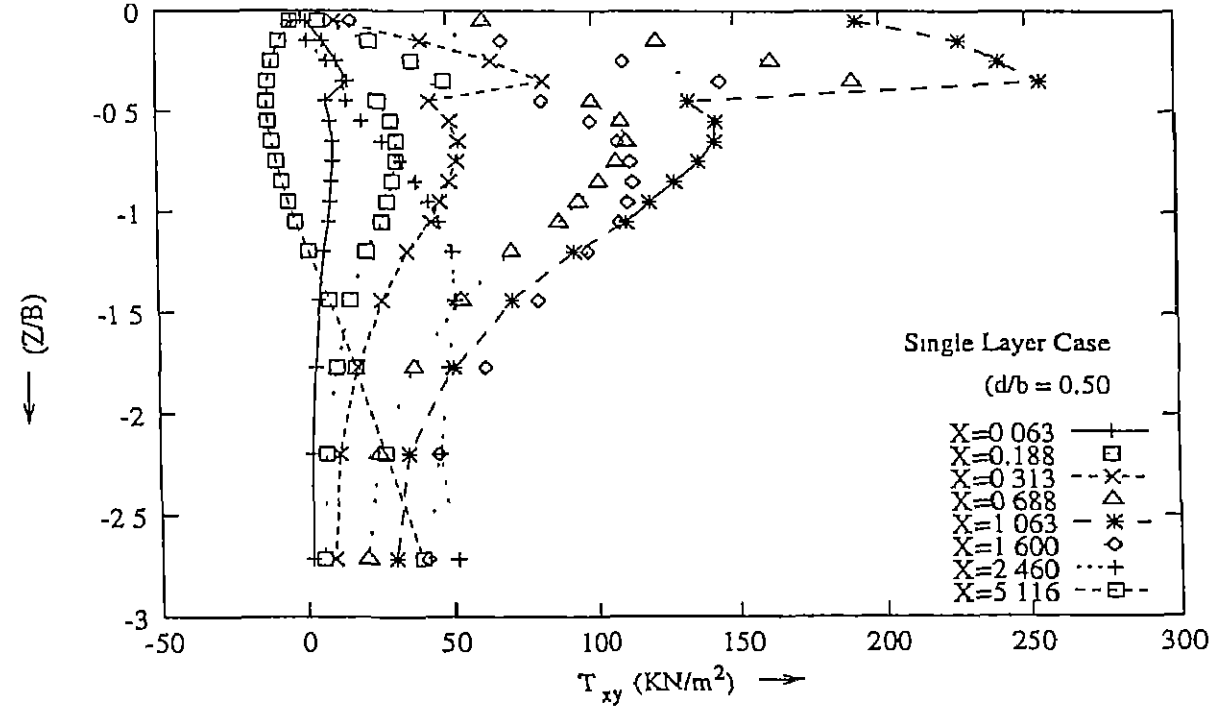

Figure 2 37· Vertical Distribution of Shear Stresses. Single Layer case

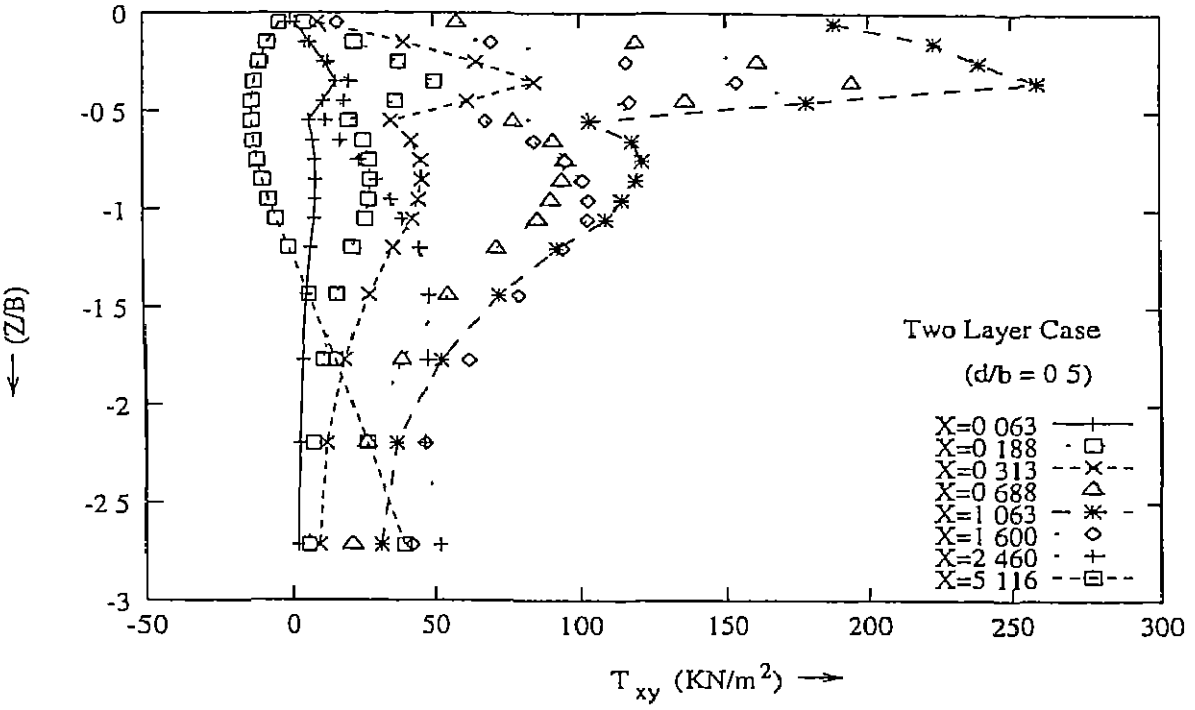

Figure 2 38 Vertical Distribution of Shear Stresses Two layer case

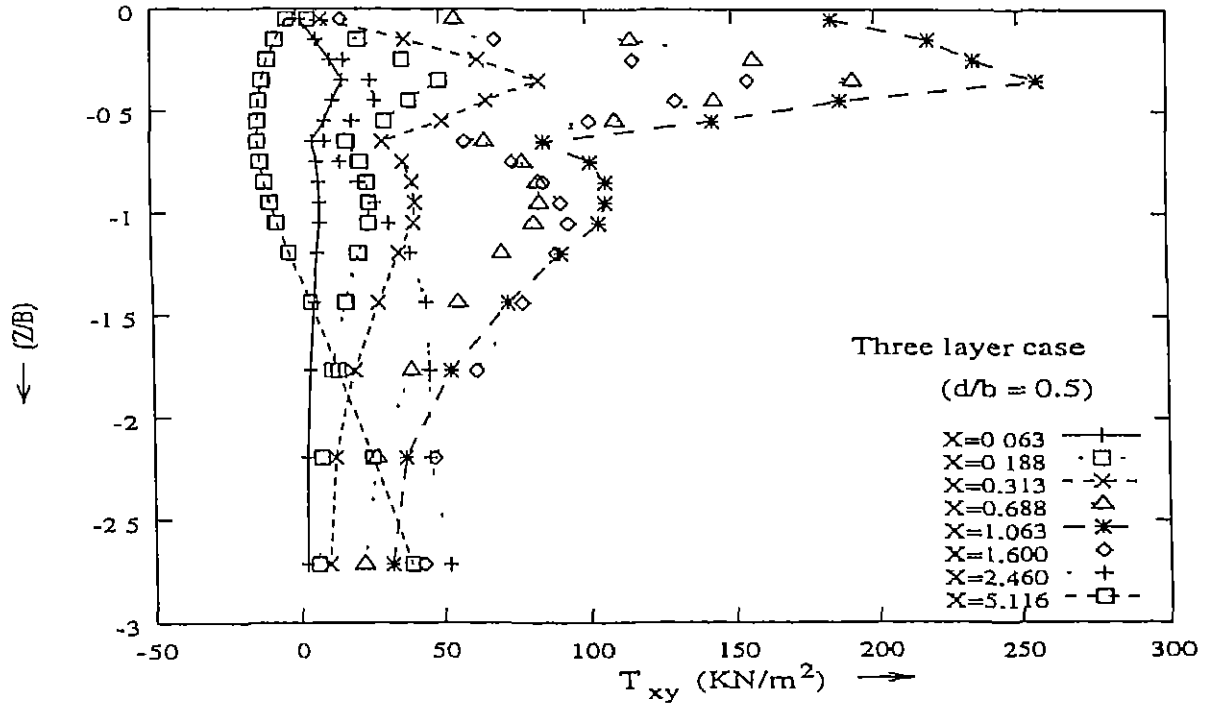

Figure 2 39 Vertical Distribution of Shear Stresses Three layer case

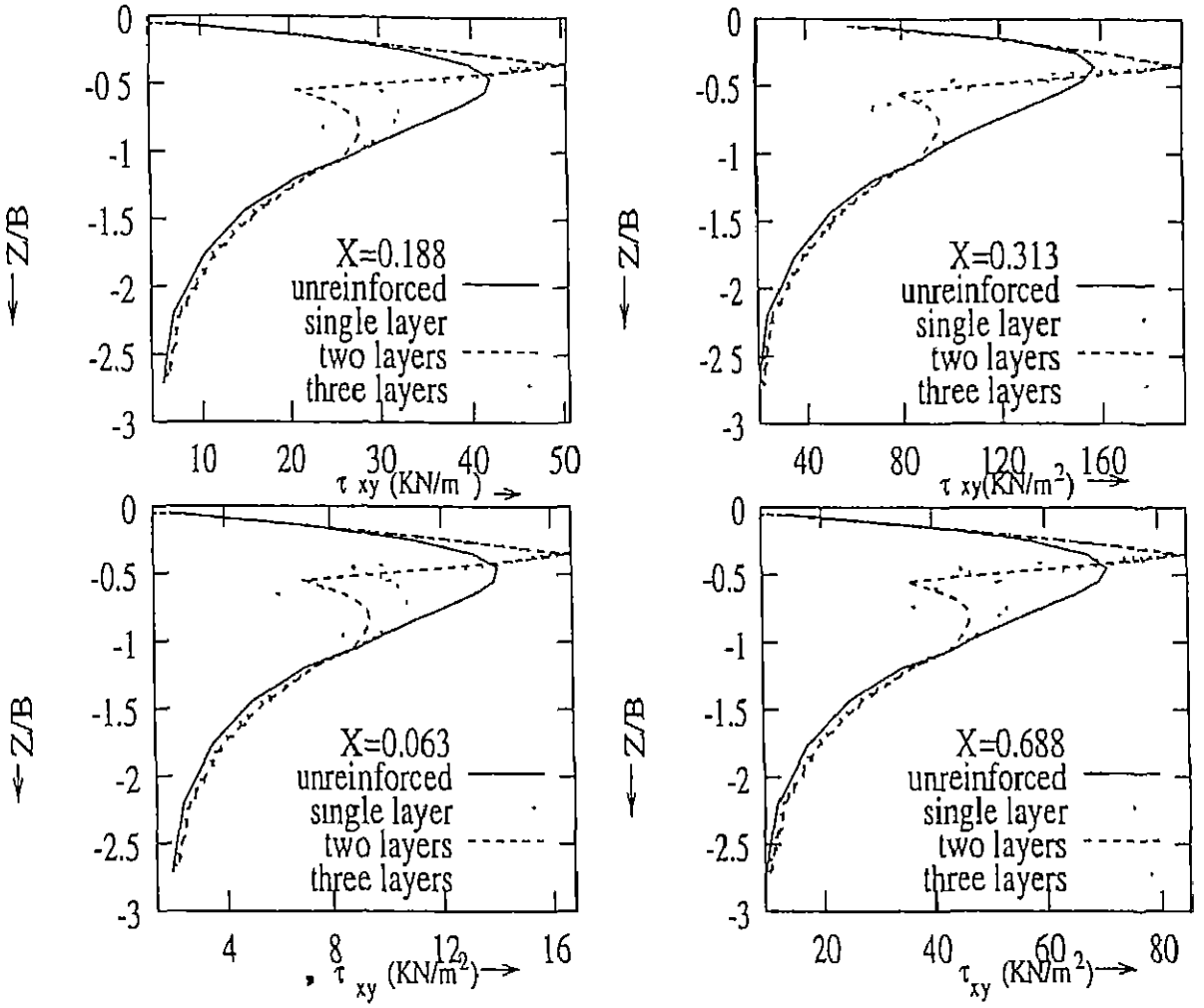

Figure 2 40 Vertical Distribution of Shear Stresses Comparison

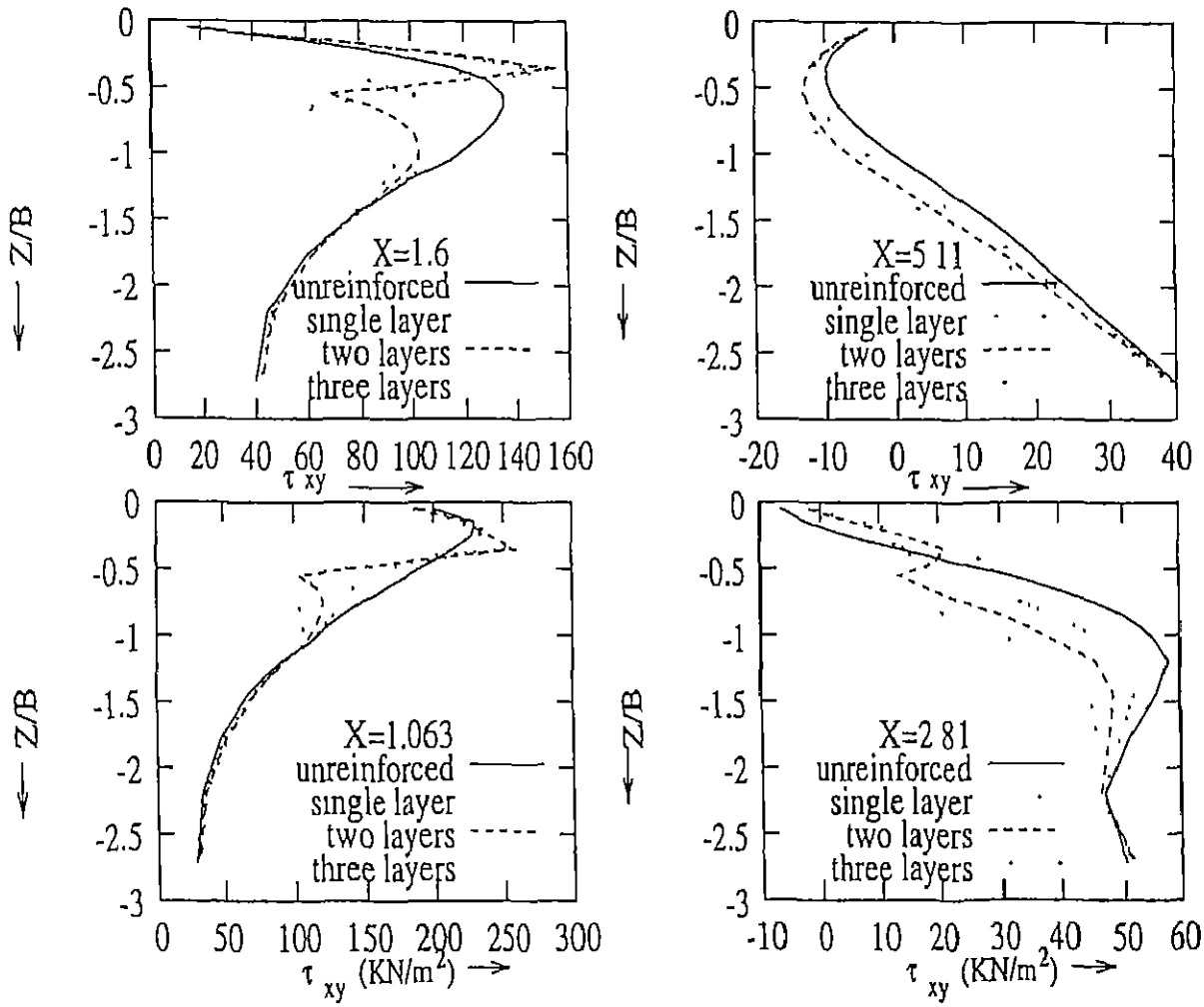

Figure 2 41 Vertical Distribution of Shear Stresses· Comparison

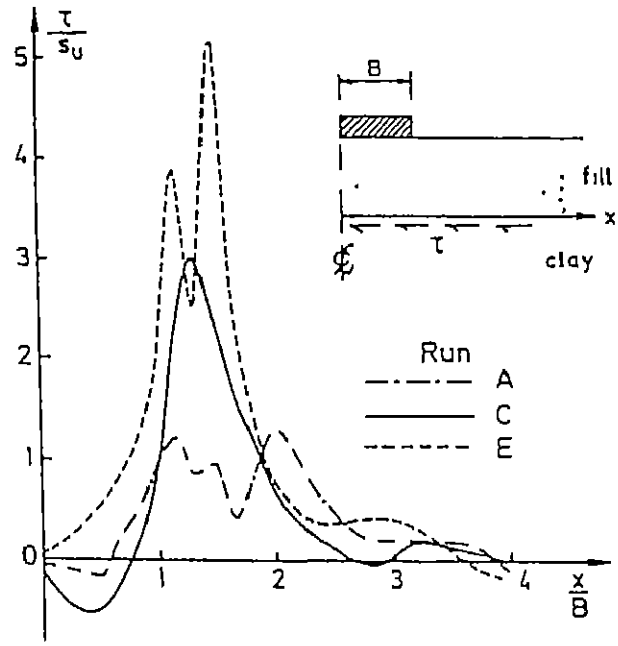

Figure 2 42· Distribution of Shear Stresses in the reinforced zone Burd et al (1990)

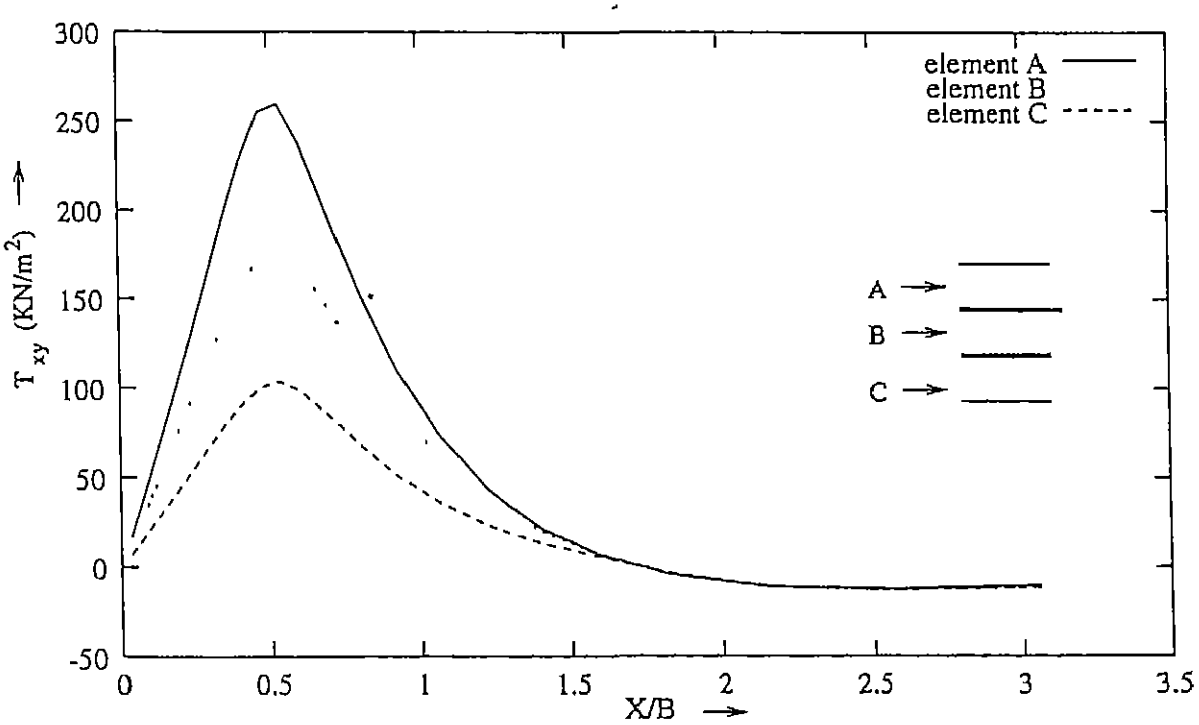

Figure 2.43: Distribution of Shear Stresses in the reinforced zone

2.2.3 Conclusions

The general conclusions that can be drawn from the present study are presented as follows

- The computer program originally developed for a single layer of reinforcement, when extended to multiple layers of reinforcements, functioned well and the predicted results are found to be compatible with experimental and theoretical studies
- Increase in the number of layers of reinforcements causes reduction in settlements, the reduction being of the order of $15 - 16\%$ for a three layer case as compared to unreinforced case
- The optimum placement depth for uniformly distributed strip loading is $0.5b$ for all the cases of reinforcements For Parabolic distribution of loading, the optimum placement depth is $0.5b$ for a single layer case and $0.4b$ for two and three layer case
- The optimum spacing of the reinforcements is $0.4b$ for both two and three layer case
- Settlement reduction for all cases is most effective when soil is in undrained state
- As Modular ratio, E_g/E_s increases, settlements reduce at an increasing rate, but for $E_g/E_s \geq 400$, the decrease is at an almost constant rate The trend is similar for one, two and three layers of reinforcements
- Tensile forces in the top layer of the reinforcement decrease with increase in the number of reinforcement layers Increase in the strip load on the footing causes greater mobilization of the tensile forces in the reinforcement

- Shear stresses are reduced sharply in the reinforced zone, the reduction being greatest for the three layer case
- Due to confinement effect, lateral stresses show an increase with increase in the number of layers of the reinforcement

Chapter 3

Optimal Cost Analysis of Reinforced Earth Walls

3.1 Introduction

The use of Reinforced earth walls for a variety of purposes was highlighted in Chapter 1. Their importance is well recognized. The use of geogrids or geotextiles rather than metallic strips (ties) is a further development of the Reinforced earth concept. Geosynthetics offer a viable and often very economical alternative to metallic reinforcements for both permanent and temporary walls, especially under certain environmental conditions The Chapter deals with an optimum cost design of Geosynthetic reinforced earth walls.

3.1.1 Brief description of the wall

A sketch of the wall is shown in Fig. 3.1. The main item is the soil backfill which is placed as the wall is constructed. For the problem considered herein, the backfill is limited to cohesionless, free draining material, i.e. sand , having the following properties : density γ and angle of internal friction ϕ. The backfill is strengthened by reinforcing members, which in the present case are geogrids and geotextiles. Since

system for long-term applications. The facings, additionally, enhance the aesthetic appeal of the completed wall For geogrid wall, Modular Concrete units (MCU) are the most common facing used They are popular because of their aesthetic appeal, easy availability and relatively low cost Geotextiles are more commonly used in wrap-around-faced MSE walls Such facings are used for temporary structures, for walls that are subject to significant post-construction settlements and where aesthetic requirements are low

3.1.2 Design approaches

A number of approaches have been developed for the design of geosynthetic soil walls. Among them, the Limit Equilibrium method and the Working Stress design method are more common The Working Stress method basically rely upon restrictive assumptions with regard to the state of stress in the soil. The Limit Equilibrium method essentially use conventional slope stability analysis, modified to account for the reinforcement effect, for the global stability of the reinforced soil mass For retaining walls, all the methods normally considered applicable to routine design, use limiting equilibrium analysis to determine factors of safety against failure, however, they vary in their assumptions regarding stress distribution, failure surfaces, safety factors and the inclination of the reinforcement at the failure surface The various design methods used in practice are Forest Service method (1977), Broms method(1978), Collin method(1986), Bonoparte et al. method(1987), Leshchinsky and Perry method(1987), Schmertmann et al method(1990) These methods typically presume a planar failure surface through the reinforced mass described by the classical Rankine active failure condition. The reinforcements extend beyond the assumed failure surface and are considered to be tension resistant tiebacks for the assumed failure wedge. As a result, these methods are collectively referred to as tied-back wedge analysis methods

For calculating maximum stress developed in the ties or reinforcements, three approaches are possible These are designated as Rankine method, Coulomb Force method and Coulomb Moment method. The Rankine method considers the equilibrium of a single representative critical element of soil at any depth, whereas the Coulomb methods consider the overall stability of the entire wall. All these methods predict maximum tension in the lowermost layer of the reinforcement But, the Rankine method necessitates a minimum embedment depth beyond the failure plane for all ties or geosynthetics, while the Coulomb method does not require that all the ties should extend behind the failure plane Hence, the Coulomb method computes the shortest length of the reinforcement , whereas the Rankine method leads to the longest tie. Thus, the Rankine method is more conservative

The earliest method to determine the lateral earth pressure on a retaining structure subjected to dynamic loading was developed by Mononobe(1929) and Okabe(1926). The approach is basically a pseudo-static approach in which the Coulomb's Earth Pressure equation was modified to account for the additional vertical and horizontal forces induced during an earthquake. The M-O method was developed for a dry, cohesionless backfill.

Factor of safety is defined as the ratio of the forces or moments resisting instability to the forces or moments tending to cause instability. Full mobilization of the soil strength is assumed to occur. This approach is unlike the one used for evaluating slope stability wherein the factor of safety is used to reduce strength parameters.

Most methods available for designing reinforced soil walls utilize the same general input parameters . First, the wall geometry must be defined in terms of height and face inclination. Most methods allow for a surcharge behind the top of the wall face. Secondly, the strength properties of the reinforced soil mass must be described The parameters used typically consist of soil unit weight and internal angle of friction, reinforcement strength and parameters describing the frictional interaction between

the soil and the reinforcement

Review of the literature revealed that eventhough lot of studies have been undertaken to develop methodologies for the analysis of reinforced earth walls, no work has been undertaken to develop methods for their optimum design Such an attempt has been made here

3.1.3 Statement of the Problem

Fig 3 2 shows the cross-section of a reinforced earth retaining wall. Given the wall geometry, the soil properties and the reinforcement properties, the problem is to define the length and strength of the reinforcement that gives the least cost estimate for construction.

3.2 Analysis

Optimal cost design of retaining walls when reinforced with either geogrids or geotextiles is carried out Standard design procedures developed by Federal Highway Authority (FHWA) have been adopted This particular analysis procedure is based on the Rankine Approach The same is cast in the frame of optimal design procedure in the following sections.

3.2.1 Assumptions

- Wall should be perfectly flexible and frictionless
- When walls are inclined, it should not interfere in the formation of the outer rupture plane and the soil should not slide on the wall
- As per Rankine's theory, the lateral pressure against the wall increases linearly with depth.

- The failure wedge slopes at an angle ($\theta = 45 + \phi/2$) to the horizontal.

3.2.2 Design guidelines

Input parameters

The input parameters for the optimal design procedure are presented in Table 3.1. Due to the lack of available manufacturer's data, the values of the allowable tensile strength of the geosynthetic are interpolated

Design variables

The design vectors chosen for the formulation are related to the reinforcement They are $\vec{D}(1) = l$=Length of the Reinforcement $\vec{D}(2) = T_a$=Long-term allowable strength of the reinforcement.

Design Steps

The Active Earth Pressure coefficients for both internal and external stability were computed using the Rankine Earth Pressure Theory. For backfill at an angle β, the coefficient of active earth pressure for external stability is defined as,

$$K_{a_e} = \cos\beta \times \frac{\cos\beta - \sqrt{\cos^2\beta - \cos^2\phi_b}}{\cos\beta + \sqrt{\cos^2\beta - \cos^2\phi_b}} \tag{3.1}$$

The coefficient of active earth pressure for internal stability is defined as,

$$K_{a_i} = \cos\beta \times \frac{\cos\beta - \sqrt{\cos^2\beta - \cos^2\phi_f}}{\cos\beta + \sqrt{\cos^2\beta - \cos^2\phi_f}} \tag{3.2}$$

The minimum recommended wall embedment depth is 0.45m Therefore, the design height of the wall is incremented by the addition of the minimum embedment depth of the wall.

Table 3 1 Input Parameters for Design of MSE wall

Parameter	Symbol	Value
Height of Wall	h	$3-10m$
Minimum Embedment depth of wall	$h_{d_{min}}$	$0\ 45m$
Angle of Internal friction of the fill	ϕ_f	35^o
Unit wt of the fill	γ_f	$20KN/m^3$
Backfill inclination	β	0.0
Angle of Internal Friction of the backfill	ϕ_b	30^o
Unit wt. of the backfill	γ_b	$18KN/m^3$
Allowable Tensile Strength of the Geosynthetic	T_a	$30-60KN/m$
Minimum spacing between the reinforcements	s_{min}	$0.2m$
Minimum Embedment length of the reinforcement	$l_{e_{min}}$	$1.0m$
Design Factors of Safety:		
Overturning	FS_{ov_d}	2.0
Sliding	FS_{sl_d}	1.5
Bearing Capacity	FS_{bc_d}	2.0
Reinforcement Strength	FS_{st_d}	1.5
Reinforcement Pullout	FS_{pl_d}	2.0
Cost Factors:		
Levelling pad	c_1	$\$10/m^2$
Wall Fill	c_2	$\$3/1000Kg$
Cost of Geotextile	$c_{3_{gx}}$	$\$(T_a(0.03)+2.6)/m^2$
Cost of Geogrid	$c_{3_{gd}}$	$\$(T_a(0.04)+2\ 0)/m^2$
Cost of MCU face units	c_4	$\$60/m^2$
Engineering and Testing Cost:		
Geotextile wall	$c_{5_{gx}}$	$\$30/m^2$
Geogrid Wall	$c_{5_{gd}}$	$\$10/m^2$
Installation Cost	c_6	$\$50/m^2$

$$h_d = h + 0.45 \tag{3 3}$$

Since the wall is to be constructed with constant total length of the geosynthetic, according to Rankine's theory, the most critical condition for pull-out occurs at the top where the embedment length, l_e, beyond the failure plane is a minimum. So, according to Fig , the minimum length of the reinforcement,

$$d_{min} = l_{e_{min}} + (h_d - s_{min}) \tan\theta \tag{3 4}$$

Initial values to the design vector are assigned For the length of the reinforcement, the recommended minimum value of $l = 0\ 7h_d$ is a rational initial value An initial value of the strength of the reinforcement is also chosen.

Checking External Stability:

Overturning.

Fig. 3.3 illustrates the forces involved in the analysis The safety factor for overturning is evaluated by considering the moment about point A, the toe of the wall Since the depth of the soil in front of the wall is small, the stabilizing passive pressure, is ignored.

$$FS_{over} = \frac{3(\gamma_f h_d + q_s)l^2}{K_{a_e} h_d^2(\gamma_b h_d + 3q_s)} \tag{3 5}$$

Sliding:

The forces involved in the sliding failure are shown in Fig. 3.4 The sliding resistance is calculated as,

$$R_s = (\gamma_f h_d + q_s) l \tan\delta \tag{3 6}$$

where δ is the interface friction angle between the soil and the fabric Bonoparte et al(1987) and Jewell(1990) have proposed that $\delta = (2/3)\phi$. The force attempting

to cause sliding is the active thrust which can be estimated from the following equation,

$$P_a = \frac{1}{2} K_{a_e} \gamma_b h_d^2 + K_{a_e} q_s h_d \tag{3 7}$$

Therefore, Factor of safety for base sliding is the ratio of the resisting force to the force causing sliding.

$$FS_{slid} = \frac{R_s}{P_a} \tag{3 8}$$

Bearing Capacity Analysis.

The overturning moment from the lateral pressure in the backfill causes a transfer of bearing pressure from the heel of the wall to the toe. Hence, the base reaction no longer acts along the centre line but is eccentric by a distance e.(Fig 3.3) Considering a unit length of the wall and taking moments about the toe,

$$e = \frac{K_{a_e} h_d^2 (\gamma_b h_d + 3q_s)}{6(\gamma_f h_d + q_s/l)} \tag{3.9}$$

As with other gravity retaining walls, the middle third rule must be complied with in order to avoid any tension between the wall base and foundation soil Hence, the trapezoidal bearing pressure distribution gave the maximum bearing pressure, q_{max}, as

$$q_{max} = (\gamma_f h_d + q_s)(1 + 6e/l) \tag{3 10}$$

The net ultimate bearing capacity was assessed using Terzaghi's equation for a strip footing,

$$q_{net} = \frac{1}{2} \gamma_f N_\gamma l + q_s N_q \tag{3 11}$$

The safety factor for bearing capacity is given by,

$$FS_{bear} = \frac{q_{net}}{q_{max}} \tag{3 12}$$

Internal Stability:

Safe design strength of the geosynthetic is equated by

$$T_d = \frac{T_a}{FS_{str}}$$

The lateral load to be resisted by the reinforcement

$$P_{lat} = \frac{1}{2} K_{a_e} \gamma_f h_d^2 + K_{a_e} q_s h_d \tag{3.13}$$

Assuming 100% geosynthetic coverage in the plan view, the geosynthetic should safely carry this load.

The approximate number of layers of the geosynthetic required is

$$n_l = \frac{P_{lat}}{T_d}$$

The number obtained is rounded and an additional layer is added to account for practical layout consideration. Assuming uniform spacing between the layers, the spacing was calculated as,

$$s = \frac{h_d - h_e}{nl} \tag{3.14}$$

Check for Pullout:

The factor of safety against pullout is given by the equation

$$FS_{pull} = \frac{2(\gamma_f z + q_s) \tan \phi_r l_e}{T_i} \tag{3 15}$$

where,

z = depth of the layer being designed.

ϕ_r = angle of frictional sliding resistance between the soil and the reinforcement.

l_e = embedment length of each layer of reinforcement beyond the failure plane

T_i is the tensile strength required at each level to resist the internal lateral pressures

$$T_i = s_i \times \sigma_h$$

where,

s_i = 1/2(distance to reinforcing layer above + distance to reinforcing layer below).

σ_h = horizontal earth pressure at the middle of the layer

$$\sigma_h = K_{a_i}(q_s + \gamma_b z)$$

Since the design is assumed for equal spacing between the reinforcements,

$$z = i \times s$$

where i varies from 1 to n_l.

The embedment length of each layer of reinforcement beyond the failure plane is calculated as,

$$l_{e_i} = l - (h_d - z)\tan\theta$$

In addition, for geotextile wrap-wall , a minimum overlap length is required for re-embedment. the total length of the geotextile is then calculated as,

$$l_{tot} = l + s + l_{ol_{min}}$$

In addition to static forces, the reinforced earth retaining wall may be subjected to dynamic forces, the following section briefly describes the procedures to be adopted in the design in such conditions.

Seismic Stability

During an earthquake, a reinforced soil wall is subjected to a dynamic soil thrust at the back of the reinforced zone and to inertial forces within the reinforced zone in

addition to the normal static forces Current design procedures use a pseudo-static approach since the dynamic response of even the simplest type of retaining walls is quite complex The common approach involves estimating the loads imposed on the wall during earthquake shaking and then ensuring that the wall can resist these loads An attempt was made to find the optimum cost of the reinforced wall when subjected to earthquake loading. The design steps are the same as for static analysis except that the earthquake loading is represented pseudostatically by the dynamic soil thrust, δP_{a_E}, and the inertial force on the reinforced zone, P_{IR} (Fig. 3 5). The external stability of the wall can be analysed by the following procedure.

- The peak accleration coefficient at the centroid of the reinforced zone is calculated from the given value of peak horizontal ground surface accleration coefficient, α_{max},

$$\alpha_c = (1.45 - \alpha_{max})\alpha_{max}$$

- The dynamic soil thrust is calculated from

$$\delta P_{a_E} = 0.375\alpha_c\gamma_b h_d^2$$

- The inertial force acting on the reinforced zone is

$$P_{IR} = \alpha\gamma_f h_d l$$

- δP_{a_e} and 50% of P_{IR} is added to the static forces acting on the reinforced zone and the usual checks for external stability are done The reduced value of P_{IR} is taken to allow for the fact that the maximum values of P_{a_E} and P_{IR} are unlikely to occur at the same time.

The internal stability is calculated using the following steps·

- The pseudostatic inertial force acting on the potentially unstable failure zone is determined by,

$$P_{IA} = \alpha_c W_a$$

wher W_a is the weight of the failure mass (mass contained within the Rankine Failure envelope).

- P_{IA} is distributed to each reinforcement layer in proportion to its resistant area (the area of the reinforcement that extends beyond the potential internal failure surface). This process produces a dynamic component of tensile force for each layer of reinforcement.
- The dynamic component of the tensile force is added to the static component to get the total tensile force for each layer of the reinforcement
- The check for the allowable tensile strength of the reinforcement is carried out
- Check for pullout failure is carried out.

3.2.3 Objective Function

The objective function is the cost estimate for the proposed design of the geosynthetic reinforced retaining wall. The costs involved per metre length of the wall are as follows:

1. Cost of Levelling Pad $=c_1$
2. Cost of the wall fill $=c_2 \times \gamma_f/g \times h_d \times l$
3. Cost of the geosynthetic used$=c_3 \times n_l \times l$
4. MCU[1] face units cost$=c_4 \times h_d$
5. Engineering and Testing Cost$=c_5 \times h_d$
6. Installation Cost$=c_6 \times h_d$

[1]Only for Geogrid Wall

The objective function is the sum of all the above costs and, thus, is a function of the length and strength of the reinforcement which are the design variables.

$$\vec{D}^T = (d_1, d_2)$$

The objective function is minimized with respect to the design vector

$$F = f(\vec{D}) = f(d_1, d_2)$$

3.2.4 Design Constraints

The various design constraints that are to be placed on the choice of design variables and other design parameters were as follows:

- The initial length of the reinforcement chosen for design is to be greater than the critical length calculated by Equation 3.4 thus, the first design constraint is,

$$g_{j1} = d_{min} - d_1 \leq 0$$

- The initial allowable strength of the geosynthetic is chosen to be greater than the minimum specified.

$$g_{j2} = T_{a_{min}} - d_2 \leq 0$$

- The allowable strength of the geosynthetic is not to exceed the maximum available.

$$g_{j3} = d_2 - T_{a_{max}} \leq 0$$

- The factor of safety for overturning calculated by the relation (Equation 3.5) is to be greater than the design factor of safety

$$g_{j4} = FS_{ov_d} - FS_{over} \leq 0$$

- The factor of safety for sliding calculated from the relation (Equation 3.8) is to be greater than the corresponding design factor of safety

$$g_{j5} = FS_{sl_d} - FS_{slid} \leq 0$$

- The factor of safety for bearing capacity calculated from Equation 3.12 is to be greater than the design safety factor.

$$g_{j6} = FS_{bc_d} - FS_{bear} \leq 0$$

- The spacing between between the reinforcements obtained from the expression (Equation 3.14) is to be greater than the recommended minimum spacing.

$$g_{j7} = s_{min} - s \leq 0$$

- At each level of reinforcement, the factor of safety against pullout calculated from Equation 3.15 is to be greater than the design safety factor

$$g_{j_1} = FS_{pl_d} - FS_{pull} \leq 0$$

The problem could be stated as an optimization problem as follows: Find the decision vector $\vec{D_m}$, such that

$$F = f(\vec{D_m})$$

is the minimum of $F(\vec{D})$ subject to

$$g_j(\vec{D_m}) \leq 0, j = 1, 2, \ldots, n$$

The Sequential Unconstrained Minimization Technique (Fox, 1971) was used in which interior penalty function methods was employed in conjunction with Powell's multidimensional search and quadratic interpolation for minimising steps. The interior penalty function approach needs a feasible starting point for initiating the

solution. Such a starting point was easy to get. Results are obtained thus for a feasible initial design vector using interior penalty function approach. A detailed description of the optimization procedures can be found in any standard text book on the optimization theory.

3.3 Results and Discussions

3.3.1 The Developed Program

The flow chart for the developed optimization procedure is presented in Fig 3.6. A brief description of the subroutines used in the procedure is presented here.

- INTPEN : This subroutine described in Fig 3.7 is the Interior Penalty Function Method in which a new function, ψ, is constructed by augmenting a penalty term to the Objective function.

$$\psi(\vec{D}, r_k) = F(\vec{D}) - r_k \sum_{j=1}^{m} \frac{1}{g_j(\vec{D})}$$

- POWEL : This subroutine utilizes Powell's Conjugate Direction method for pattern move in order to find the minima.

- QFIT : This subroutine approximates the given function by a quadratic function for which finite minimum can exist.

- FUN : The subroutine calculates the value of the objective function.

- CONSTR : This subroutine calculates the value of the design constraints.

- Convergence is assumed to be achieved when the change in the value of the objective function between two consecutive cycles is less than the desired accuracy. The same convergence criterion is used althrough wherever convergence is to be checked.

The effectiveness of the developed methodology for the optimum design has been demonstrated with an example problem. Following the standard procedure in practice, as enunciated earlier, the cost of construction of the reinforced wall is estimated With the design parameters of the example problem (FHWA Manual) as the starting point design vector, optimal cost for the wall is obtained

3.3.2 The Example Problem

Wall Description: The wall is about 200m long and exposed wall height is 5m. Surcharge and seismic effect are ignored. The reinforced fill is imported to the site at a cost of \$3 per 1000Kg. An effective angle of internal friction, ϕ, of 34^o and unit weight of $20KN/m^3$ is assumed for the fill. The retained backfill is assumed to have $\phi = 30^o$ and $\gamma_b = 19^o$

Factors of Safety

The design factors of safety chosen are,

For external stability,

- Sliding = 1.5
- Overturning = 2
- Bearing Capacity = 2.0

For Internal Stability,

Reinforcement failure = 1.5.

Pullout failure = 1.5.

Calculations:

The Active earth pressure Coefficients are calculated from Equations 3 1 and 3.2. The values are

$$K_{a_i} = 0.283$$

$$K_{a_e} = 0.333$$

Design height, $h_d = 5\ 45m$,from Eq. 3.3

Assume l/h ratio of 0 7 so, $l = 0.7 \times 5.45$

$$l = 3\ 815 \approx 4m$$

Checks for external stability using equations 3.5,3 8 and 3.12 gave the following values of factors of safety.

$$FS_{over} = 5\ 11$$

$$FS_{slid} = 1\ 91$$

$$FS_{bear} = 8\ 62$$

All these values are above the design factor of safety values, so the wall fulfills external stability requirements.

The Lateral Load to be resisted by the geogrid is:

$$\frac{1}{2}K_{a,}\gamma_f h_d^2 = \frac{1}{2}(0\ 283)(20)(5.45)^2 = 84\ 06KN/m$$

Assuming that a georid with a long term design strength of $20KN/m$ is chosen, the safe design strength of the geogrid is given by :

$$T_d = T_a/1.5 = 13.33$$

The approximate number of layers of the geogrid required are

$$\frac{84.06}{13\ 33} = 6.2$$

This number is approximated to 8 to account for practical layout considerations and 5.1 slope. Spacing of the layers is calculated by Eq 3.14

$$sp = 5/8 = 0.625m$$

COST ESTIMATE:

1 Cost of the Levelling Pad= $(200m)(\$10/m) = \$2000$

2 Cost of the reinforced wall fill.

$$(200m)(5\ 45m)(4m)(20KN/m^3)/(9.8) \times \$3/1000Kg = \$26670$$

3 Cost of Geogrid soil Reinforcement·

$$8\ \text{layers}(4m)(200m)(\$5/m^2) = \$32000$$

4. Cost of MCU face units:

$$(200m)(5\ 45m)(\$60/m^2) = \$65400$$

5. Engineering and Testing Cost:

$$(200m)(5.45m)(\$10/m^2) = \$10900$$

6. Installation Cost:

$$(200m)(5.45m)(\$50/m^2) = \$54500$$

The total cost estimate=\$191470

Cost estimate from Optimization Program = \$176536

Total Net Saving = \$14934

The percentage saving=7.79%.

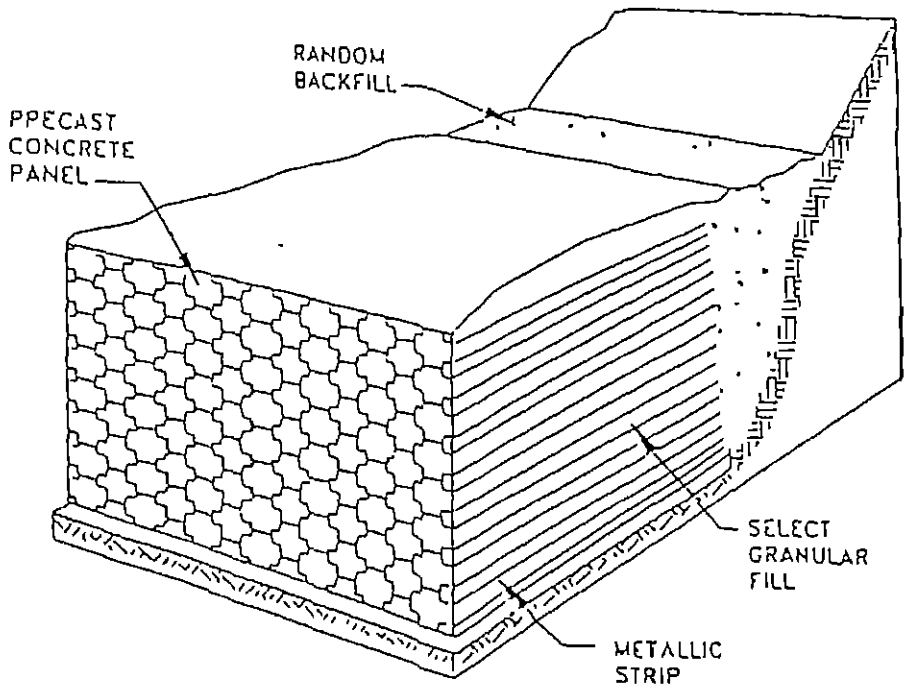

Figure 3.1 Sketch of MSE wall

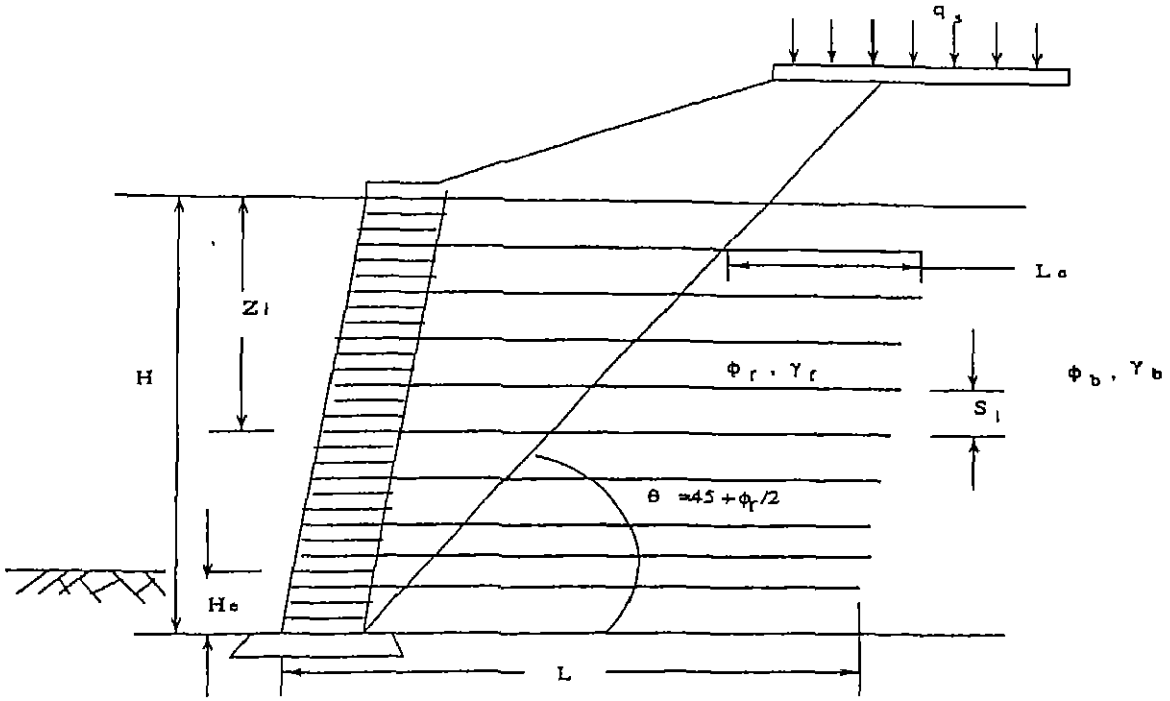

Figure 3.2 Cross-section of MSE wall

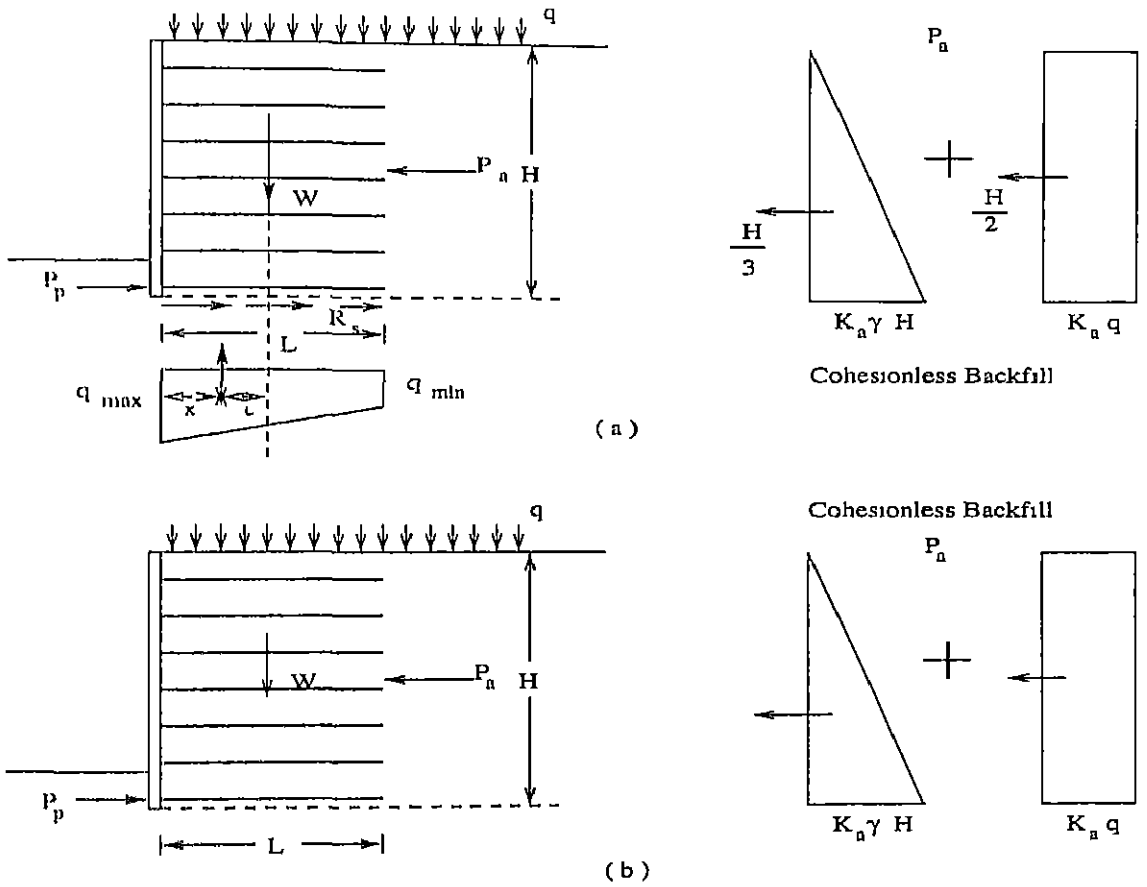

Figure 3.3: Forces for External Stability Analysis

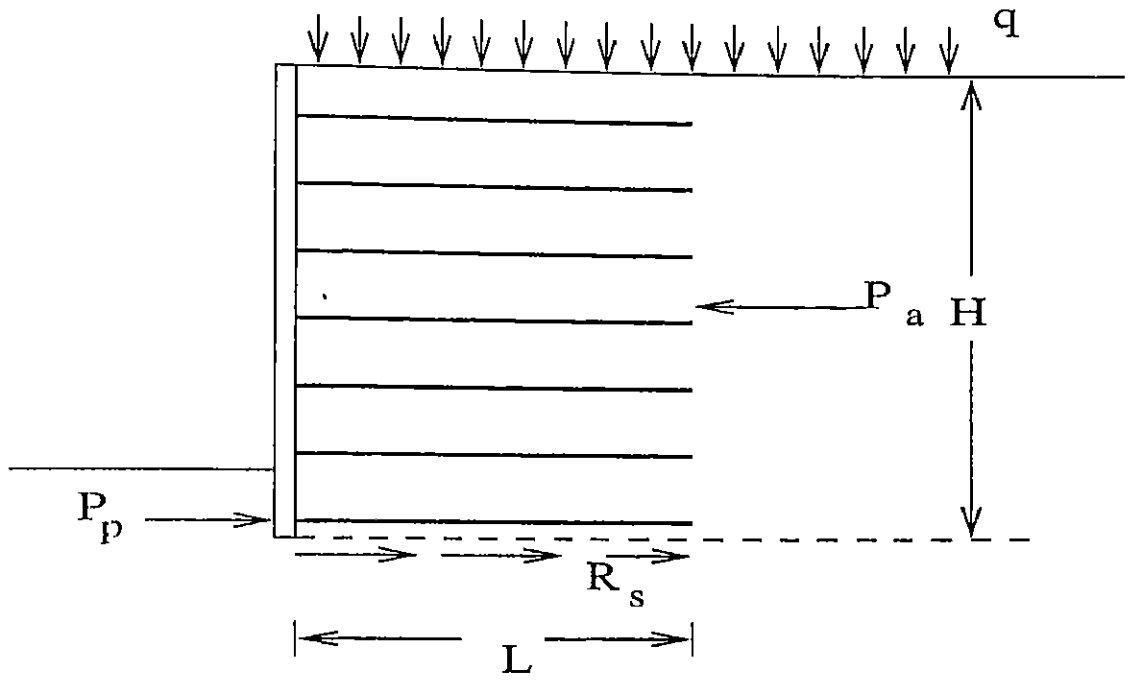

Figure 3.4: Forces for External Stability Analysis (Sliding)

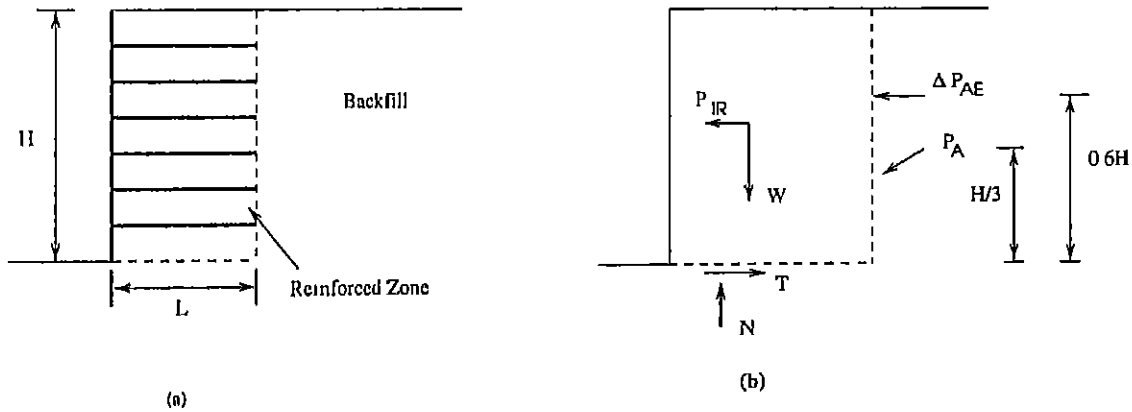

Figure 3.5: Seismic Stability Analysis :(a)Geometry and notation for reinforced soil walls, (b) Static and pseudostatic forces acting on reinforced zone

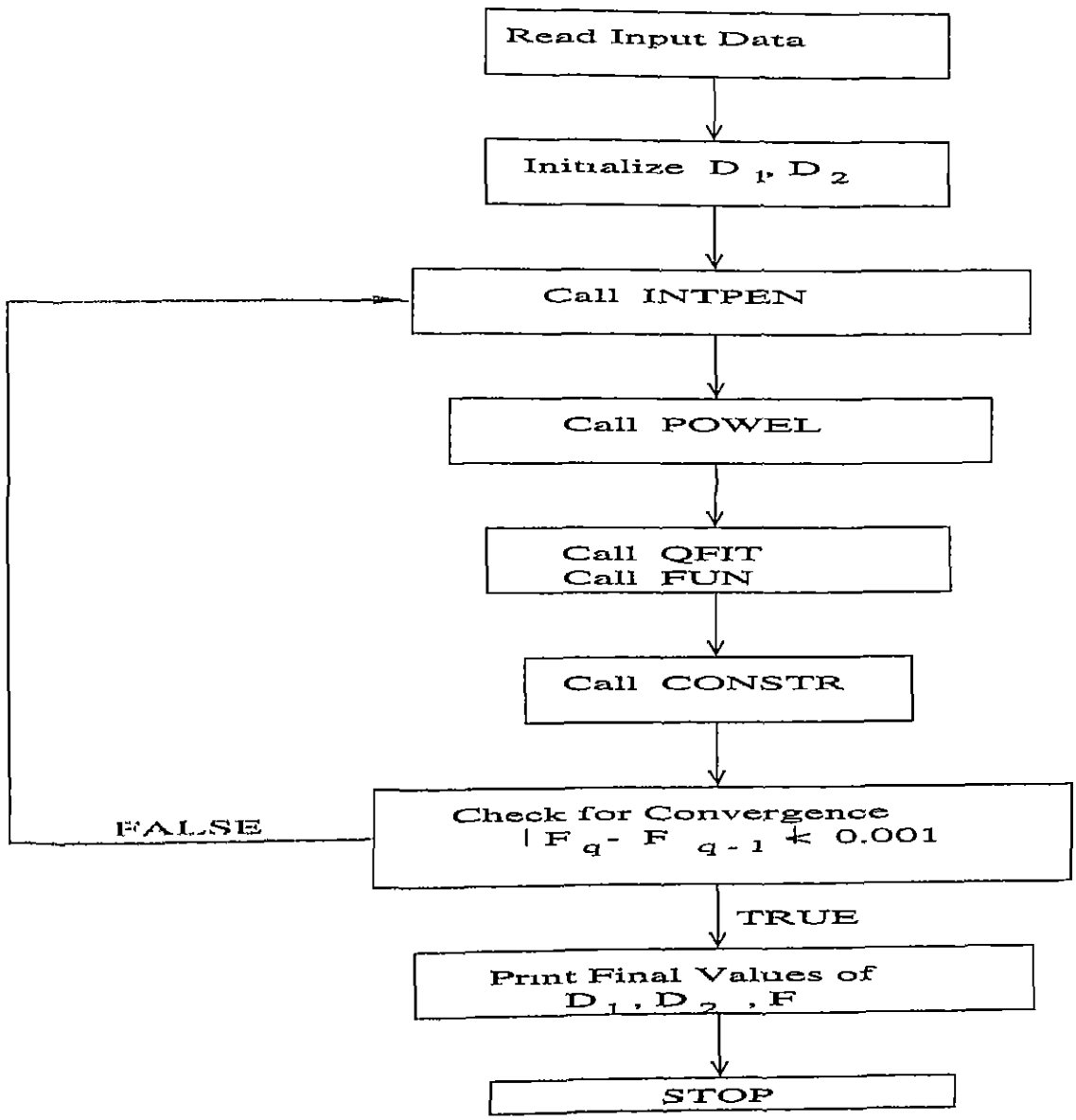

Figure 3.6: Flow Chart for the Developed Program

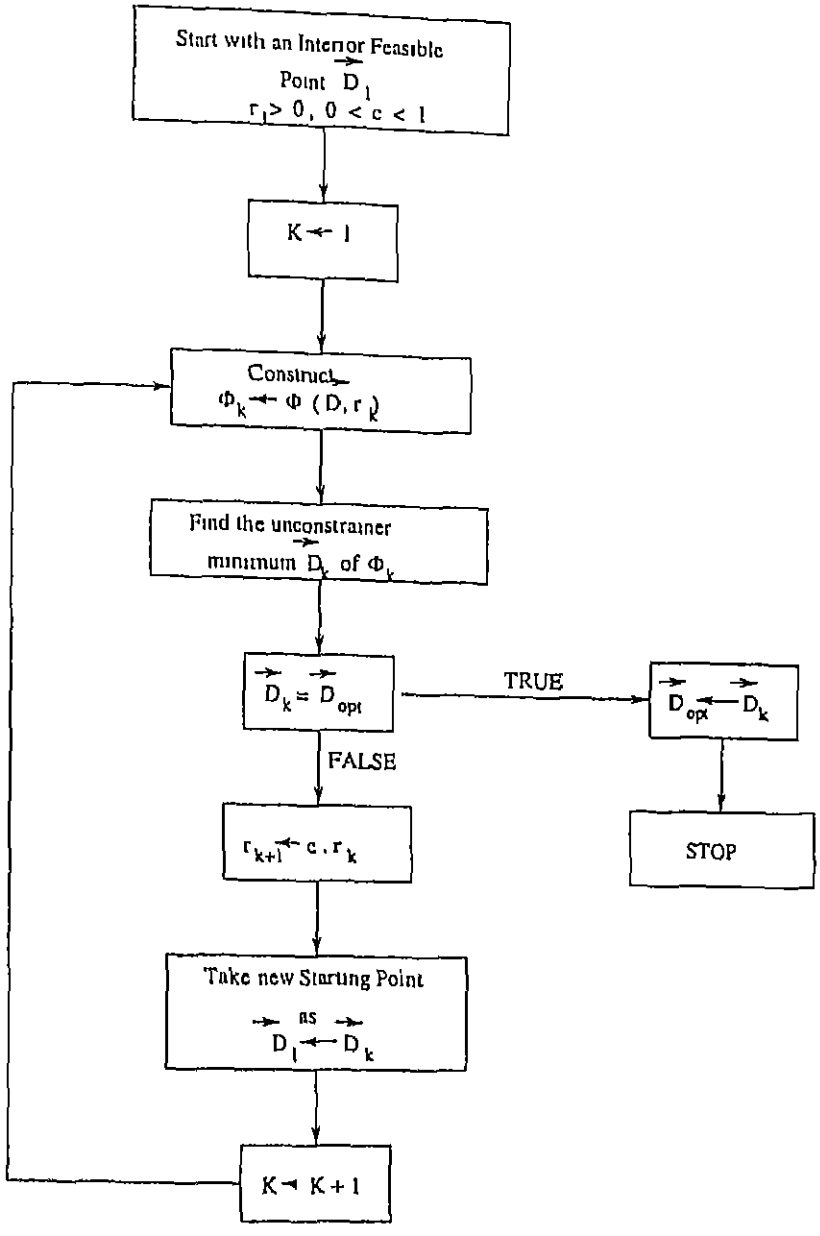

Figure 3.7: Flow Diagram for the Interior Penalty Function Approach

3.3.3 Optimum Cost Tables

Typical optimum cost tables for different wall heights(3 to 10m) are prepared for design parameters as specified in Table 3.1. The walls are designed for different combinations of static and dynamic loading conditions. The results are presented in Tables 3.2 to 3.9 for both geotextile Wrap wall and Geogrid wall. The tables show that the optimum costs increase for increasing wall heights. The optimum design vector for a particular combination of loadings and wall height is almost the same for both the types of walls since they have essentially the same design procedure. The geogrid type wall shows more costs because of the additional cost of the MCU face units. For example, for a $7m$ high wall, the percent increase in cost for a loading of $10KN/m$ is 10.2% over the no-loading case, and for a loading of $20KN/m$, the corresponding percent increase is around 21%. The general observation is that for the same height of the wall and same loading condition, the geogrid wall shows higher costs in the range of $20-30\%$ for low wall heights (3m to 6m), while the increase is $10-20\%$ for heights greater than 6m.

Table 3 2 Optimum Cost Table for Geotextile-wrap Wall, $\alpha_h = 0$, $q_s = 0$

Ht. (m)	l (m)	T_a (KN/m)	Fill Vol	geotextile area (m^2/m)	n_l	spacing (m)	Cost $\$/m^2$
3	2.69	48 38	9.29	10.39	2	1.5	77.73
4	3 21	40 25	14.3	16 64	3	1 33	92 87
5	3 73	40 24	20.35	23 94	4	1 25	108 37
6	4.25	56.37	27.44	27 02	4	1 5	112 49
7	4.78	45.12	35.57	41.65	6	1.67	139 67
8	5.29	41.46	44 74	58 36	8	1.0	167.1
9	5.84	45 38	55 21	70.59	9	1 0	183 19
10	6.49	56.02	68 16	77 43	9	1 11	188 75

Table 3.3: Optimum Cost Table for Geotextile-wrap Wall, $\alpha_h = 0$, $q_s = 10KN/m$

Ht. (m)	l (m)	T_a (KN/m)	Fill Vol.	geotextile area (m^2/m)	n_l	spacing (m)	Cost $\$/m^2$
3	2.69	31.20	9.29	14 09	3	1 0	90.04
4	3.21	32.86	14.3	20.85	4	1.0	105.42
5	3.73	35.72	20.35	28 67	5	1 0	120.91
6	4.25	39.06	27.44	37 52	6	1 0	136 49
7	4.96	42.65	36.95	48.73	7	1 0	153 94
8	5.29	40.57	44.74	64 65	9	0 89	179 64
9	5.82	44.60	54.96	77 15	10	0 9	195.48
10	6.49	44.82	68.16	92.41	11	0 91	211 97

Table 3.4. Optimum Cost Table for Geotextile-wrap Wall, $\alpha_h = 0$, $q_s = 20KN/m$

Ht (m)	l (m)	T_a (KN/m)	Fill Vol	geotextile area (m^2/m)	n_l	spacing (m)	Cost $\$/m^2$
3	2 72	30.00	9 39	17 88	4	0.75	103 79
4	3 37	30.00	14.99	25.85	5	0 8	119 78
5	4 01	41.26	21 84	30 04	5	1.0	124 23
6	4.64	44 31	29 94	39.85	6	1 0	140 95
7	5 27	40.88	39 28	57 18	8	0.88	169.66
8	5.90	44.87	49 85	70.10	9	0 89	186.54
9	6.53	48 87	61 67	84 26	10	0.9	203 54
10	7 18	48.50	75 40	108 18	12	0.83	232 72

Table 3 5. Optimum Cost Table for Geotextile-wrap Wall, $\alpha_h = 0\ 05$, $q_s = 0$

Ht. (m)	l (m)	T_a (KN/m)	Fill Vol.	geotextile area (m^2/m)	n_l	spacing (m)	Cost $\$/m^2$
3	2.88	30.00	9.96	14.66	3	1.00	91.64
4	3.72	45.66	16.56	18.16	3	1.33	97.73
5	4.55	45.66	24.84	27.23	4	1 25	116 20
6	5.39	47.96	34.79	37 97	5	1 2	134 93
7	6.23	51.19	46.41	50.38	6	1 17	153.86
8	7.07	54.88	59.72	64.46	7	1 14	172 99
9	7.90	58.83	74.68	80.22	8	1 125	192 34
10	8.78	56.49	92.20	107.81	10	1.0	224 30

Table 3.6 Optimum Cost Table for Geogrid Wall, $\alpha_h = 0$, $q_s = 0$

Ht. (m)	l (m)	T_a (KN/m)	Fill Vol	geotextile area (m^2/m)	n_l	spacing (m)	Cost $\$/m^2$
3	2 69	48.38	9 29	5.39	2	1.5	105 41
4	3.21	40.25	14 3	9.64	3	1 33	119 59
5	3.73	40.25	20 35	14.94	4	1 25	134 45
6	4.25	56.37	27.44	17 02	4	1 5	138 73
7	4.77	45 12	35.57	28 64	6	1.67	165.12
8	5.29	41.46	44 74	42.36	8	1 0	191 89
9	5 84	45 38	55.21	52 58	9	1 0	208 06
10	6 49	56 02	68.17	58 43	9	1 11	214 39

Table 3 7. Optimum Cost Table for Geogrid Wall, $\alpha_h = 0$, $q_s = 10KN/m$

Ht. (m)	l (m)	T_a (KN/m)	Fill Vol.	geotextile area (m^2/m)	n_l	spacing (m)	Cost $\$/m^2$
3	2.69	31.20	9.29	8.08	3	1.0	116.87
4	3.21	32.86	14.3	12 85	4	1 0	131 37
5	3.73	35.72	20.35	18.67	5	1 0	146.33
6	4.25	39.07	27.44	25.52	6	1 0	161.61
7	4.96	42.65	36 95	34 72	7	1 0	178.94
8	5.58	40.57	47.16	50 22	9	0.89	206.89
9	5.82	44.60	54.96	58.15	10	0 9	220.02
10	6.49	44.82	68 16	71 41	11	0 91	236.56

Table 3.8 Optimum Cost Table for Geogrid Wall, $\alpha_h = 0$, $q_s = 20KN/m$

Ht. (m)	l (m)	T_a (KN/m)	Fill Vol.	geotextile area (m^2/m)	n_l	spacing (m)	Cost $\$/m^2$
3	2 72	30.00	9.38	10 88	4	0.75	129 57
4	3 37	30.00	14 99	16 85	5	0 8	144.89
5	4 01	41.26	21.84	20 04	5	1.0	149.74
6	4 64	44.31	29 94	27 85	6	1.0	166 23
7	5.27	40.88	39 28	42.18	8	0 88	194.22
8	5.90	44 87	49 85	53 10	9	0 89	211 23
9	6 53	48.87	61 67	65.26	10	0 9	228 49
10	7.18	48 50	75 41	86.18	12	0 83	257 52

Table 3.9 Optimum Cost Table for Geogrid Wall, $\alpha_h = 0\ 05$, $q_s = 0$

Ht. (m)	l (m)	T_a (KN/m)	Fill Vol.	geotextile area (m^2/m)	n_l	spacing (m)	Cost $\$/m^2$
3	2.89	30.00	9.96	8.66	3	1.00	118 46
4	3.72	45.66	16.56	11.16	3	1.33	124 51
5	4.55	45.66	24.84	18.23	4	1.25	142 42
6	5.39	47.96	34 79	26.97	5	1 2	160.88
7	6.23	51.19	46.41	37.38	6	1.17	179.76
8	7.07	54.88	59.71	49 46	7	1.14	199 06
9	7.90	58.83	74.68	63.22	8	1.125	218.73
10	8.78	56.49	92.20	87 81	10	1 0	250 61

3.3.4 Conclusions

Optimal cost tables are presented for different combinations of loading The Geogrid walls show greater optimal costs because of the inherent design involving MCU face units The saving is of the order of $7 - 8\%$ for the optimum design procedure developed here over the standard design

Chapter 4

Scope of Future Studies

The present study, with regards to reinforced foundation beds, may be further extended to consider-

- The effect of non-linearity of both soil and geotextile on the settlement and stress response.
- The bending stiffness of the reinforcement in the analysis.
- Further refining of the mesh to study the effect on the stresses
- Higher order elements to increase the computational efficiency

As for the reinforced earth walls, future works may involve one of the following.

- Optimal design of other reinforcing structures.
- Finite Element Analysis of Reinforced Earth Walls

References

[1] Adams, M. T. and Collin, J. G (1997), "Large Model Spread Footing Load Tests on Geosynthetic Reinforced Soil Foundations," *Jr. of Geotech. and Geoenvironmental Engg.*, Vol. 123, No 1, pp 66-72.

[2] Akinmusuru, J. O., and Akinbolade, J. A (1981), "Stability of Loaded Footings on Reinforced Soil," *Jr. of Geotech. Engg. Div.*, ASCE, Vol 107, No. GT6, pp. 819-827

[3] Andrawes, K. Z., McGown, A., Wilson-Fahmy, R. F. and Mashhour M. M. (1982), "Finite Element Method of Analysis applied to Soil-Geotextile System," *Second Int. Conf on Geotextiles*, Vol. 3, Las Vegas, Aug., pp. 695-699

[4] Bastick, M. and Segrestin, P. (1996), "Use of Double Wedge Equilibrium for reinforced earth structures design," *Earth Reinforcement*, (Ochiai, Yasufuku and Omine, Eds.), Balkema, Proc. of the Int. Symp. on Earth Reinforcement, IS-Kyushu '96, Fukuoka, Japan, Nov. 1996, pp. 309-314

[5] Binquet, A. M. and Lee, K. L. (1975a), "Bearing Capacity Tests on Reinforced Earth Slabs," *Jr. of Geotech. Engg. Div.*, ASCE, Vol. 101, No. GT12, pp. 1241-1255.

[6] Binquet, A. M. and Lee, K. L (1975b), "Bearing Capacity Analysis of Reinforced Earth Slabs," *Jr of Geotech. Engg Div*, ASCE, Vol 101, No. GT12, pp. 1257-1276

[7] Brown, B. S. and Poulos, H G. (1981), "Analysis of Foundations on Reinforced Soil," *Proc. of the Tenth Int. Conf on Reinforced Soil*, Stockholm, Vol. 3, pp 595-598

[8] Burd, H. J. and Brocklehurst, C. J. (1990), "Finite Element Studies of the Mechanics of Reinforced Roads," *Proc. Int. Conf on Geotextiles, Geomembranes and Related Products*, Netherlands, pp. 217-221

[9] Burd, H. J. and Houlsby, G. T. (1989), "Numerical modelling of reinforced unpaved roads," *Numerical Models in Geomechanics*, NUMOG III, pp. 699-709.

[10] Claybourn, A. F. and Wu, J. T. H. (1993), "Geosynthetic-Reinforced soil wall design," *Geotextiles and Geomembranes*, 12, pp 707-724

[11] Desai, I. D. (1995), "Nonlinear Finite Element Analysis of a Strip Footing on Reinforced Sand," *Foundation Engineer*, Vol. 1, No. 2, April-June 1995, pp 77-82.

[12] Fragaszy, R. J. and Lawton, E. (1984), "Bearing Capacity of Reinforced Sand Subgrades," *Jr. of the Geotech. Engg. Div.*, ASCE, Vol. 110, No. 10, pp. 1500-1507

[13] Gharpure, A (1995), "Finite Element Analysis of Geotextile Reinforced Sand-bed Subjected to Strip Loadings," *M. Tech. Thesis*, Deptt. of Civil Engg., IIT Kanpur.

[14] Ghosh, C. and Madhav, M. R. (1994), "Settlement Response of a Reinforced Shallow Earth Bed," *Geotextiles and Geomembranes*, Vol. 13, pp 643-656.

[15] Ghosh, C. and Madhav, M. R (1994), "Reinforced Granular Fill - Soft Soil System : Confinement Effect," *Geotextiles and Geomembranes*, Vol. 13, pp. 727-741.

[16] Ghosh, C. and Madhav, M. R. (1994), "Reinforced Granular Fill - Soft Soil System : Membrane Effect," *Geotextiles and Geomembranes*, Vol 13, pp. 743-759

[17] Giroud, J P. and Noiray, L. (1981), "Geotextile-Reinforced Unpaved Road Design," *Jr. of Geotech. Engg. Div.*, ASCE, Vol 107, No GT9, pp. 1223-1254.

[18] Gofar. N. and Bourdeau, P. L (1994), "Transmission of Surface Applied Load in Geosynthetic-Reinforced Soil Structures," *Fifth Int Conf on Geotextiles, Geomembranes and Related Products*, Singapore, 5-9 Sept 1994, pp. 207-210.

[19] Guido, V. A., Chang, D. K. and Sweeney, M. A. (1986), "Comparison of geogrid and geotextile reinforced earth slabs," *Can. Geotech. J.*, 23, pp 435-440.

[20] Hausmann, M. R. (1990), *Engineering Principles of Ground Modification*, McGraw-Hill, New York.

[21] Hyodo, M., Matsuoka, H., Nakata, Y. and Murata, H. (1996), "Stability and Deformation of geosynthetic reinforced soil retaining wall," *Earth Reinforcement*, (Ochiai, Yasufuku and Omine, Eds.), Balkema, Proc. of

the Int Symp. on Earth Reinforcement, IS-Kyushu '96, Fukuoka, Japan, Nov 1996, pp 379-384

[22] Ingold, T. S. and Miller, K. S. (1982), "Analytical and Model investigations of Reinforced clay," *Second Int. Conf. on Geotextiles*, Las Vegas, Vol. 3, Aug , pp. 587-592.

[23] Jewell, R. A. and Milligan G. W E. (1985), "Deformation calculations for reinforced soil walls," *Proc. of the Eleventh Int Conf on reinforced soil*, pp. 1257-1262.

[24] Juran, I. and Christopher, B. (1989), "Laboratory Model Study on Geosynthetic Reinforced soil Retaining Wall," *Jr of the Geotech. Engg. Div.*, ASCE, Vol 115, No. 7, pp. 905-926.

[25] Juran, I., Ider, H. M. and Farrag, K. (1990), "Strain Compatibility Analysis for Geosynthetic Reinforced soil Walls," *Jr. of the Geotech. Engg. Div.*, ASCE, Vol. 116, No. 2, pp 312-328

[26] Karpurapu, R and Bathurst, R. J. (1995), "Behaviour of Geosynthetic reinforced soil retaining walls using the finite element method," *Computers and Geotechnics*, Vol. 17, No. 3, pp. 279-299.

[27] Kennedy, J. B., Laba, J. T. and Mossaad, M A. (1980), "Reinforced Earth Retaining Walls under strip Load," *Can. Geotech. J.*, 17, pp.382-394.

[28] Khing, K. H., Das, B. M., Puri, V. K., Cook, E E. and Yen, S C. (1993), "The Bearing-Capacity of a Strip Foundation on Geogrid-Reinforced Sand," *Geotextiles and Geomembranes*, 12, pp. 351-361

[29] Kramer, S L (1996), *Geotechnical Earthquake Engineering*, Prentice-Hall, New Jersey, USA.

[30] Laba, J. T. and Kennedy, J. B (1986), "Reinforced Earth Retaining Wall analysis and Design," CAN geotech J , 23, pp. 317-326

[31] Lambe, T. W. and Whitman, R. V. (1979), *Soil Mechanics - SI version*, John Wiley and Sons

[32] Lee, K. L., Adams, B. D. and Vagneron, J. J. (1973), "Reinforced Earth retaining walls," *Jr. of the Geotech. Engg. Div.*, ASCE, Vol. 99, No SM10, pp. 745-763.

[33] Leshchinsky, D. and Boedeker, R. H. (1989), "Geosynthetic reinforced Soil Structures," *Jr. of the Geotech. Engg. Div* , ASCE, Vol 115, No 10, pp. 1459-1477.

[34] Ling, H. I., Leshchinsky, D. and Perry, E. B. (1996), "A new concept on seismic design of geosynthetic-reinforced soil-structures permanent displacement limit," *Earth Reinforcement*, (Ochiai, Yasufuku and Omine, Eds.), Balkema, Proc. of the Int. Symp. on Earth Reinforcement, IS-Kyushu '96, Fukuoka, Japan, Nov. 1996, pp. 797-801

[35] Love, J. P., Burd, H. J., Milligan, G W. E. and Houlsby, G. T. (1987), "Analytical and Model Studies of reinforcement of a layer of granular fill on a soft clay subgrade," *Canadian Geotech. J.*, 24, pp. 611-622.

[36] Madhav, M. R. and Poorooshasb, H. B. (1989), "Modeling of Embankment on near surface reinforced soils," *Numerical Models in Geotechnics*, NUMOG III, pp. 657-666.

[37] McGown, A , Andrawes, K. Z and Pradhan, S M (1994), "The Applicability of Limit State Design to Polymer Reinforced Soil Structures," *Fifth Int Conf. on Geotextiles, Geomembranes and Related Products*, Singapore, Sept. 1994, pp 237-242.

[38] Nishimura, J , Hirai, T ,Iwasaki, K ,Saito, Y. and Morishima, M. (1996), "Earthquake resistance of geogrid-reinforced soil walls based on a study following the southern Hyogo earthquake," *Earth Reinforcement*, (Ochiai, Yasufuku and Omine, Eds.), Balkema, Proc of the Int. Symp on Earth Reinforcement, IS-Kyushu '96, Fukuoka, Japan, Nov. 1996, pp. 797-801

[39] Omar, M. T., Das, B. M., Puri, V. K. and Yen, S C. (1983), "Ultimate Bearing Capacity of shallow foundations on sand with geogrid reinforcement," *Canadian Geotech. J.*, 30, pp. 545-549.

[40] Otani, J., Ochiai, H., Tsukamato, Y. and Hayashi, S. (1994), "Supporting capability of Geogrid-Mattress Foundation," *Fifth Int. Conf on Geotextiles, Geomembranes and Related Products*, Singapore, Sept 1994, pp 321-327.

[41] Patel, N. M and Chandrashekharam, Y. (1992), "FEM studies on Geosynthetic-Reinforced Soil structures," *Geotechnique Today*, Proc Indian Geotechnical Conf., Calcutta, 1992, pp 247-250

[42] Pitchumani, N. K. (1992), *Reinforcement Foundation Beds : Soil Reinforcement Interaction Analysis*, Ph. D. Thesis, Deptt. of Civil Engg., IIT Kanpur.

[43] Poorooshasb, H. B. (1991), "On Mechanics of Heavily Reinforced Granular Mats," *Soils and Foundations*, Vol. 31, No. 2, pp 134-152.

[44] Porbaha, A and Goodings, D. J. (1996), "Centrifuge Modeling of Geotextile-Reinforced Cohesive Soil Retaining Walls," *Jr. of the Geotech. Engg Div.* ASCE, Vol. 122, No 10, pp. 840-848

[45] Raghavendra, H. B., Sitharam, T. G., Srinivas Murthy, B. R and Balakrishna, C K (1996), "Bearing Capacity Analysis of Reinforced Two Layered Soil System," *Indian Geotechnical Journal.* Vol 2, pp. 122-140

[46] Ramaswamy, S. V. and Purushothaman, P. (1992), "Model Footings on Geogrid Reinforced Clay," *Geotechnique Today*, Proc. Indian Geotechnical Conf., Calcutta, 1992, pp. 183-186.

[47] Rao, G. V. and Raju, G. V. S S (1990), *Engineering with Geosynthetics*, Tata-McGraw Hill Publishing Company Ltd., New Delhi.

[48] Rao, S. S. (1989), *Optimization · Theory and Applications*, Wiley Eastern Ltd.

[49] Rowe, R. K. and Sodermann, K. L. (1987), "Stabilization of very soft soil using high strength Geosynthetic: Role of FEM," *Geotextiles and Geomembranes*, 6, pp. 53-80.

[50] Shukla, S. K. and Chandra, S. (1994), "A study of settlement response of a Geosynthetic-Reinforced Granular Fill-Soft Soil System," *Geotextiles and Geomembranes*, 13, pp 627-639.

[51] Singh, D. N. and Basudhar, P. K (1993), "Determination of Optimal Lower-Bound Bearing Capacity of Reinforced Soil- Walls by usinf Finite Element and Linear Programming," *Geotextiles and Geomembranes*, 12, pp. 665-686.

[52] Sitharam, T G., Srinivas Murthy, B. R. and Raghvendra, H. B. (1996), "Tensile Force Distribution along the reinforcement for reinforced soil foundations," *Earth Reinforcement*, (Ochiai, Yasufuku and Omine, Eds.), Balkema, Proc. of the Int. Symp. on Earth Reinforcement, IS-Kyushu '96, Fukuoka, Japan, Nov 1996, pp. 797-801

[53] Terzaghi, K. (1943), *Theoretical Soil Mechanics*, John Wiley and sons, Inc. New York.

[54] Wilson-Fahmy, R. F. and Koerner, R. M (1993), "Finite Element Modeling of soil Geogrid Interaction with application to the behaviour of the geogrids in a pullout loading condition," *Geotextiles and Geomembranes*, 12, pp. 479-501.

[55] Wong, K. S., Broms, B. B. and Chandrasekaran, B. (1994), "Failure Modes at model tests of a geotextile reinforced wall," *Geotextiles and Geomembranes*, 13, pp. 475-493.

[56] Yetimoglu, T., Wu, J. T. H. and Saglamer, A. (1994), "Bearing Capacity of Rectangular Footings on Geogrid-Reinforced Sand," *Jr. of Geotech. Engg. Div.*, ASCE, Vol. 120, No 12, pp. 2083-2099.

123350

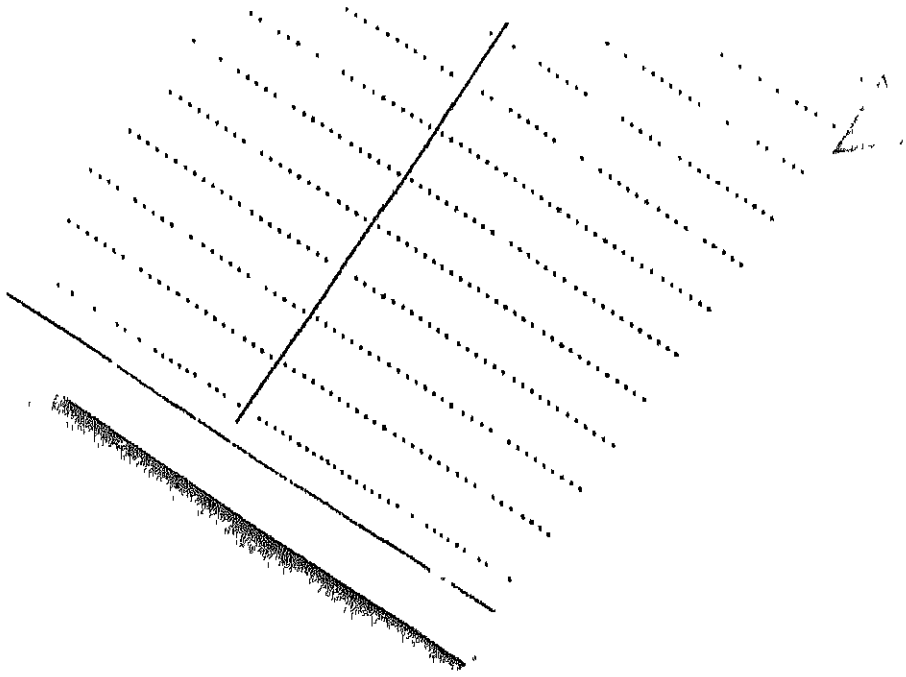

CE-1997-M-VAS-REI